

mi  
NAS8-2696-QPR-1204

FOURTH QUARTERLY PROGRESS REPORT  
For Period  
JANUARY 8, 1967 to APRIL 8, 1967

CONTRACT NAS 8-2696, Mod 12.

Prepared for  
NATIONAL AERONAUTICS & SPACE  
ADMINISTRATION  
GEORGE C. MARSHALL SPACE FLIGHT CENTER  
HUNTSVILLE, ALABAMA 35812

MAY 8, 1967

## FUEL CELL RELIABILITY ASSESSMENT

GPO PRICE \$                      ✓  
CFSTI PRICE(S) \$                     

Hard copy (HC) 2.00

Microfiche (MF) 1.65

ff 653 July 65

FACILITY FORM 902

107-20786  
(ACCESSION NUMBER)  
65  
(PAGES)  
CR-94826  
(NASA CR OR TMX OR AD NUMBER)

1  
(THRU)  
1  
(CODE)  
03  
(CATEGORY)

 **ALLIS-CHALMERS**  
RESEARCH DIVISION  
MILWAUKEE, WISCONSIN 53201

Fourth Quarterly Progress Report

FUEL CELL SYSTEMS  
RELIABILITY ASSESSMENT

Contract Number NAS8-2696, Mod 12

Prepared for  
George C. Marshall Space Flight Center  
NATIONAL AERONAUTICS AND SPACE ADMINISTRATION  
Huntsville, Alabama

Prepared by  
Systems Technology Section  
NASA Fuel Cell Systems Program  
Research Division  
ALLIS-CHALMERS  
Milwaukee, Wisconsin

Prepared By: R. P. Bruno  
R. P. Bruno, Manager  
Reliability Testing

## TABLE OF CONTENTS

	Page
SUMMARY . . . . .	1
INTRODUCTION . . . . .	3
FUEL CELL CONSTRUCTION . . . . .	4
Group I Stacks (131 through 135) . . . . .	4
Group II Stacks (136 through 138) . . . . .	4
TEST BENCH CONSTRUCTION . . . . .	5
STACK TESTING PROGRAM . . . . .	5
Start-Up Test - Stack 134 . . . . .	8
Acceptance Test . . . . .	8
Performance Evaluation Test . . . . .	10
Start-Up Test . . . . .	10
Load Cycle Test - Stack 135 . . . . .	10
Acceptance Test . . . . .	10
Performance Evaluation Test . . . . .	10
Load Cycle Test . . . . .	10
Low Power Life Test - Stack 136 . . . . .	13
Acceptance Test . . . . .	13
Performance Evaluation Test . . . . .	13
Low Power Life Test . . . . .	13
Thermal Cycle Test - Stack 137 . . . . .	19
Acceptance Test . . . . .	19
Performance Evaluation Test . . . . .	19
Thermal Cycle Test . . . . .	23
High Power Life Test - Stack 138 . . . . .	28
Acceptance Test . . . . .	28
Performance Evaluation Test . . . . .	28
High Power Life Test . . . . .	28
DISASSEMBLY ANALYSIS . . . . .	34
Anode Extrusion . . . . .	34
Cathode Extrusion . . . . .	34
Discoloration and Markings . . . . .	36
Corrosion . . . . .	36
ANALYTICAL STUDIES . . . . .	37
Effect of KOH Concentration on Stack Degradation . . . . .	37
Reactant Purging . . . . .	59
Cell Matrix Compression . . . . .	61

# SUMMARY

The fuel cell reliability assessment program was undertaken in April 1966 under Contract NAS8-2696, Modification 12. This is the fourth and final quarterly report covering effort under Modification 12.

The program was directed toward the determination of hydrogen - oxygen fuel cell performance under high stress conditions, and toward the establishment of reliable operation limits. Eight complete 29 volt 2 kw fuel cell stacks were fabricated under the program.

Tests of the first five stacks have been completed. Test status is as follows:

<u>Test</u>	<u>Stack Number</u>	<u>Total Hrs on Test</u>
Load Failure	131	640.7
Reactant Pressure	132	774.8
Low Power Life	133	1507.5
Startup	134	1535.0
Load Cycle	135	575.1

Testing of the above five stacks has demonstrated the following capabilities of the present design Allis-Chalmers 2 kw fuel cell stacks.

- a. Capability of sustaining a continuous load in excess of 3 KW
- b. Brief (one minute) power output capabilities above 5 KW.
- c. Brief (15 second) current output capabilities in excess of 400 amperes.
- d. Capability of over 1000 hours of continuous on-line power production at a 1200 watt level.
- e. Capability of over 40 startup cycles without detrimental effect upon performance or life.
- f. Bootstrap startup capability from room temperature to operating temperature in less than seven minutes.
- g. Useful lifetime in excess of 1500 hours.

Testing of the last three stacks is in process, and will be continued under Modification 18 to Contract NAS8-2696. The three latter tests are Lower Power Life, Thermal Cycle, and High Power Life, being conducted on Stacks 136, 137, and 138 respectively.

The last three stacks (136 through 138) of this program have been loaded with electrolyte by means of a recently developed vacuum loading technique. These stacks have demonstrated a significant improvement in stability over the first five stacks which were filled with electrolyte using the wet stacking method. After 715, 887, and 515 hours on test, these last three stacks are completely free of any crossleaks.

Disassembly analyses were performed on Stacks 131, 132 and 133 after completion of their tests. The major items noted were electrode extrusion into the reactant gas plates and corrosion deposits in the oxygen outlet manifold.

Anode Extrusion. - In the region of the hydrogen inlet port, the anode material is weakened and extruded into the hydrogen plate. The area affected is approximately 2 square inches. The continual wetting and drying of the anode in the vicinity of the hydrogen inlet port, higher temperatures in this area, and the pressure exerted by the cell asbestos matrix may result in the extrusion of the anode into the hydrogen plate. This anode disfigurement may have contributed to the crossleaks that developed on Stack 132 (reactant pressure test) and Stack 133 (low power life test).

The stacks involved were wet stacked, and the electrodes may not have been completely filled at the time of fabrication. Because a certain amount of operating time is necessary for the anodes to lose their water repellancy, these stacks may have been particularly susceptible to this extrusion problem. A new KOH loading procedure (vacuum loading) prevents crossleaks (see page 19), and has been used for the second group of stacks (136 through 138).

Crossleaks in this fuel cell do not result in catastrophic failures or hazardous operating conditions. Crossleaks in Stack 133 occurred at 300 hours operating time; however, the stack was operated for more than an additional 1000 hours by using corrective action. This consists of applying a 1 psi pressure differential to the reactant gases ( $O_2$  higher than  $H_2$ ). The pressure differential maintains an acceptable voltage on the cell having the crossleak by preventing the transport of hydrogen across the cell matrix.

Cathode Extrusion. - An extrusion of the cathode into the oxygen cavity was noted at the oxygen inlet. The extent of cathode extrusion is relatively minor. It has been observed in about 10 percent of the cathodes during stack disassembly.

Corrosion. - When some of the fuel cell stacks were prepared for flushing, after they had accumulated several hundred hours of operating time, removal of the gas and water manifolding at the bottom end plate exposed a deposit at the bottom of the oxygen purge port. Analysis of these deposits showed them to be various hydrates of KOH along with small quantities of nickel, copper, and magnesium, and trace quantities of other elements used in the stack. Stack disassemblies have shown these same corrosion deposits throughout the entire oxygen purge manifold. The bottom water plate usually shows the most severe corrosion because of the high drop ( $\approx 30$  volts) between the bottom section and the bottom end plate. The oxygen inlet manifold is free of corrosion due to the dry incoming reactant gas which inhibits the formation of the KOH film.

Several methods can be employed in future stacks to inhibit this corrosion; these include reaming of fuel cell plate manifold holes to provide a better plating surface, reversing the electrical output leads to eliminate the 30 volt drop to the bottom end plate, and coating manifolds or providing manifold inserts which will break up the KOH film into discontinuous droplets.

Analytical studies were conducted during this quarter to investigate the following effects:

a. Electrolyte concentration upon stack voltage degradation, in which it appears that a significant portion of apparent stack voltage degradation is attributable to the effect of operating fuel cells at non-optimum KOH concentrations.

b. Reactant purging upon fuel cell performance. The average, standard, deviation, and range of the section voltages were used as performance indicators. The voltage data was obtained from Stack 131 operating at a load of 100 amperes. Voltage data was obtained for eleven consecutive purge cycles of Stack 131 at a load of 100 amperes.

The average section voltage increased after each of the 11 purges. The average increase was slightly less than 1 millivolt. The standard deviation of the section voltages decreased after 9 of the 11 purges. Neither the low nor the high voltage section was uniformly affected by purging.

For several purges, more sections decreased in voltage than increased. No apparent reason could be found for this. Some sections showed a significant increase in voltage for all of the purges studied. This is especially true for section number 33. Comparison of the KOH optimization curves for several sections showed no cause for some sections to increase voltage after purge and not the others. The sections studied appeared to be operating under their optimum at 25.5 percent KOH.

c. Matrix compression upon performance. Because of the stringent construction tolerances of these stacks, a variation in bulk asbestos density was small (1.20 to 1.39 gm/cc for a 30 mil matrix). Within this variation in bulk density, no relationship was found between matrix compression and fuel cell performance (see page 61 for detailed data).

## INTRODUCTION

This report covers the technical progress accomplished under Mod 12 to Contract NAS8-2696, "Fuel Cell Reliability Assessment" for the period January 8, 1967 to March 20, 1967. The program was directed toward determining fuel cell stack performance under conditions of high stress, and establishing limitations of reliable operation. In addition, a number of analytical studies relating to fuel cell operation were made. Portions of this effort will be continued under the follow-on program authorized and funded by Modification 18 to Contract NAS8-2696.

# FUEL CELL CONSTRUCTION

Eight stacks were fabricated and categorized into two groups.

All Group I stacks had identical electrode weight distribution. These stacks were wet stacked with quantities of electrolyte determined by a computer program to achieve uniform wetting of the electrodes.

Because electrodes from the same lot were not available, the Group II stacks were not fabricated with the same electrode weight statistics as Group I. Further, the Group II stacks were vacuum loaded with electrolyte. In accordance with a NASA request, the Group II stacks were also equipped with conical washers to maintain stack compression.

## Group I Stacks (131 through 135)

All Group I stacks were wet stacked and delivered to the testing section on the dates listed below:

<u>STACK</u>	<u>DATE</u>
131	October 5, 1966
132	October 27, 1966
133	September 28, 1966
134	September 20, 1966
135	November 28, 1966

## Group II Stacks (136 through 138)

All Group II stacks were flushed with electrolyte prior to operation and were delivered to the testing section on the dates listed below:

<u>STACK</u>	<u>DATE</u>
136	February 13, 1967
137	February 6, 1967
138	February 20, 1967

All Group II stacks were equipped with conical washers to maintain stack compression.

# TEST BENCH CONSTRUCTION

Four stack test benches have been constructed and are in operation.

A Data Acquisition System (DAS) is being used to obtain and record the bulk of the fuel cell data being generated. The DAS provides a paper tape printout and magnetic tape storage for an 800 channel input.

## STACK TESTING PROGRAM

The eight stacks, eight tests, and four test benches are related as follows:

<u>Stack</u>	<u>Test*</u>	<u>Test Bench</u>	<u>Status</u>
131	RA-LF-1	I	Complete**
132	RA-RP-2	K	Complete**
133	RA-LL-3	J	Complete**
134	RA-SU-4	H	Complete
135	RA-LC-5	I	Complete
136	RA-LL-6	K	In Progress
137	RA-TC-7	J	In Progress
138	RA-HL-8	H	In Progress

\*RA = Reliability Assessment

LF = Load Failure Test

RP = Reactant Pressure Test

LL = Low Power Life (two stacks)

SU = Startup Test

LC = Load Cycle Test

TC = Thermal Cycle Test

HL = High Power Life

\*\* Test results are presented in  
NAS8-2696-QPR-1203

Each of the above tests is segmented into three parts as described below.

- a. Acceptance Test. - This phase of testing requires 40 hours, during which 1600 ampere hours of electricity are produced. The load profile is shown in Figure 1. The two main objectives of this test are to verify the compatibility of test bench and test stack, and to optimize the KOH concentration for the test stack. At the end of the acceptance testing, the elapsed time meter is reset to zero.

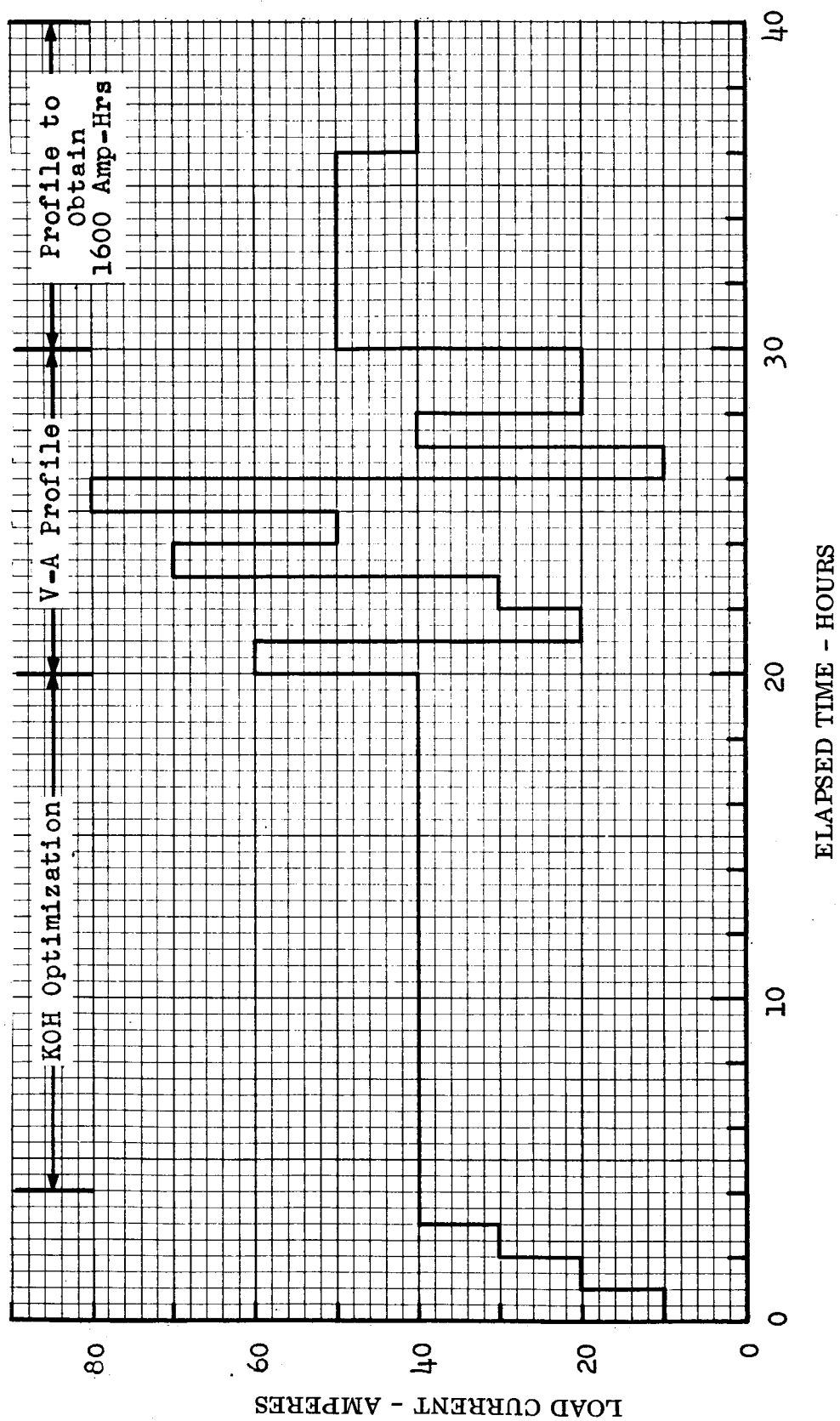


Figure 1. Stack Acceptance Test Load Profile

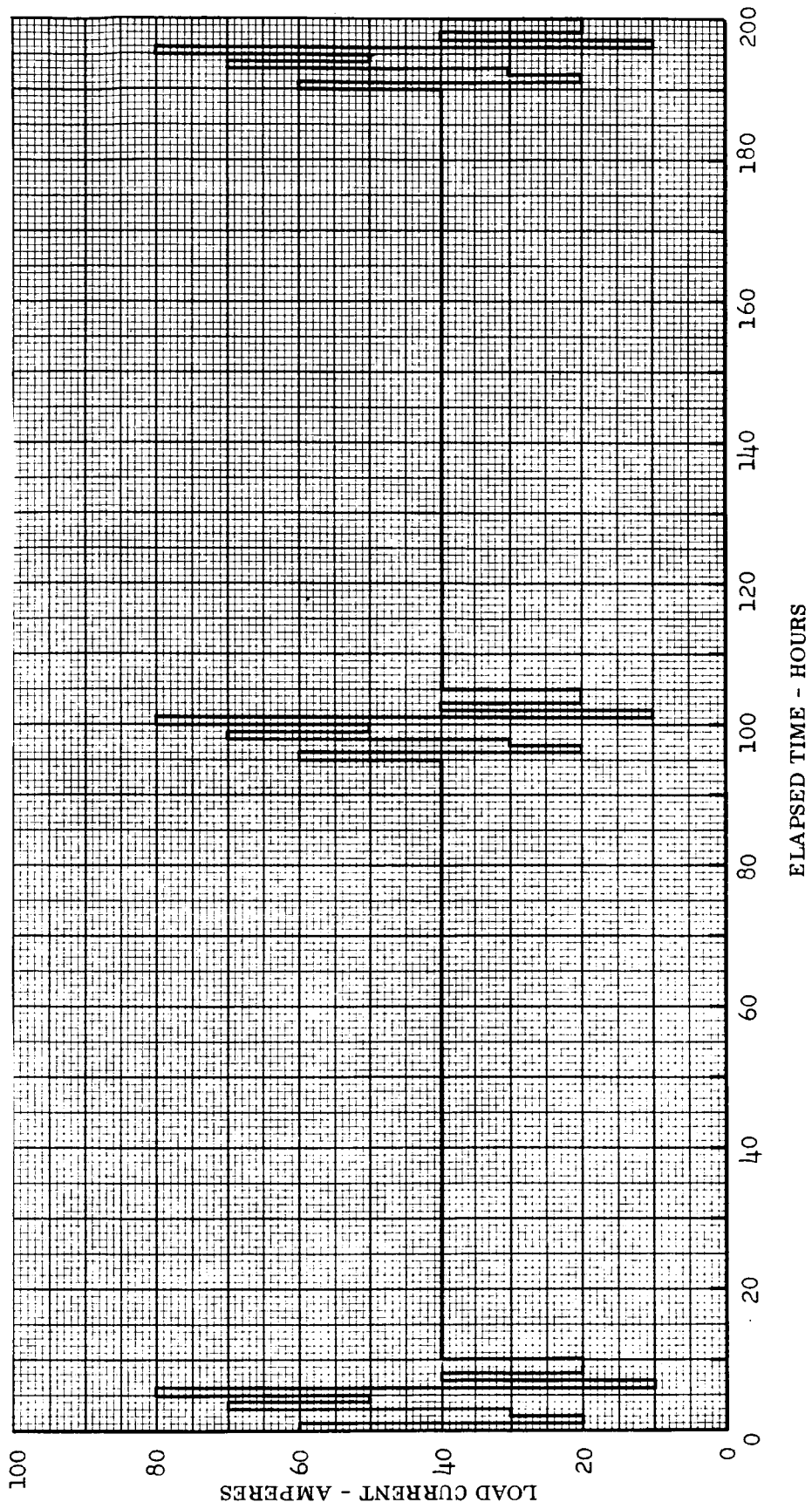


Figure 2. Performance Evaluation Load Profile

- b. Performance Evaluation Test. - This phase of testing is of 200 hours duration. The stack is operated at standard conditions (temperature:  $190 \pm 2^\circ\text{F}$ ; reactant pressure:  $37 \pm 1$  psia; KOH concentration: 1% less than optimum) at a load current of 40 amperes, except during three 10-hour segments where the load is varied from 10 to 80 amperes to permit the generation of steady state volt-ampere characteristics. See Figure 2.
- c. Reliability Test. - This phase of testing begins at 200 hours elapsed on-load time and is scheduled to continue to 500 or 1300 hours dependent upon the particular test. It is here that the primary objectives of this testing program are achieved; i.e., to determine performance characteristics under abnormal stress conditions.

### Startup Test - Stack 134

Acceptance Test. - Stack 134 has completed its acceptance test.

Performance Evaluation Test. - Stack 134 has completed its performance evaluation test. Test results were presented in NAS8-2696-QPR-1203.

Start-Up Test. - Stack 134 has accumulated 1495 hours of elapsed on-load time and has completed all scheduled tests. Seven types of startup and standby cycles were performed for this test. Cycles A, B, C and D, which compare methods of holding the stack in four different shutdown conditions, and Cycle E which determined startup capabilities for a fuel cell system without using the warm-up or standby heaters, have been reported in detail in QPR-1203. These tests have demonstrated that the stack may be held in a hot ( $180^\circ\text{F}$ ) or cold ( $70^\circ\text{F}$ ) shutdown condition, with or without the use of an inert gas (helium) to fill the reactant cavities for an extended time with no detrimental effects upon fuel cell performance. The tests also investigated bootstrap startup capabilities demonstrating a non-detrimental startup from room temperature to operating temperature in less than seven minutes.

Cycles F and G involved two methods of holding the stack in a hot standby condition. The load profile for both standby conditions is shown in Figure 3. During the off-load segments for Cycle F, the reactant valves were closed while the load remained on. This procedure consumed the reactants, leaving a 4 to 5 psia water vapor pressure in the reactant cavities. For Cycle G, the off-load segment consisted of dropping the load and leaving the reactant valves open. A temperature of  $180^\circ\text{F}$  was maintained during all off-load segments by the standby heaters.

Cycle F and part of Cycle G were completed when a crossleak prevented operation at 80 amps without excessive purging. The test was interrupted to perform an electrolyte optimization. At ET 970 hours the optimum concentration was determined to be 34% KOH by weight. Until then, the stack was operated at 37% KOH. The stack still had crossleaks when

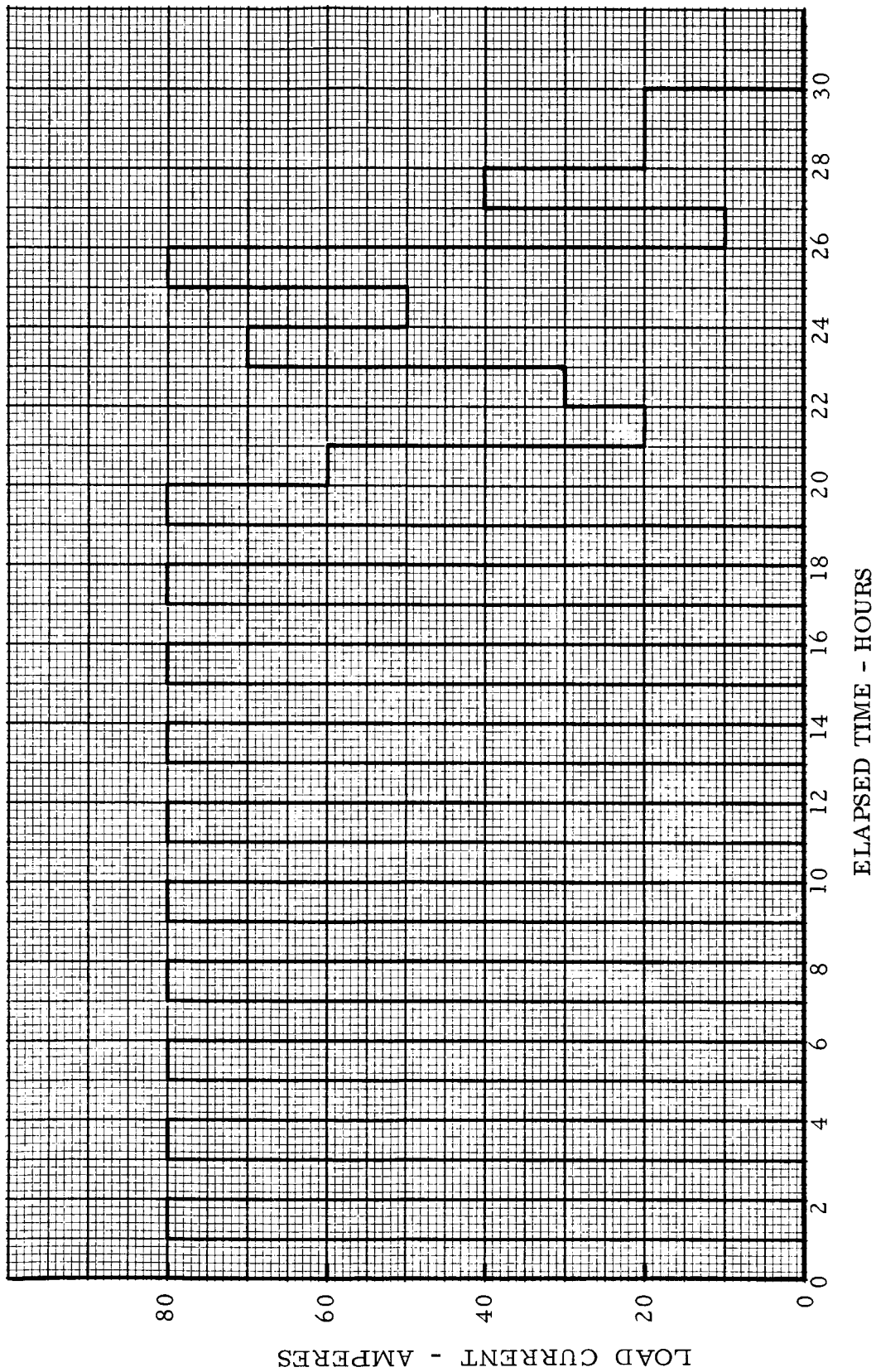


Figure 3. System 134 - Load Profile For Cycles F & G

Cycle F was restarted, using a 40 amp load in lieu of the original 80 amps. A plot of stack voltage at the 40 amp load level is summarized in Figure 4. The degradation rate during this period was 490 microvolts per hour per section. This relatively high degradation rate may be due to the fact that the stack was operated for almost 1000 hours without adjustment of electrolyte concentration. According to information derived from this stack testing program, this may not have been the optimum operating condition for that entire time. Just prior to the hot standby segment of the test, the stack was operating at a constant 40 ampere load and was degrading at approximately the same rate as during the hot standby runs. Further hot standby testing should be performed on another stack.

Upon completion of the scheduled startup tests, Stack 134 was used to verify the apparatus developed and built for vacuum loading (fill and flush) the Group II stacks.

After flushing, Stack 134 was subjected to an additional unscheduled test which increased the total elapsed time on load to 1495 hours. The test was performed to determine the capabilities of a present design fuel cell stack operating at a very low power level (300 watts). The reactant pressures were reduced to 2 psi above atmospheric pressure. The canister was removed and the fans were turned off. The stack was therefore operating without temperature control except for convection in the atmosphere.

The net power output of the stack was continually adjusted to 300 watts as the temperature rose. Stable operation was achieved at 115° F at a voltage of 27.8 volts. This test demonstrated the feasibility of low pressure, low temperature operation for low power requirements. Degradation data is not available because the test duration was not sufficient.

### Load Cycle Test - Stack 135

Acceptance Test.- Stack 135 has completed its acceptance test. The optimum concentration was determined to be 37-1/2% KOH by weight and the system was operated at 36-1/2%.

Performance Evaluation Test.- During this 200 hour segment of testing the stack voltage of stack 135 degraded at a rate of 66 microvolts per hour per section. Voltage-Power characteristics at the beginning and end of the performance evaluation test are shown by the first two curves of Figure 5.

Load Cycle Test.- Stack 135 has accumulated 535 hours of elapsed on-load time. The optimum electrolyte concentration was determined to be 36% and 34% KOH by weight at ET 210 and 510 hours, respectively. The load profile shown in Figure 6 was followed from ET 220 hours to ET 500 hours. The V-P characteristics of the stack at the end of this load cycle is shown as Curve 3 in Figure 5. The stack degraded at a rate of 164 microvolts per hour per section during this time interval. The accumulated degradation rate from ET 0 hours to ET 535 hours is 119 microvolts per hour per section. The individual section voltage data indicated gradual development of crossleaks in three sections. The stack design improvements (electrolyte vacuum loadings, and installation of stack compression devices) had been incorporated in the Group II stacks. It was decided that more bountiful information could be obtained from the testing of the Group II stacks. Testing of stack 135 was terminated at ET 535.1 hours.

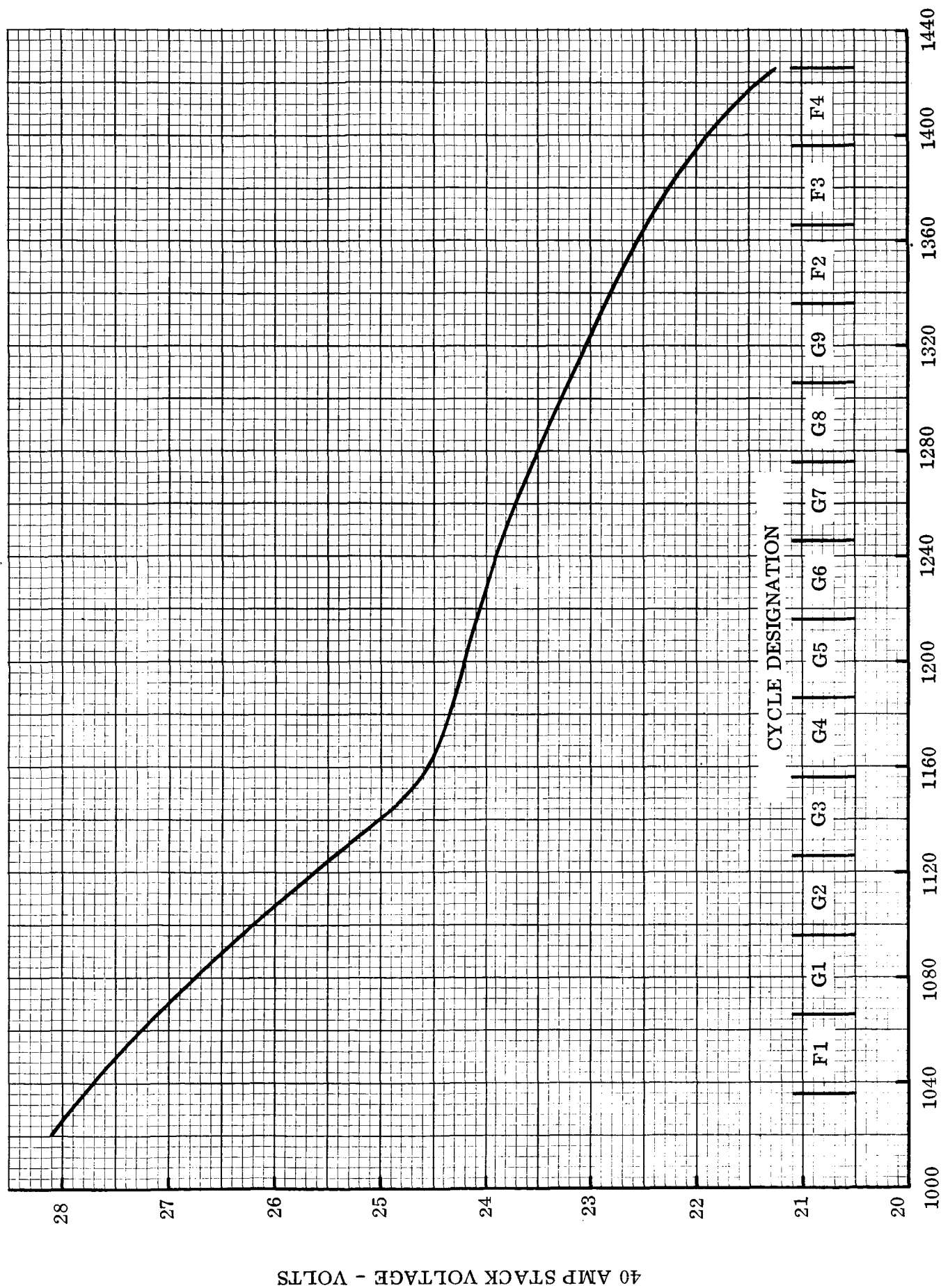
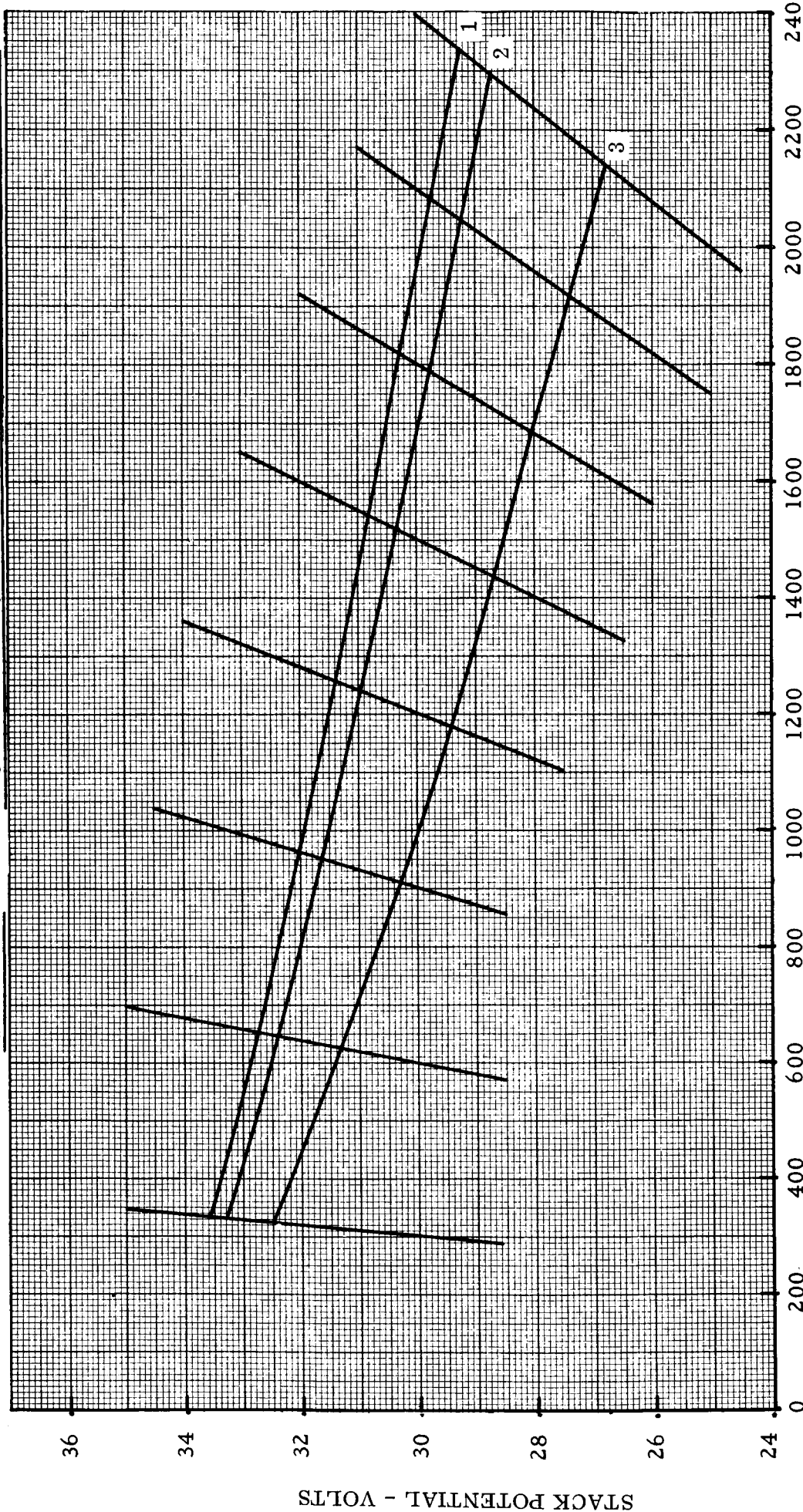


Figure 4. Stack 134 Voltage at 40 Amps - Cycles F & G

Stack Temperature  $190 \pm 2^{\circ}\text{F}$   
 Reactant Pressure  $37 \pm 1 \text{ psia}$   
 KOH Concentration SEE TABLE

CURVE	E. T	% KOH	COMMENTS
1	5	36.5	Beginning of performance evaluation test
2	195	36.5	End of performance evaluation test
3	495	35.0	End of load cycle



STACK POWER OUTPUT - WATTS

Figure 5. Voltage Power Characteristics Stack 135

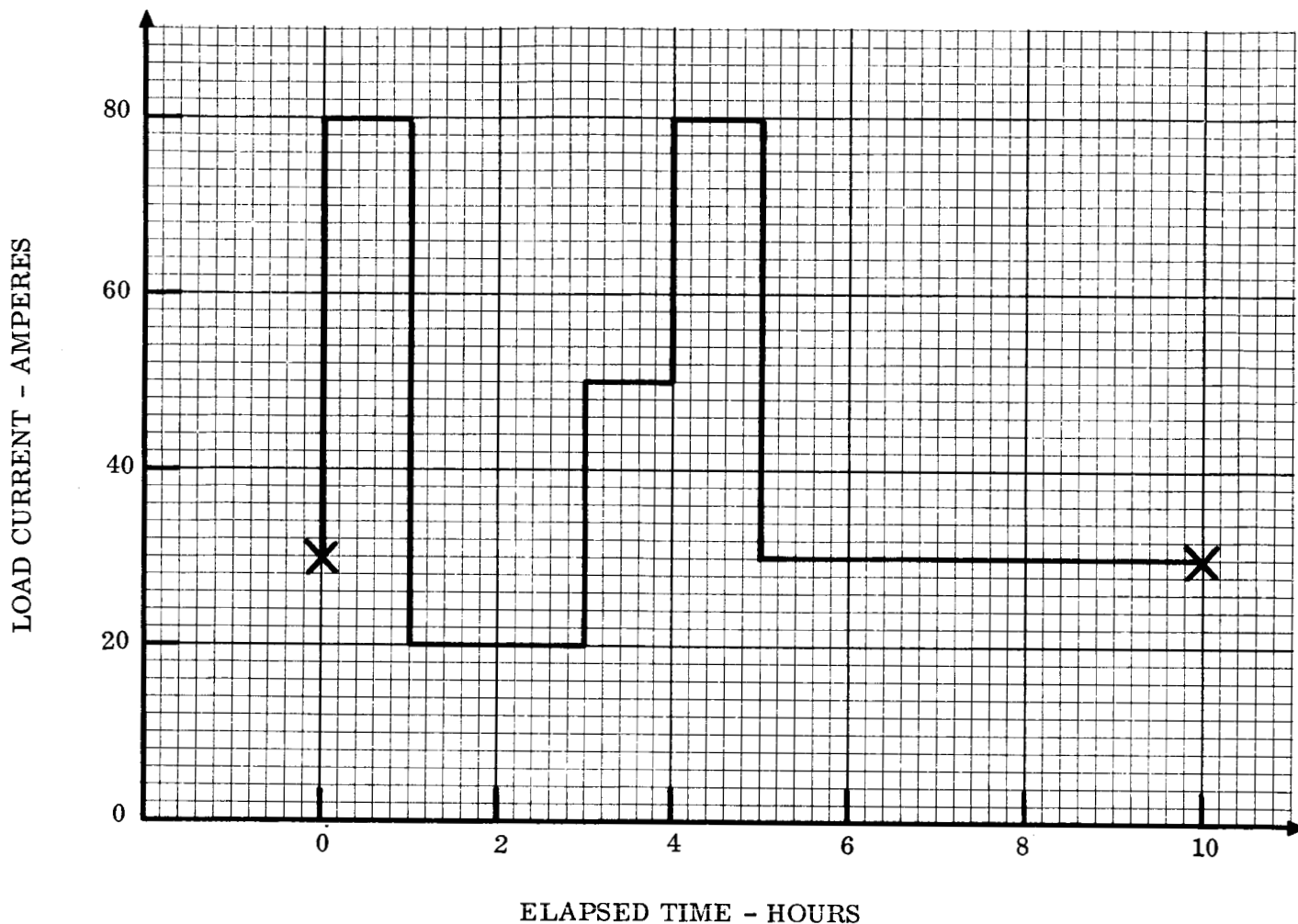


Figure 6. Load Profile - Stack 135

### Low Power Life Test - Stack 136

**Acceptance Test.** - Stack 136 has completed its acceptance test. Figure 7A shows the optimum electrolyte concentration was determined to be 42% KOH by weight. The volt-ampere characteristic shown in Figure 7B was obtained at a KOH concentration of 41%.

**Performance Evaluation Test.** - Stack 136 has accumulated 715 hours of elapsed on-load time. Voltage-Power characteristics taken at the beginning and end of the 200 hour performance evaluation test are shown by the first two curves of Figure 8. During this time the stack voltage degraded at a rate of 62 microvolts per hour per section.

**Low Power Life Test.** - This is the second low power life test of this program. The load profile consists of continuous operation at 40 amperes, interrupted every 100 hours for a 10-hour varying load profile from which voltage-power characteristics are obtained. Stack 133 was the first stack to be operated under these conditions. After 300 hours of

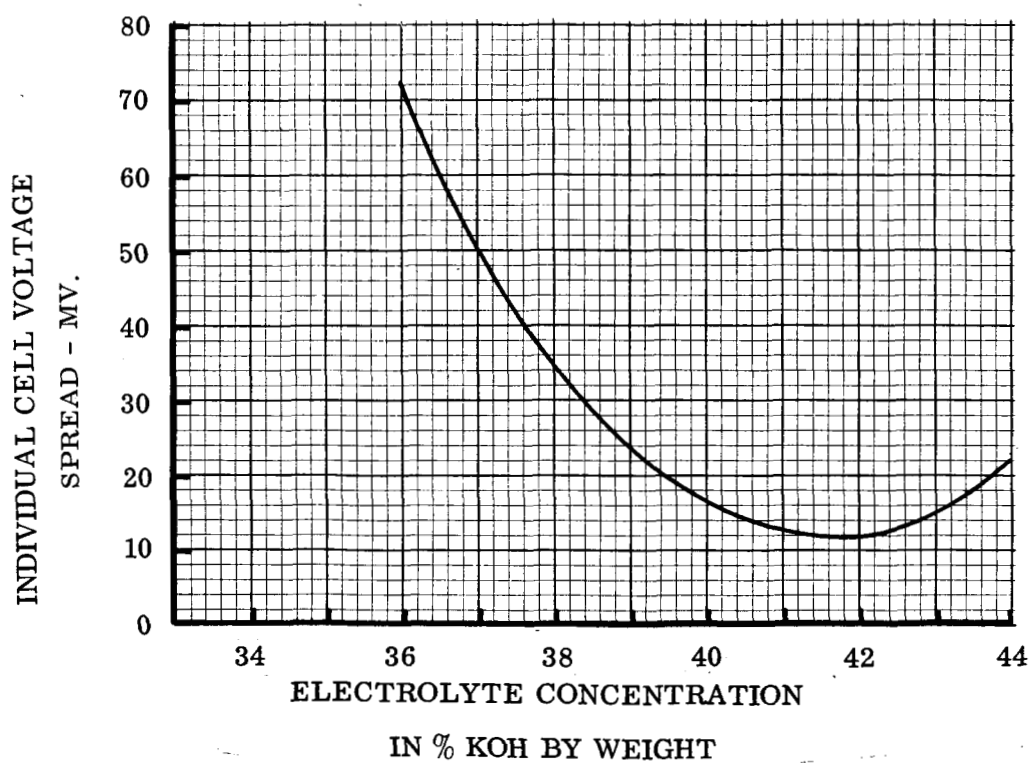
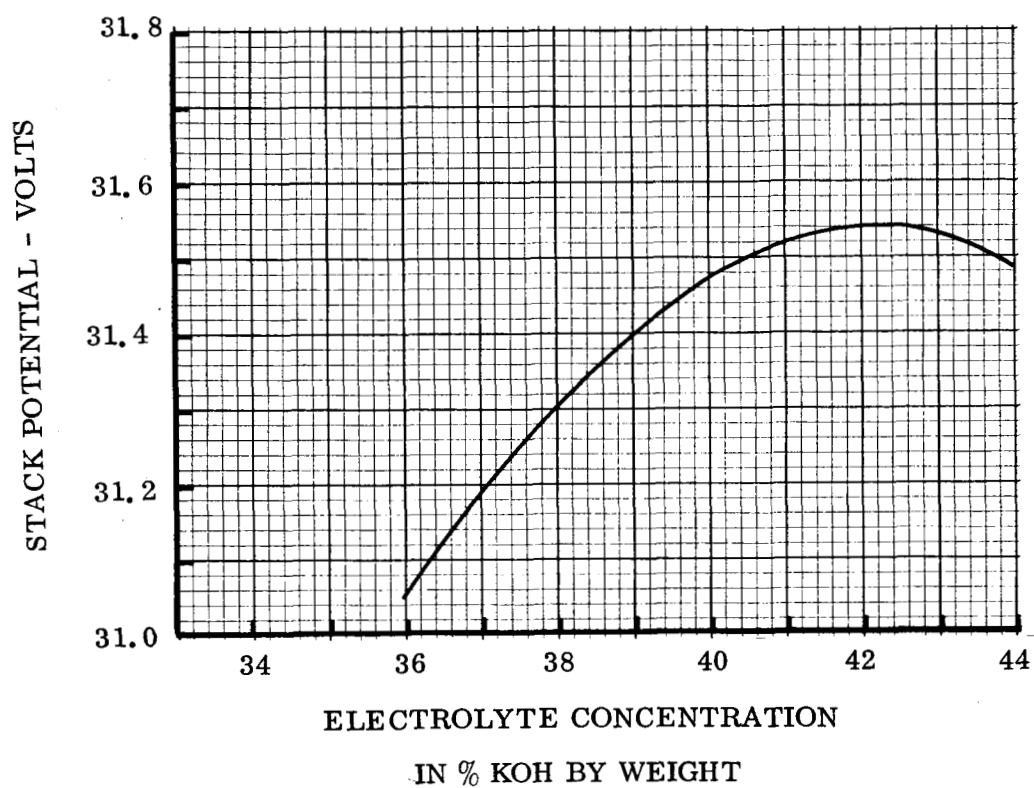


Figure 7A. Acceptance Test KOH Optimization - Stack 136

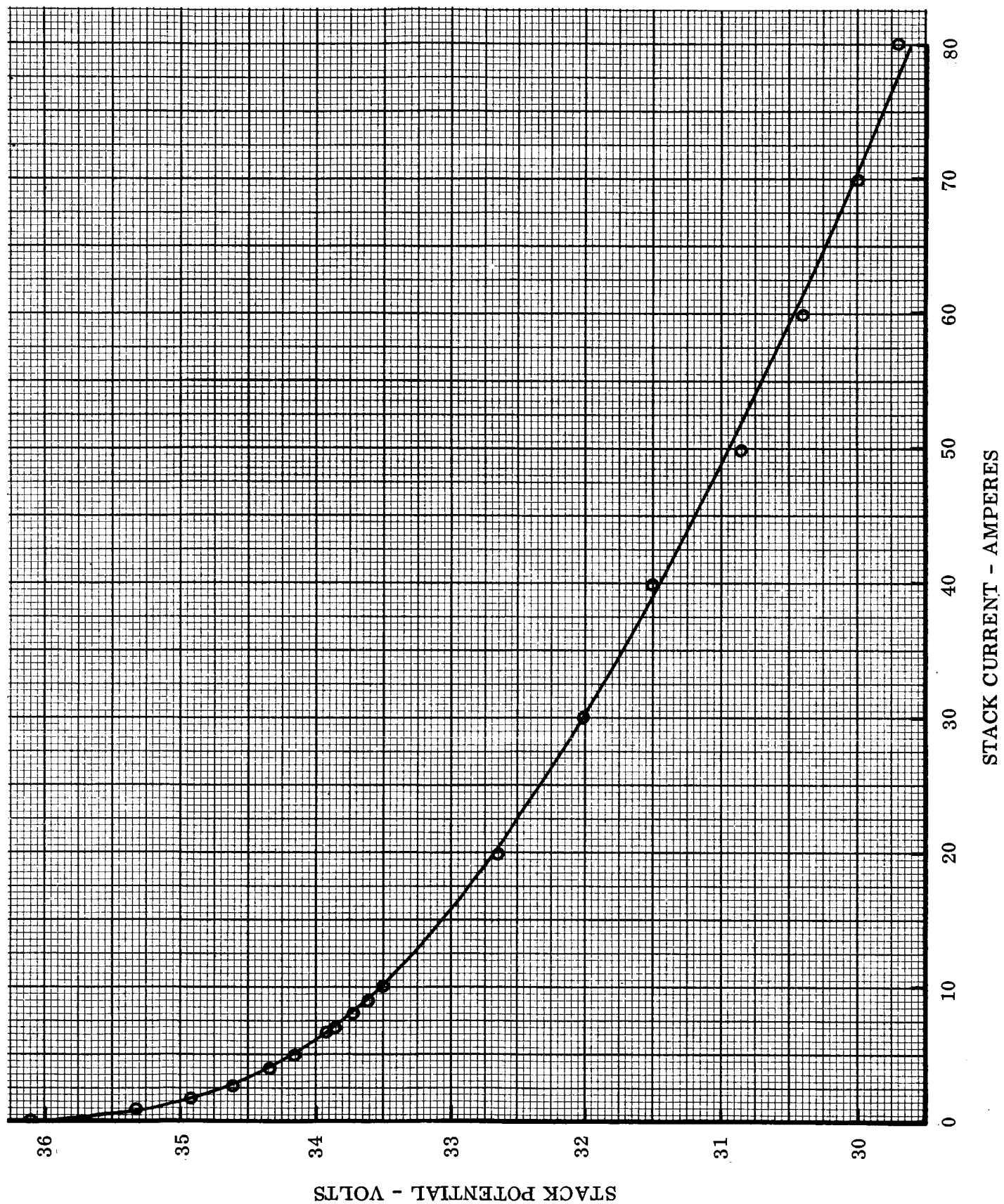


Figure 7B. Acceptance Test VA Curve - Stack 136

Stack Temperature  $190 \pm 2^{\circ}\text{F}$   
 Reactant Pressure  $37 \pm 1 \text{ psia}$   
 KOH Concentration See Table

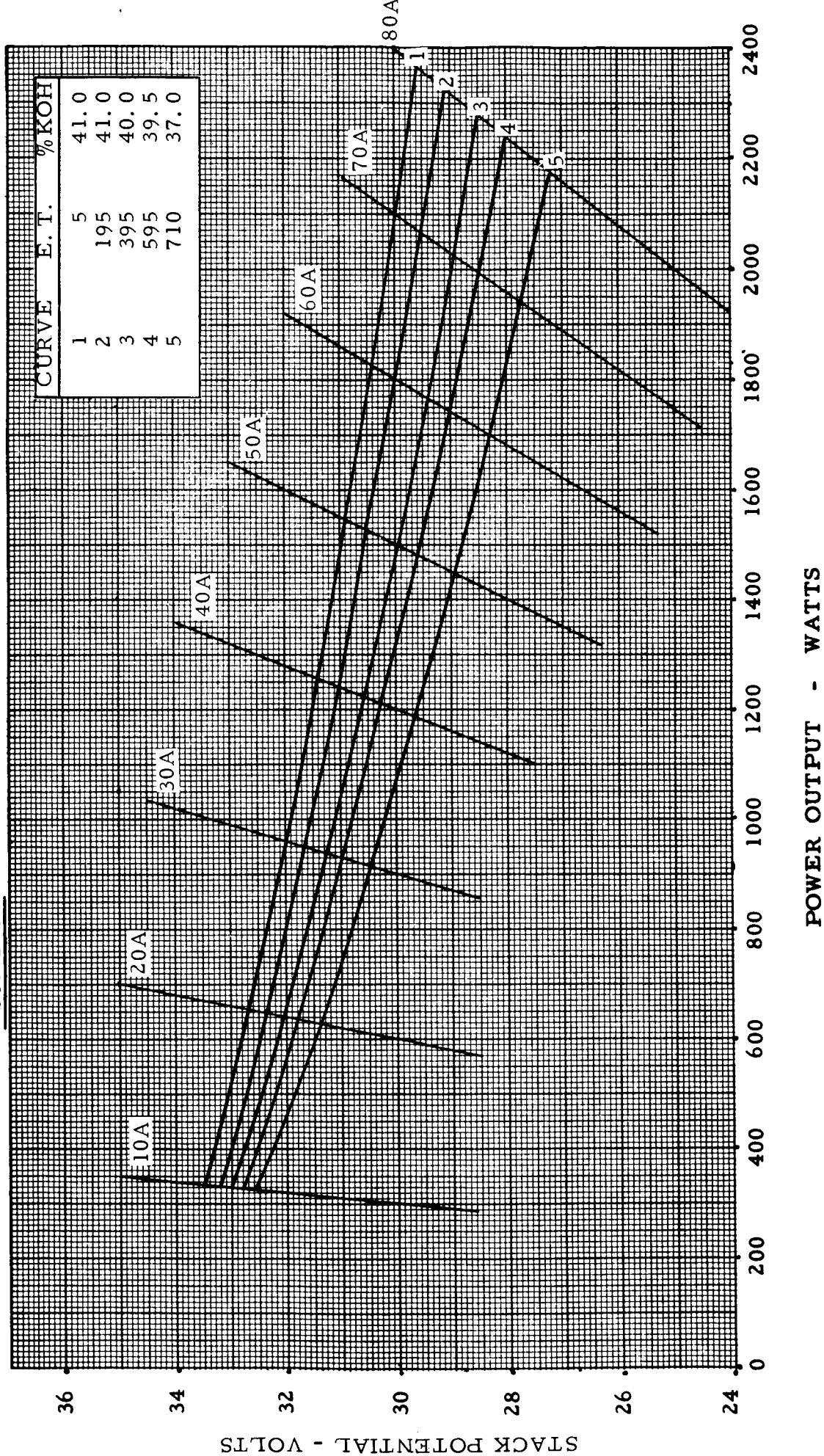


Figure 8. Performance Curves - Stack 136

operation of the stack developed crossleaks which could not be sealed. Stack 133 accumulated 1082 hours of continuous operation while experiencing crossleaks. There are two basic improvements in the construction of Stack 136 (Group II) over Stack 133 (Group I). First, a series of conical washers were affixed to the Group II stacks between the stud bolts and the top end plate, applying constant compression to compensate for stack relaxation. Second, the Group I stacks were wet stacked. During fabrication electrolyte was applied to each asbestos matrix as the particular piece was inserted into the stack. Testing of the Group I stacks has shown that the quality of the electrolyte that could be added to the stack by this method was insufficient. The anodes, during fabrication, are relatively water repellant. However, during operation the current draw on the electrodes destroys the repellancy of the anodes, which then demands an increased supply of electrolyte. This additional volume of electrolyte can be supplied by altering the operational parameters (increasing the water cavity pressure) to dilute the electrolyte. If the quantity (weight) of potassium hydroxide is unaltered, the dilution will provide the additional volume required by the electrode. This increased demand for electrolyte can be observed by noting the rapidly changing optimum KOH concentrations of the Group I stacks (see Figure 9).

A compounding problem, caused by the inherent nature of the anodes, also exists. The 66 anodes in a 2 kw stack do not lose their water repellancy in unison. Hence, there are varying demands for the degree of electrolyte dilution which cannot be simultaneously satisfied because each section is operated at the same water cavity pressure. During "conditioning" of the fuel cell electrodes some cells are therefore operating "dry" (at a higher electrolyte concentration than the particular section demands) while others are operating "wet". The cells that are operating dry are particularly susceptible to crossleaks, while the cells that are operating wet show a slightly reduced performance. Very wet cells show pronounced voltage changes during purging, which for a short period of time evaporates some water and artificially and temporarily reduces the electrolyte volume.

In addition, very wet cells may physically lose electrolyte by ejecting droplets of KOH solution out of reach of the electrodes (i.e. droplet formation on the fuel cell plates themselves). This irreplaceable loss of potassium ions is detrimental to fuel cell life. Because of the different characteristics exhibited with operating cells too wet or too dry, all stacks of this program have been operated (whenever possible) at electrolyte concentrations 1 percent below the optimum; i.e. slightly wet. Occasionally, the performance of one or two sections in the stack required stack operation at percentages that differ from that specified above. It is therefore important to prevent wide variation of electrolyte concentration from cell to cell.

The anodes being used at present produce the highest possible voltage and hence efficiency of all known available anodes, so that changing anodes is inadvisable.

Single cell tests conducted under another Contract NAS8-20573 have been used to establish two methods of overcoming this problem. Both methods are means of forcing the anodes to accept electrolyte before initial operation as a fuel cell. These methods have been termed "preconditioning" and "dry stacking-vacuum loading". In the former, the bare electrodes are placed in a jar which is subsequently evacuated of air, filled with electrolyte, and pressurized back to atmospheric pressure. When the anode is removed from the jar, it retains the electrolyte that was forced into it. The stack would then be built using the wet stacking method.

# LEGEND



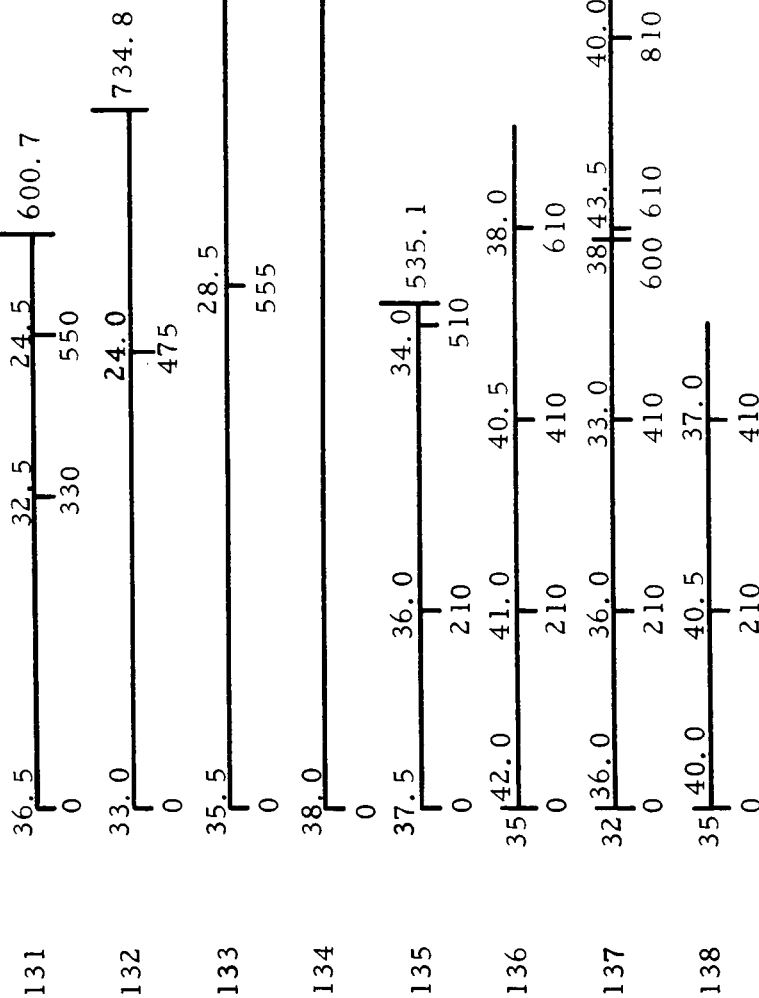
A = % KOH used to flush stack

B = Time at which A or C occurred

C = Optimum % KOH concentration

D = Time at end of test

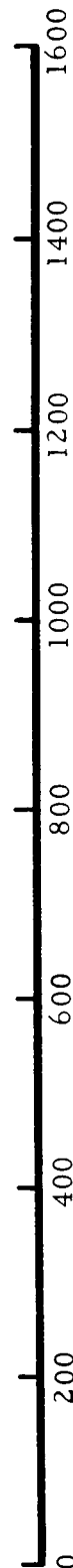
## Stack



Stacks 131 thru 135 were wet stacked with 40 % KOH.

Stacks 136 and 138 were dry stacked and flushed with 35 % KOH.

Stack 137 was wet stacked with 40 % KOH, then flushed with 32 % KOH.



ELAPSED TIME IN HOURS

Figure 9. Optimum Electrolyte Concentrations

The vacuum loading technique uses the same principle except that the entire stack is fabricated dry. The stack is then evacuated, filled with electrolyte, repressurized, and drained of excess electrolyte. The effect of the two methods of force wetting the anodes is identical. The dry stacking-vacuum loading method was chosen for the Group II stacks because of its relative simplicity.

Stack 136 was optimized with respect to KOH concentration according to the schedule and at the percentages noted in Figure 9. Voltage-power characteristics for the 700 hour period are given in Figure 8. During this time the stack voltage degraded at a rate of 76 microvolts per hour per section. It is significant that during this period no crossleaks were identified for any sections.

During the initial operation of Stack 136 (and, in general, for all Group II stacks) a problem arose which is believed to be associated with the vacuum loading technique. Occasionally, during operation, a few sections began decreasing in voltage at a constant rate. A purge restored the voltage, only to have the voltage again drop off at about the same rate. The rates vary from section to section but remain fairly constant for any one section. The stacks were subjected to unrestricted purges (where the purge flow rate is equal to approximately a 400 amp stoichiometric flow as compared with the 200 amp flow of a normal purge) and depressurization purges (where the load is dropped, reactant pressure bled to atmospheric and repressurized to the normal 37 psia, and the load reapplied). These more severe purge modes had the effect of restoring low cells to more respectable voltages where they remained stable. It is possible that after loading and draining the Group II stacks, droplets of electrolyte were still clinging to the fuel cell plates and manifolds, and during operation these droplets lodged in the inlet or outlet EDM ports of the reactant gas plates. Blockage of this sort would result in abnormal accumulation of inert gases leading to the gradual voltage dropoff observed. The severe purges might then have the effect of dislodging the droplets, in which case the section would resume its normal operation.

The major conclusions drawn from the testing of this stack are the increased stability of all 33 sections of the stack and the total absence of crossleaks. Both are affected by the improved electrolyte loading technique and the use of stack compression devices.

Continued testing of this stack beyond March 20, 1967, will be reported under Modification 18 of NAS8-2696.

### **Thermal Cycle Test - Stack 137**

Acceptance Test. - Stack 137 was wet stacked with 40 percent KOH according to Group I procedures because the vacuum loading technique had not yet been developed. Stacks 136 and 138 were vacuum loaded with a 35 percent KOH concentration using the newly developed technique. Stack 137 was then vacuum loaded according to the Group II procedures, except that it was loaded with 32 percent KOH to compensate for the original 40 percent KOH. The optimum KOH concentration determined during the acceptance test was 36.0 percent, as shown in Figure 10. In general, the Group II stacks optimized at approximately 5 percent higher than the concentration at which they were vacuum loaded. The volt - ampere characteristics for operation at 35% KOH is shown in Figure 11.

Performance Evaluation Test. - Stack 137 has accumulated 887 hours elapsed on-load time. Voltage-power characteristics taken at the beginning and end of the 200 hour performance evaluation test are shown by the first two curves of Figure 12. The blockage of some EDM ports by droplets of electrolyte, as discussed previously, was first noted on Stack 137 because this was the first vacuum loaded stack to be tested. Identification and correction of this condition was accomplished throughout this 200 hour test. During this time the stack voltage degraded at a rate of 92 microvolts per hour per section.

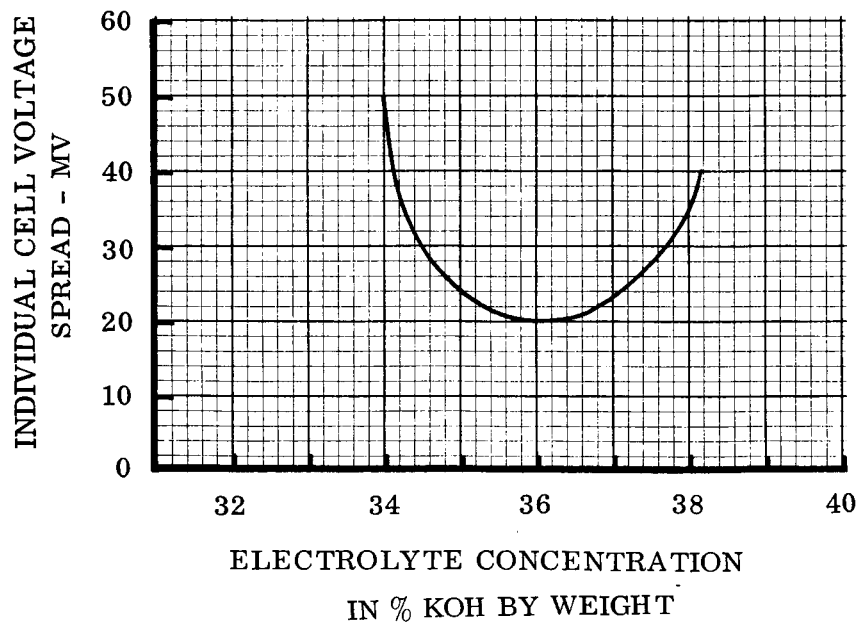
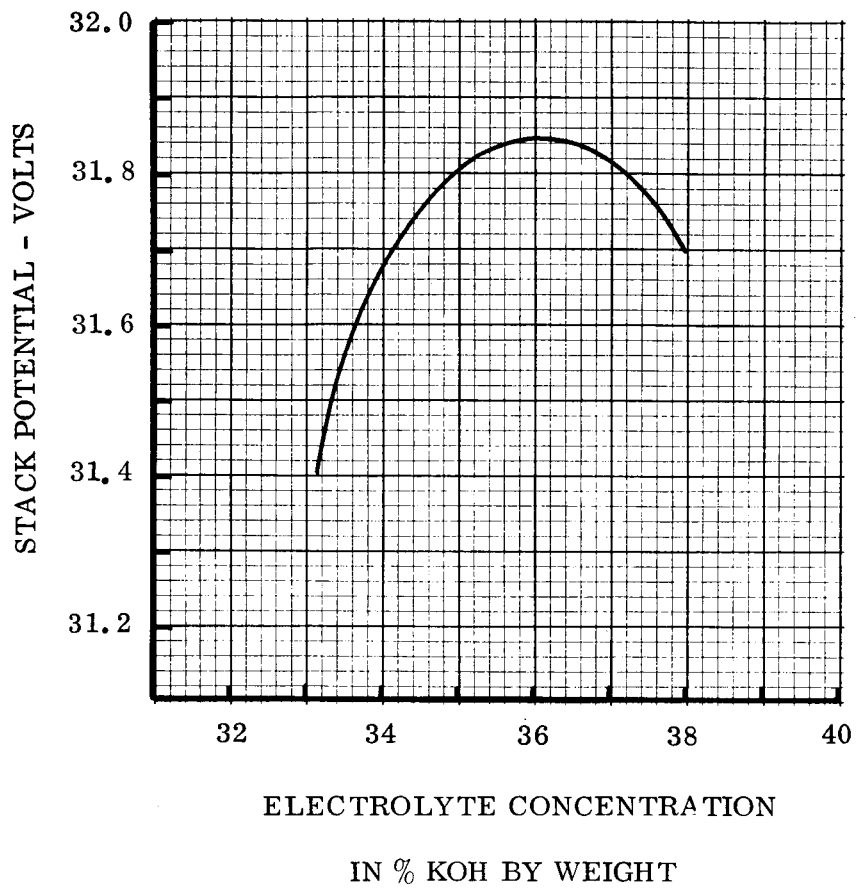


Figure 10. Acceptance Test KOH Optimization - Stack 137

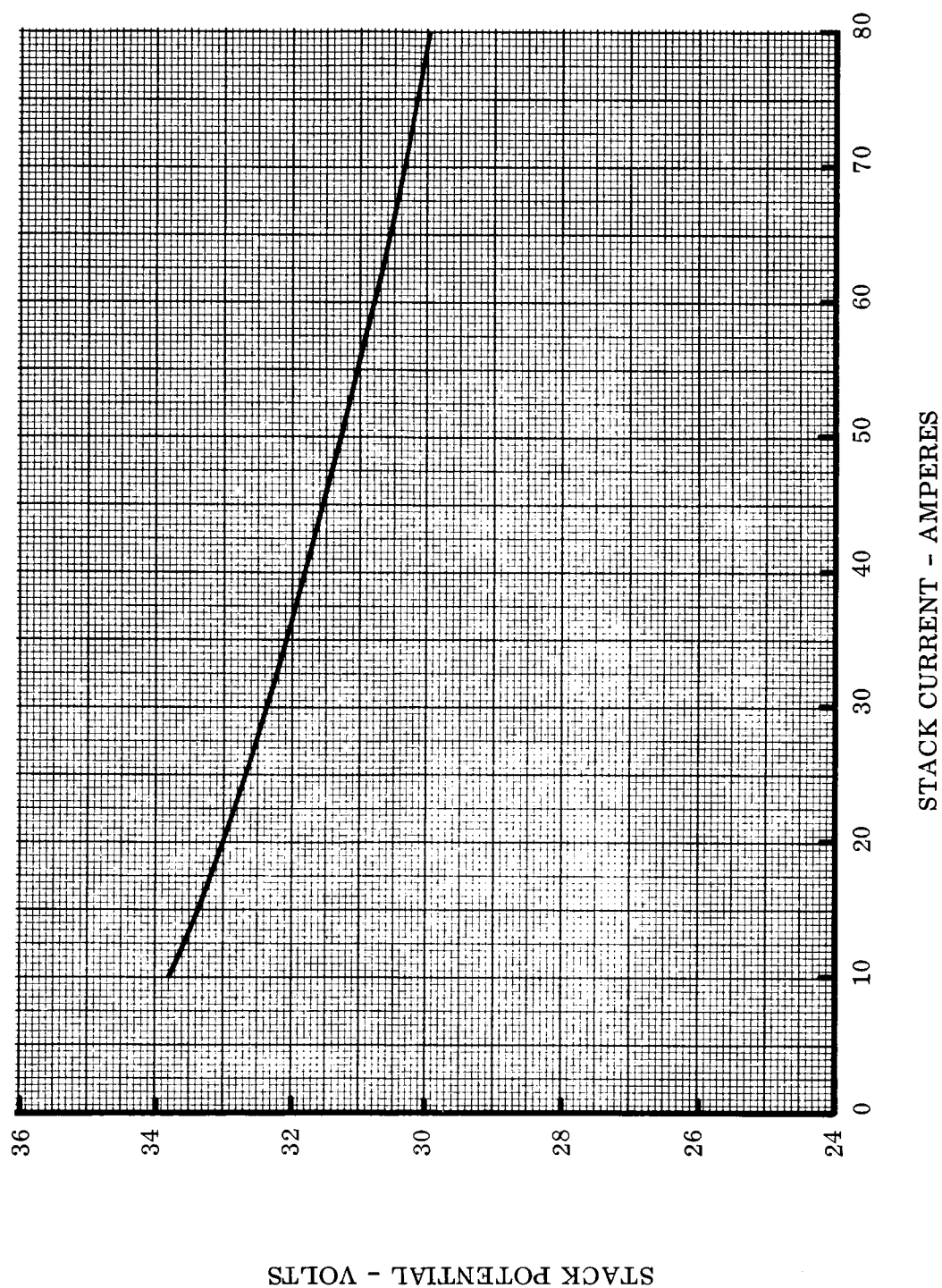
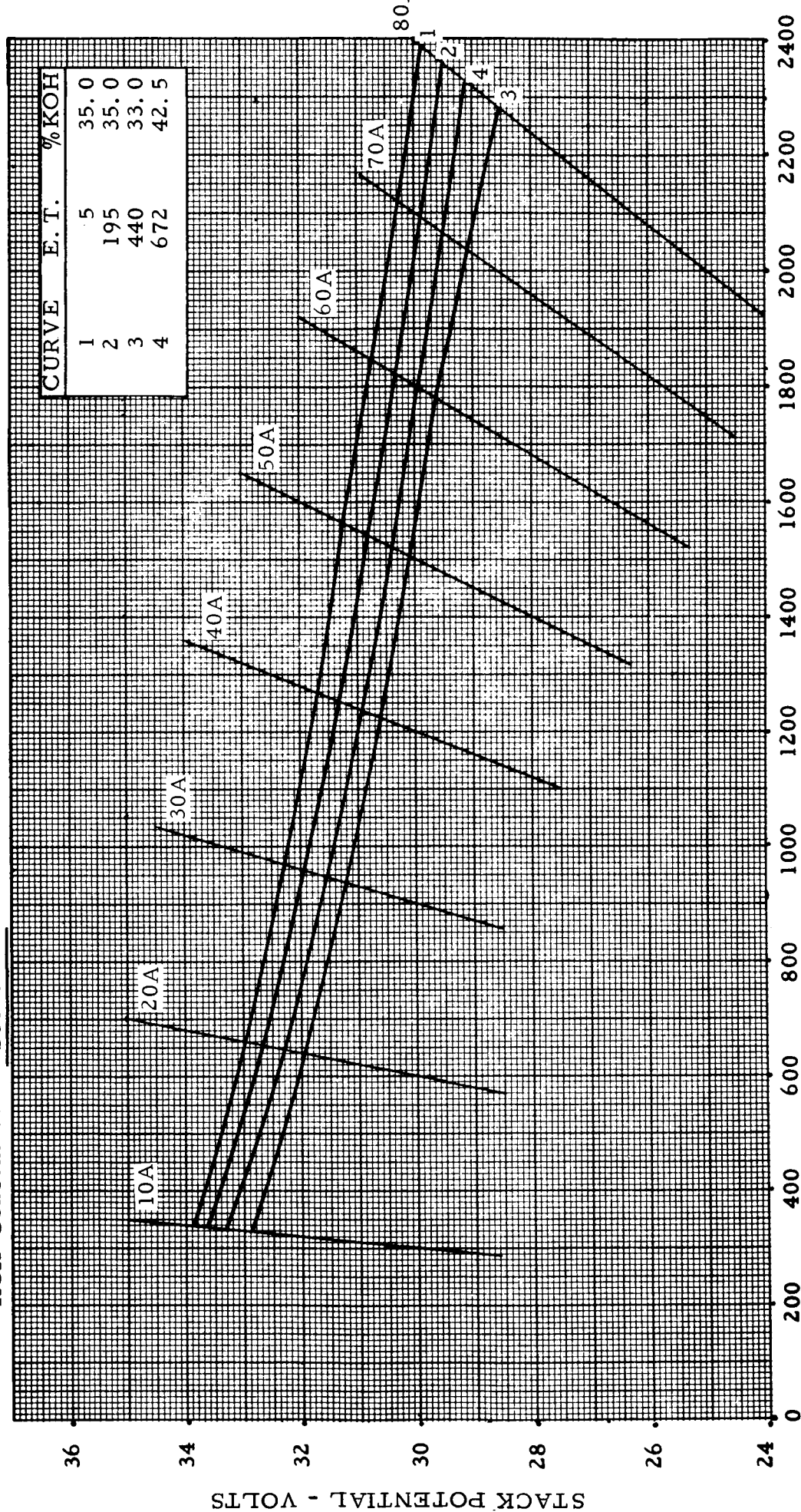


Figure 11. Acceptance Test VA Curve - Stack 137

Stack Temperature  $190 \pm 2^\circ\text{F}$   
 Reactant Pressure  $37 \pm 1$  psia  
 KOH Concentration See Table



STACK OUTPUT POWER - WATTS

Figure 12. Performance Curves - Stack 137

Thermal Cycle Test. - This test has three main objectives:

1. Investigate the variation of electrolyte concentration as a function of temperature cycling.
2. Determine voltage - power characteristics as a function of temperature in the 160 to 220° F range.
3. Determine the life characteristics of low temperature operation.

In pursuit of the first objective, Stack 137 was permitted to cycle in a 14°F temperature band during the time period ET 450 to 600 hours. During the warmup portion of the temperature cycle the liquid coolant does not flow and the stack is heated by its own heat of reaction. When the high temperature limit is reached, the coolant is turned on and the stack is cooled to the lower temperature limit. With the stack producing 80 amperes, the stack temperature and water cavity pressure were measured using a strip chart recorder. The corresponding electrolyte concentration can be calculated from these measurements. The results for a typical thermal cycle are presented in Figure 13, The cyclic variation of electrolyte concentration as a function of temperature and pressure is shown in Figure 14, which provides an indication of the effectiveness of the EMCS in controlling electrolyte concentration. During the entire 14°F temperature swing the electrolyte concentration remained within the acceptable band of  $\pm 1\%$  KOH by weight. The stack, in conjunction with the electrolyte control subsystem, therefore accepted a large temperature excursion without harmful effect.

By ET 600 hours, the optimum electrolyte concentration of Stack 137 had decreased to 33 percent KOH by weight. (See Figure 9.) The volume of electrolyte contained in the anode-cell matrix-cathode sandwich may be altered by changes in the operating temperature and water cavity pressure. The increased controllability of electrolyte volume associated with high electrolyte concentrations is desirable. Stack 137 was refilled at ET 600 hours with 38 percent KOH by weight and optimized at 43.5 percent KOH.

From ET 620 to 680 hours, Stack 137 was operated at seven temperature levels between 160 and 220°F. The voltage-power characteristics of Stack 137 as a function of temperature are shown in Figure 15.

At ET 680 hours, Stack 137 began a life test at 165°F. The objectives of this test are to establish the performance characteristics of low temperature operation and to provide support information for low temperature, low power testing to be conducted under the follow-on effort of this contract. During the 200 hours that Stack 137 has been at 165°F, the stack voltage has degraded at a rate of 76 microvolts per hour per section. The degradation rate at 190°F was 80 microvolts per hour per section. The voltage-power characteristics for Stack 137 at 165°F are shown in Figure 16. Continued testing of this stack beyond March 20, 1967, will be reported under Modification 18 of NAS8-2696.

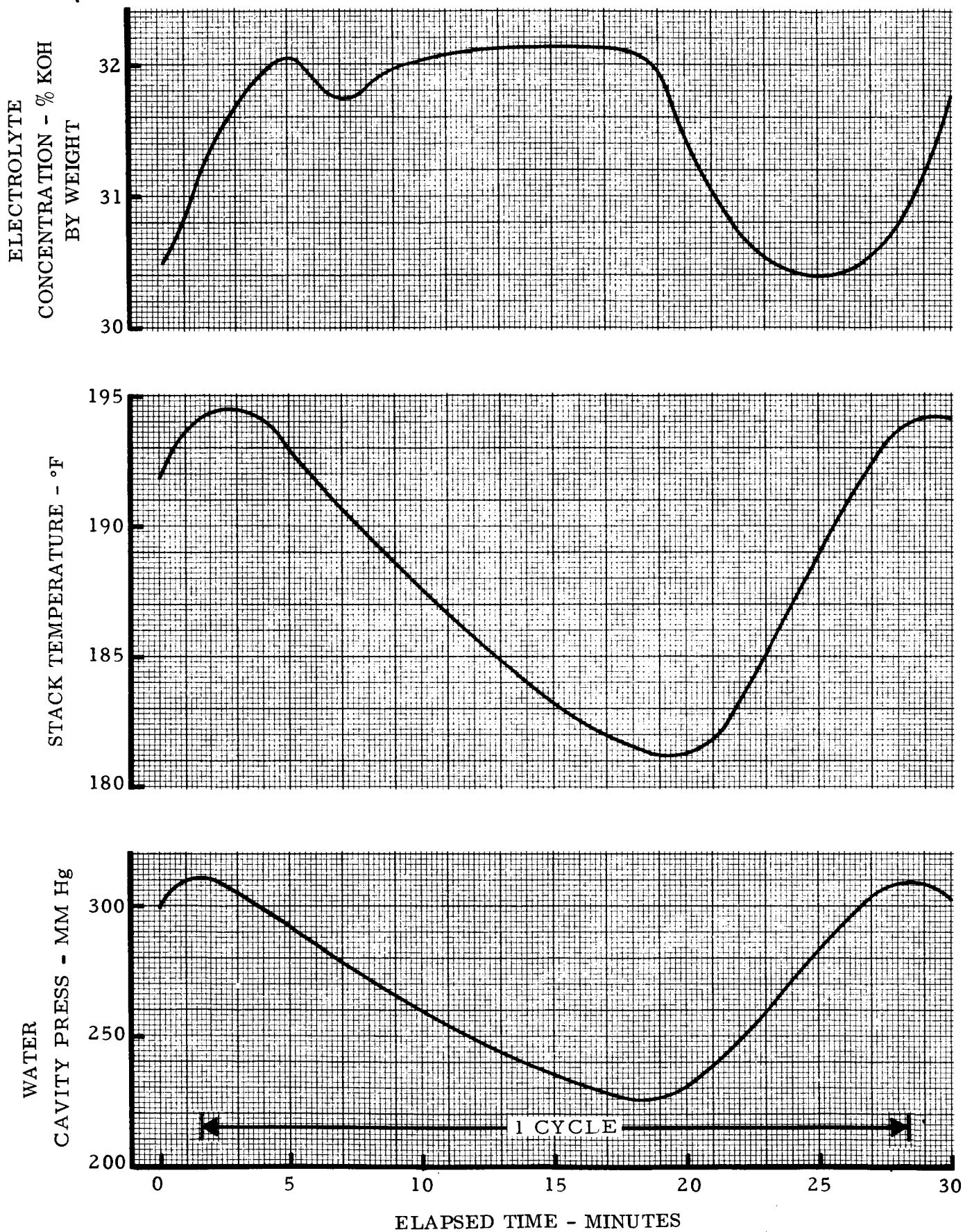


Figure 13. Temperature Cycle Test - Stack 137

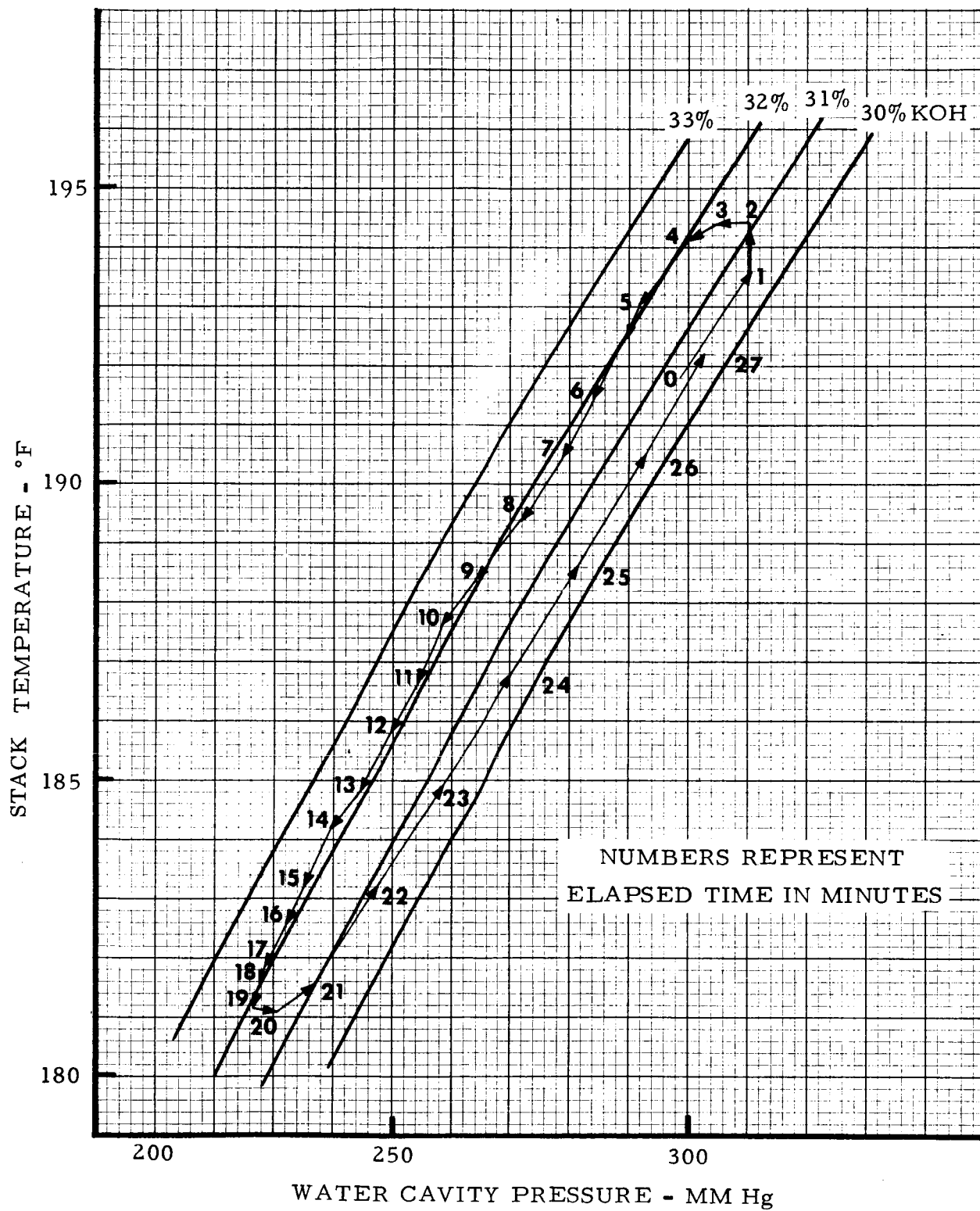


Figure 14. Temperature Cycle Test at 80 Amps - Stack 137

Stack Temperature    See Table  
 Reactant Pressure    37 ± 1 psia  
 KOH Concentration    42.5 %

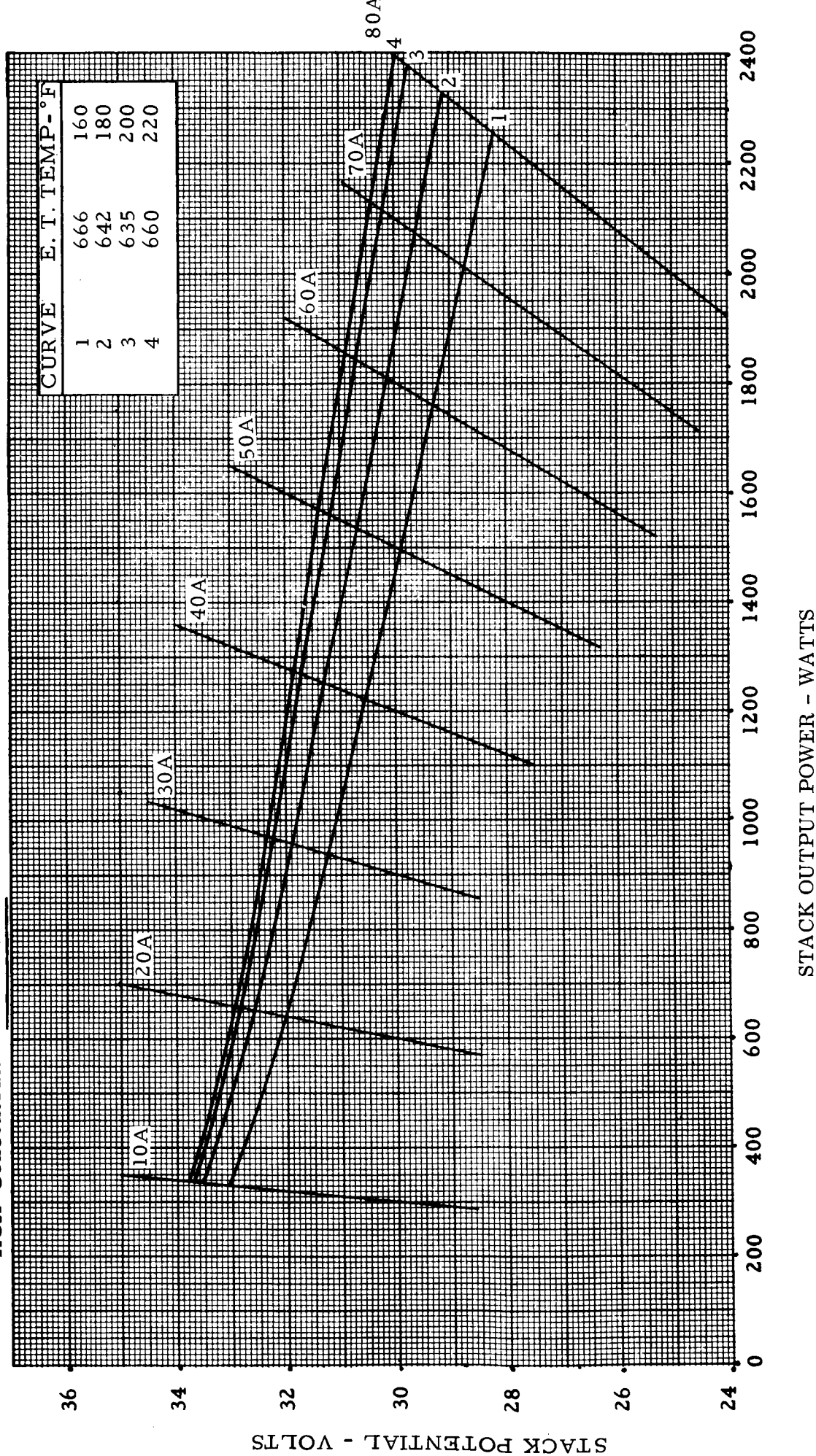


Figure 15. Performance Characteristics as a Function of Temperature - Stack 137

Stack Temperature  $165 \pm 2^{\circ}\text{F}$   
 Reactant Pressure  $37 \pm 1 \text{ psia}$   
 KOH Concentration See Table

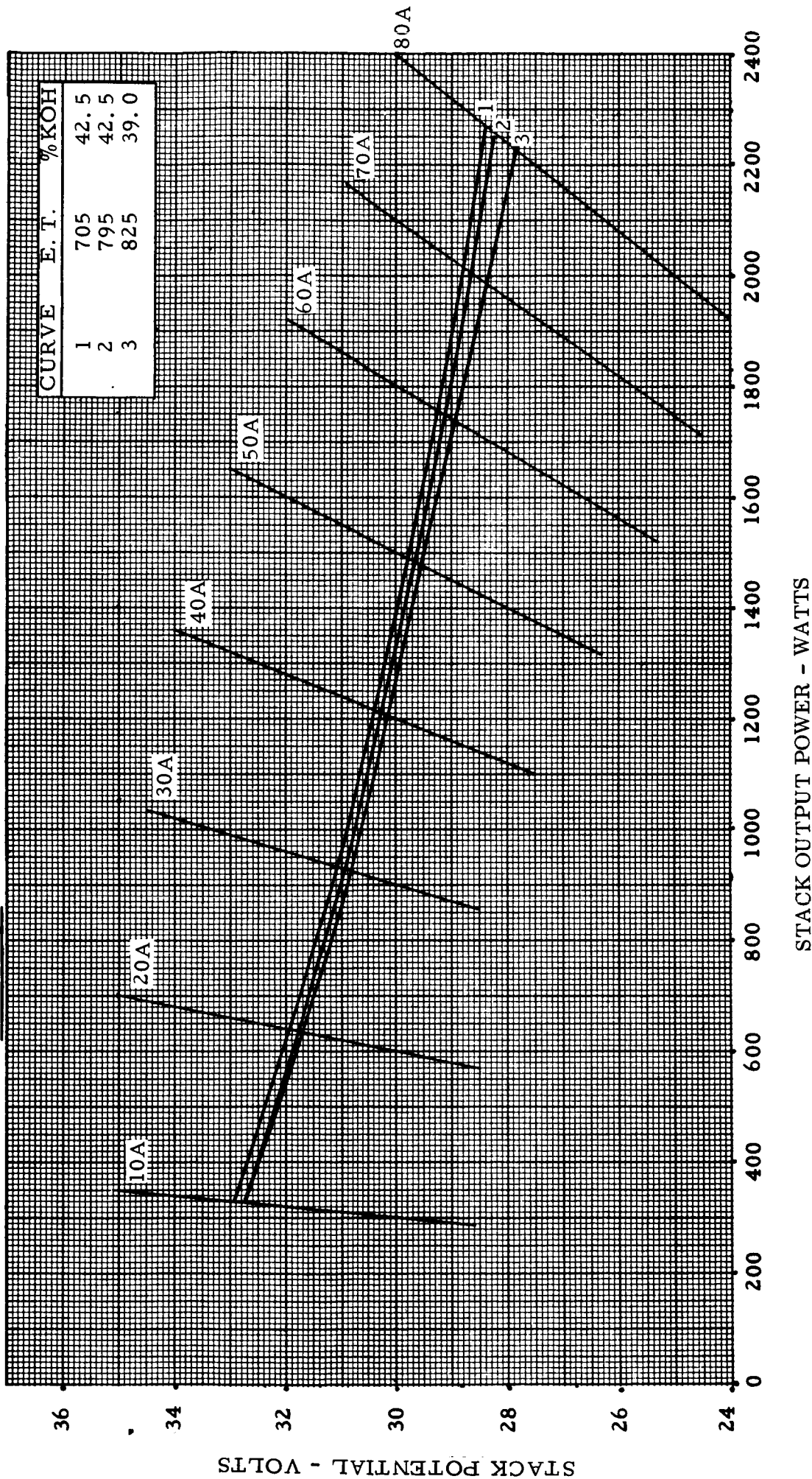


Figure 16. Performance Characteristics at  $165^{\circ}\text{F}$  - Stack 137

## High Power Life Test - Stack 138

Acceptance Test. - Stack 138 has completed its acceptance test. The optimum electrolyte concentration was determined to be 40 percent KOH by weight, as shown in Figure 17. The volt-ampere characteristic for operation at 39 percent KOH is shown in Figure 18.

Performance Evaluation Test. - Stack 138 has accumulated 515 hours of elapsed on-load time. Voltage-power characteristics taken at the beginning and end of the 200 hour performance evaluation test are shown by the first two curves of Figure 19. During this period the stack voltage degraded at a rate of 74 microvolts per hour per section.

High Power Life Test. - Stack 138 was originally scheduled for a 500 hour Water Removal Unbalance Test (RA-WR-8). However, information obtained from testing the other stacks under this program is sufficient to satisfy the objectives of test RA-WR-8. Therefore, Stack 138 has been rescheduled for a High Power Life Test of 1300 hours duration.

The electrolyte wetting problems associated with the anode were evident on the Group I stacks, as was discussed previously in this report. A solution to this problem is currently being evaluated using the Group II stacks. Reoptimization of the Group II stacks every 200 hours will provide more information on the changes in electrolyte concentration as a function of time than could have been accomplished with the RA-WR-8 test.

The load profile to be used for the High Power Life test is shown in Figure 20. the average output will be over 2 kw. This profile will be repeated as necessary to determine high power life capabilities.

Voltage-power characteristics for Stack 138 over the range of 0 to 3 kw are shown in Figure 21. The stack voltage degradation rate for the high load period already performed (ET 200 to 515 hours) and for the entire test period (0 to 515 hours) are 52 and 63 microvolts per hour per section, respectively.

This stack has provided an average power output of over 2 kilowatts for more than 300 hours and has performed at least as well at the high power level as any stack of this same design has at the one kilowatt level.

Continued testing of this stack beyond March 20, 1967, will be reported under Mod 18 to Contract NAS8-2696.

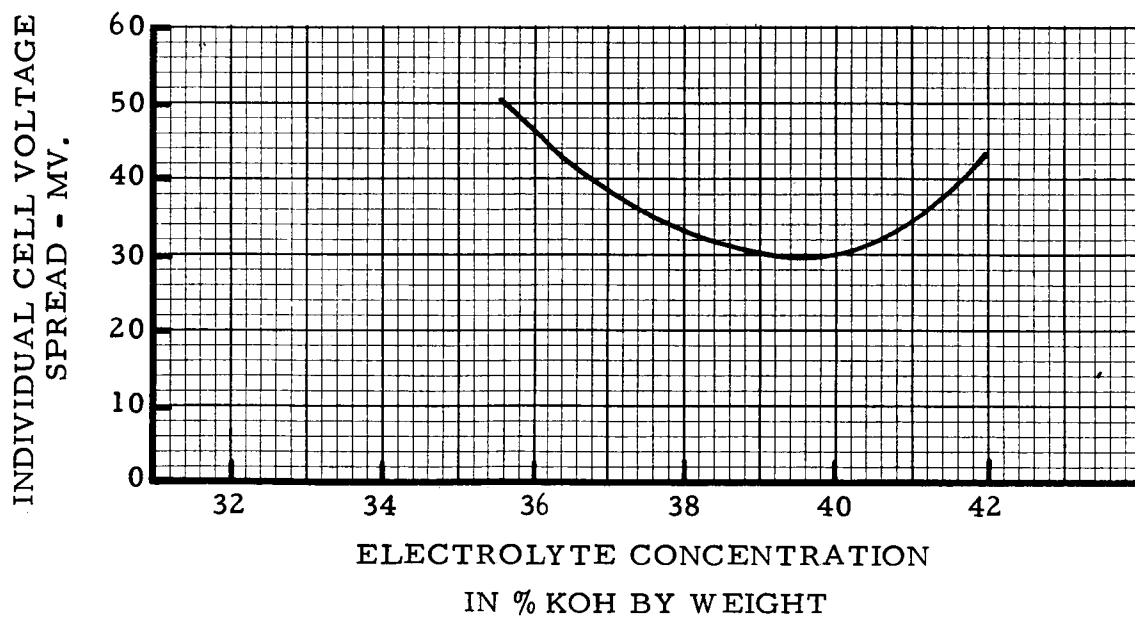
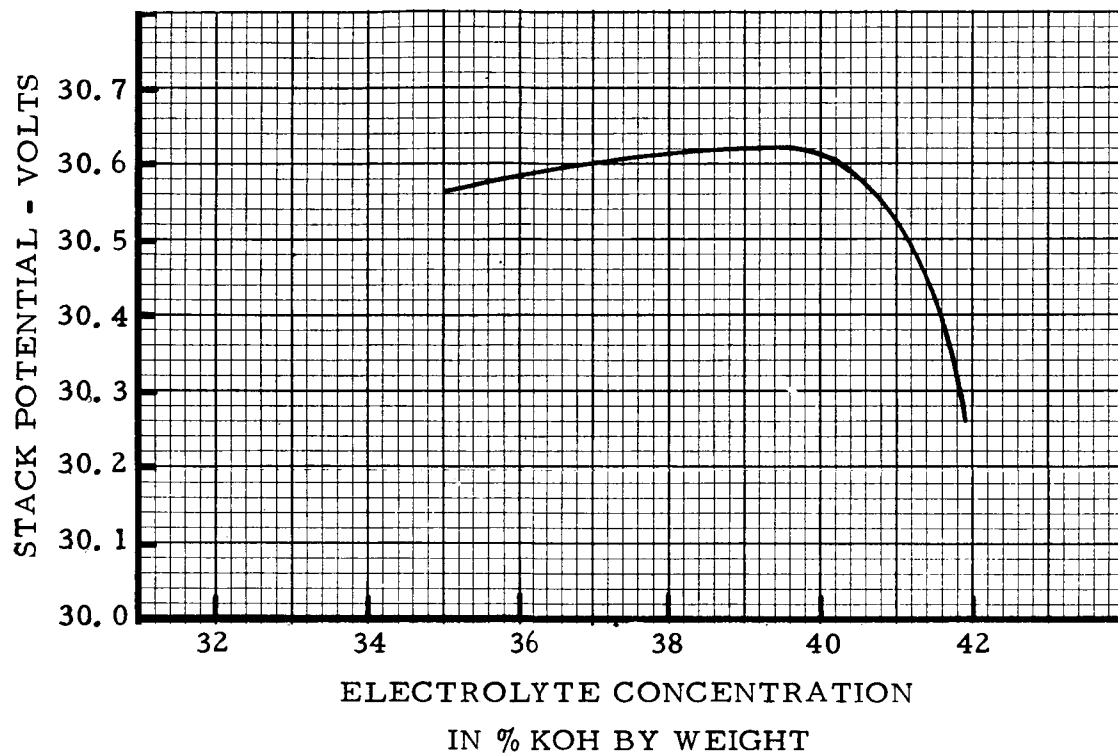


Figure 17. Acceptance Test KOH Optimization - Stack 138

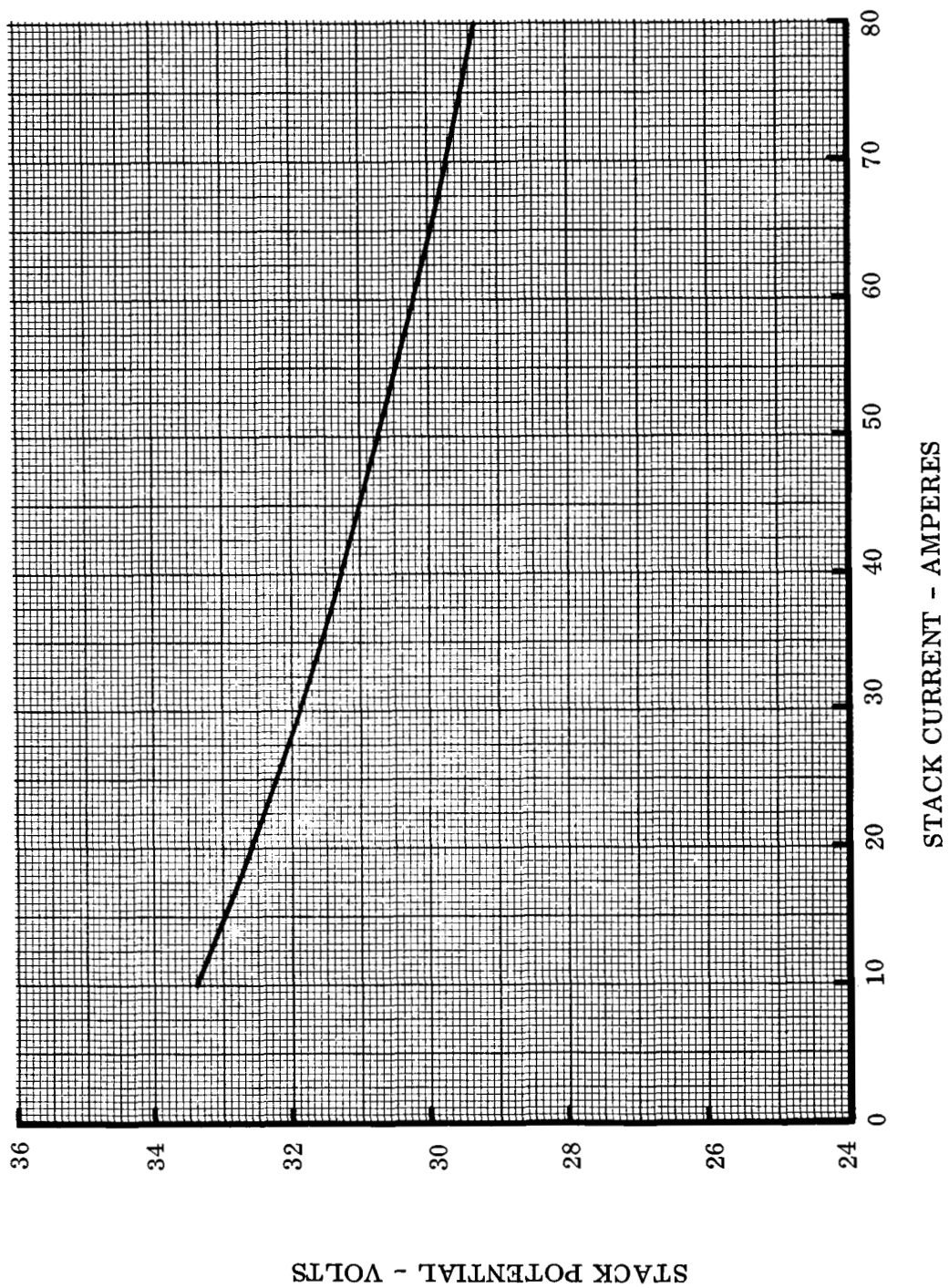
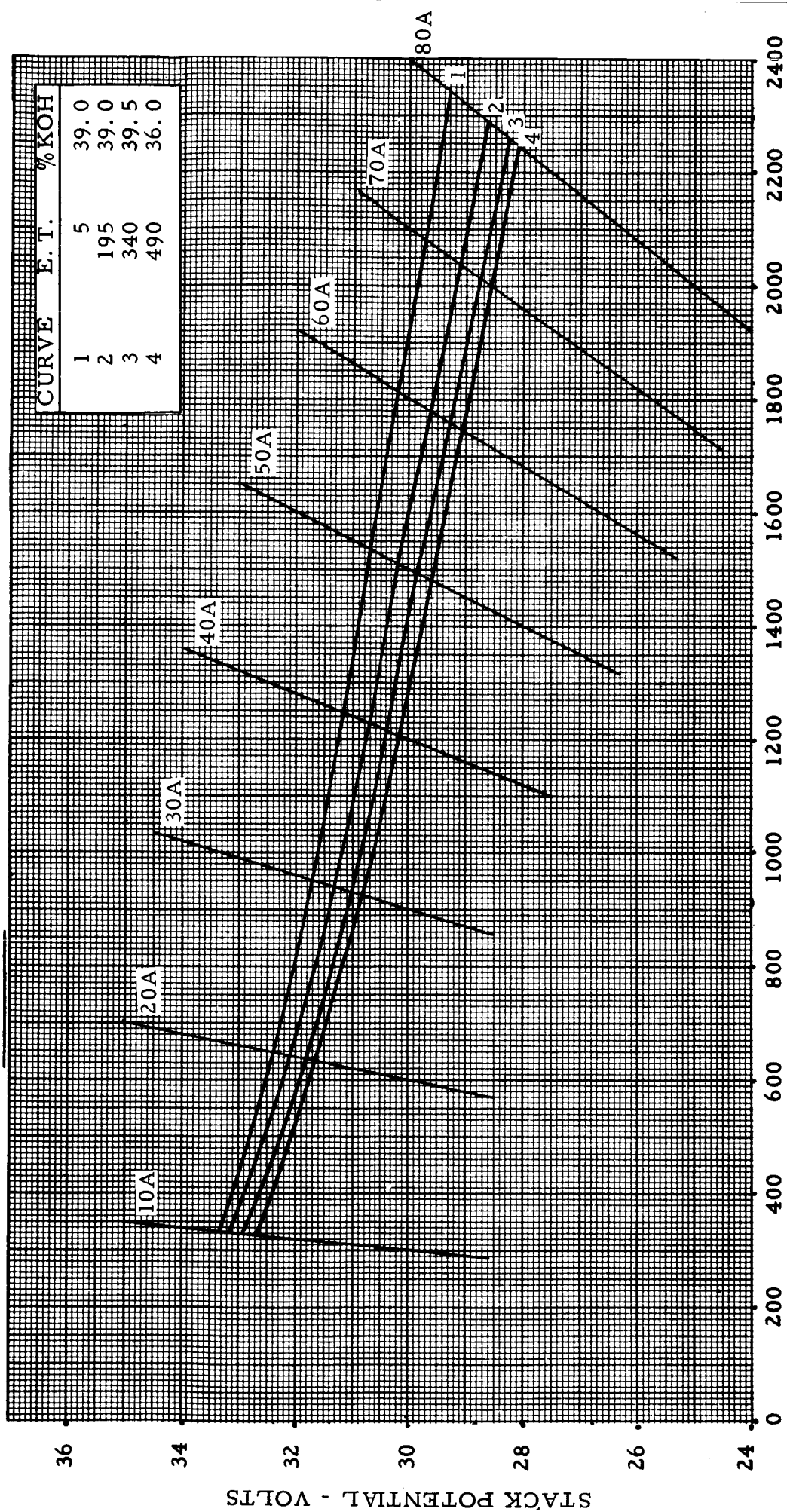


Figure 18. Acceptance Test Performance - Stack 138

Stack Temperature 190 ± 2 °F  
 Reactant Pressure 37 ± 1 psia  
 KOH Concentration See Table



STACK OUTPUT POWER - WATTS

Figure 19. Performance Curves - Stack 138

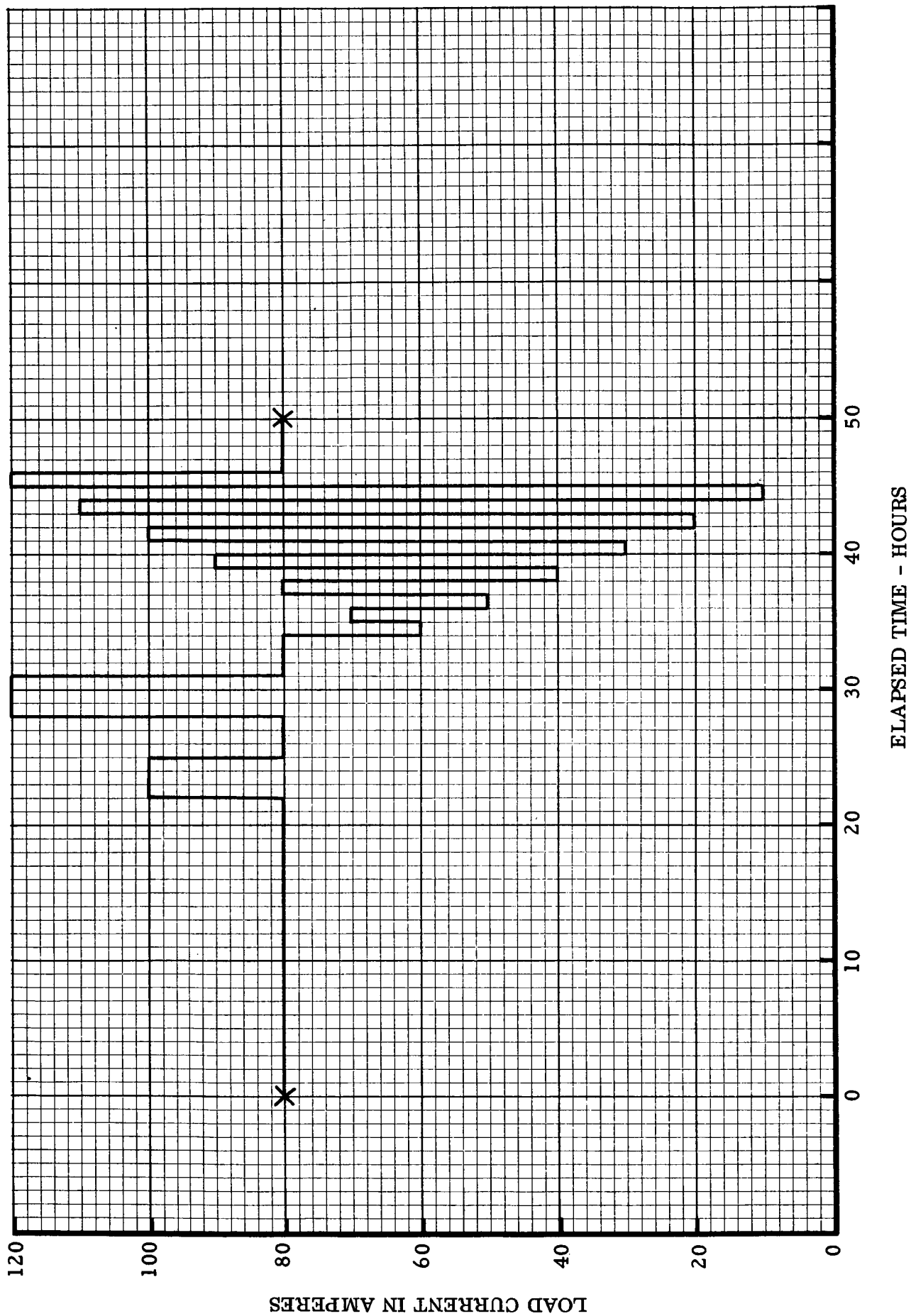
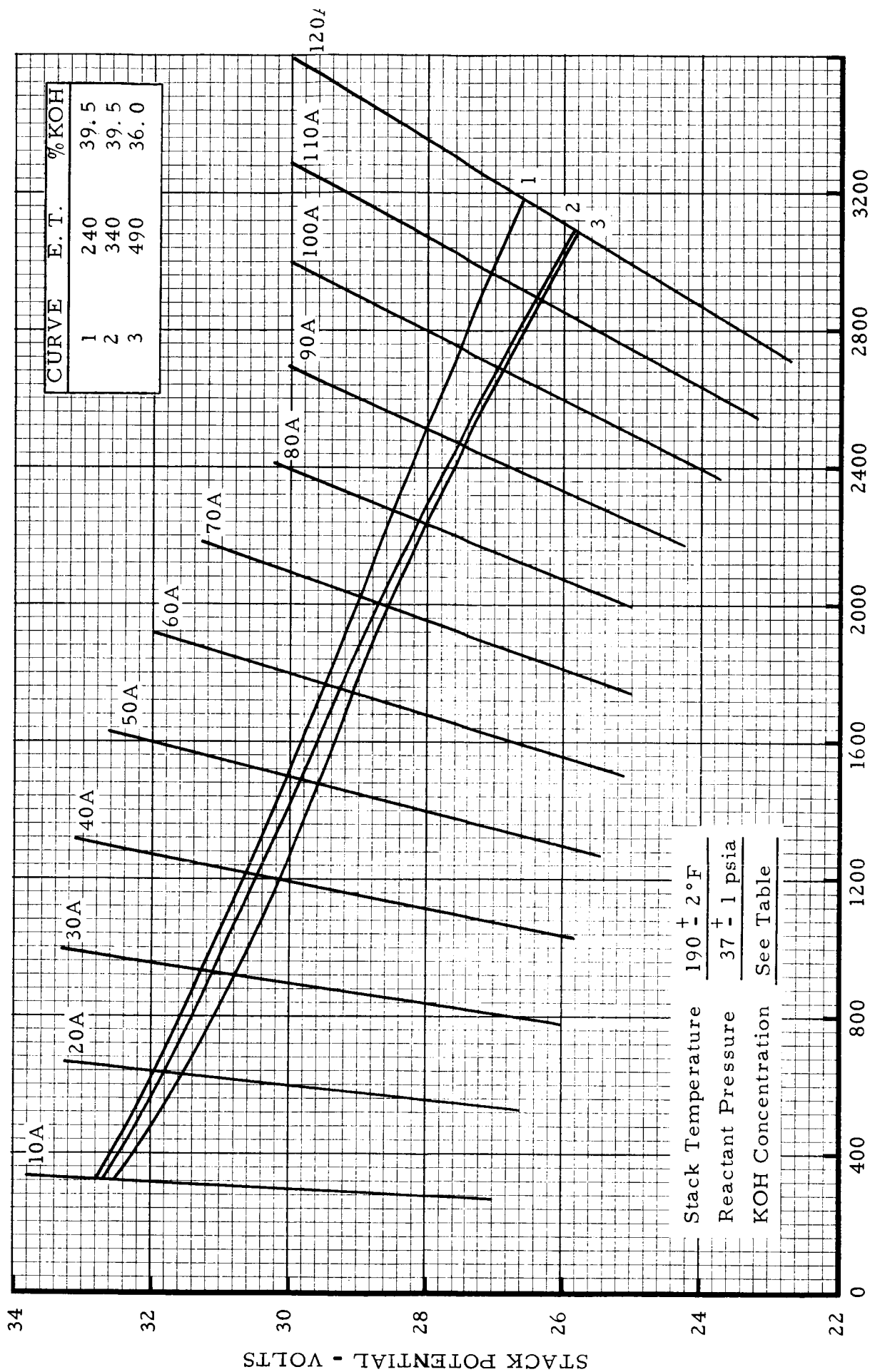


Figure 20. High Power Life Test Load Profile - Stack 138



STACK POWER OUTPUT- WATTS

Figure 21. High Power Life Performance - Stack 138

## DISASSEMBLY ANALYSIS

Stacks 131, 132 and 133 have been completely disassembled. The following is a description of the items of wear that were found on these three stacks. A description of how extensive each of these items is on each particular stack as a function of the operation of the particular stack will also be discussed.

Anode Extrusion. - It was observed that in the region of the hydrogen inlet port the anode material was weakened and actually extruded into the hydrogen plate. This extrusion was found only in the vicinity of the hydrogen inlet port. Drying, which may occur at the hydrogen inlet port, may eventually result in a crossleak between the hydrogen and oxygen plate and thru the anode-cell matrix-cathode sandwich. If a crossleak does occur at that point the reactant gas would be consumed with the production of water and heat but not electricity. Under this condition, that area of the cell would attain a higher temperature than the rest of the cell. It is therefore possible that the high temperature, the continual wetting and drying of the anode in the vicinity of the hydrogen inlet port, and the pressure exerted by the cell asbestos matrix may result in the extrusion of the anode into the hydrogen plate. In some cases the extrusion of the anode through the hydrogen plate extended to the screen on the water removal side of the hydrogen plate, staining the water removal matrix. See Figure 22. This anode disfigurement may have contributed to the crossleaks that developed on Stack 132 (reactant pressure test) and Stack 133 (low power life test). Crossleaks did not, however, result in fuel cell failure or hazzardous operation.

Anode extrusion was most discernable on Stack 131. Stack 131 was subjected to high power outputs where the current exceeded 400 amps for brief periods of time (15 seconds). This type of testing resulted in swift temperature excursions, which may have emphasized the extrusion of the anode. Every section of Stack 131 exhibited this extrusion.

The area affected is approximately 2 square inches. During the testing of Stack 132 the inlet and outlet ports for both reactant gases were interchanged midway during the test. On this stack, the anode extrusion was noted at both the hydrogen inlet port and the hydrogen purge port (which had been used as an inlet for half the test).

The Group I stacks (131 thru 135) were wet stacked. Since the electrodes may not have been less completely filled at the time of fabrication, and because a certain amount of operating time is necessary for the anodes to lose their water repellancy, the Group I stacks may have been particularly susceptible to this extrusion problem. Group II stacks, in which the electrolyte is forced into the anodes may be at an advantage. As of yet an indisputable relationship between crossleaks and extrusion has not been definitely established.

Fuel cell systems to be built in the future under other contracts will employ remedies for this problem. This new vacuum loading procedure prevents crossleaks. (See page 19.)

Cathode Extrusion. - An extrusion of the cathode into the oxygen cavity was noted at the oxygen inlet. The extent of cathode extrusion is relatively minor. It has been observed in about 10 percent of the cathodes during stack disassembly.

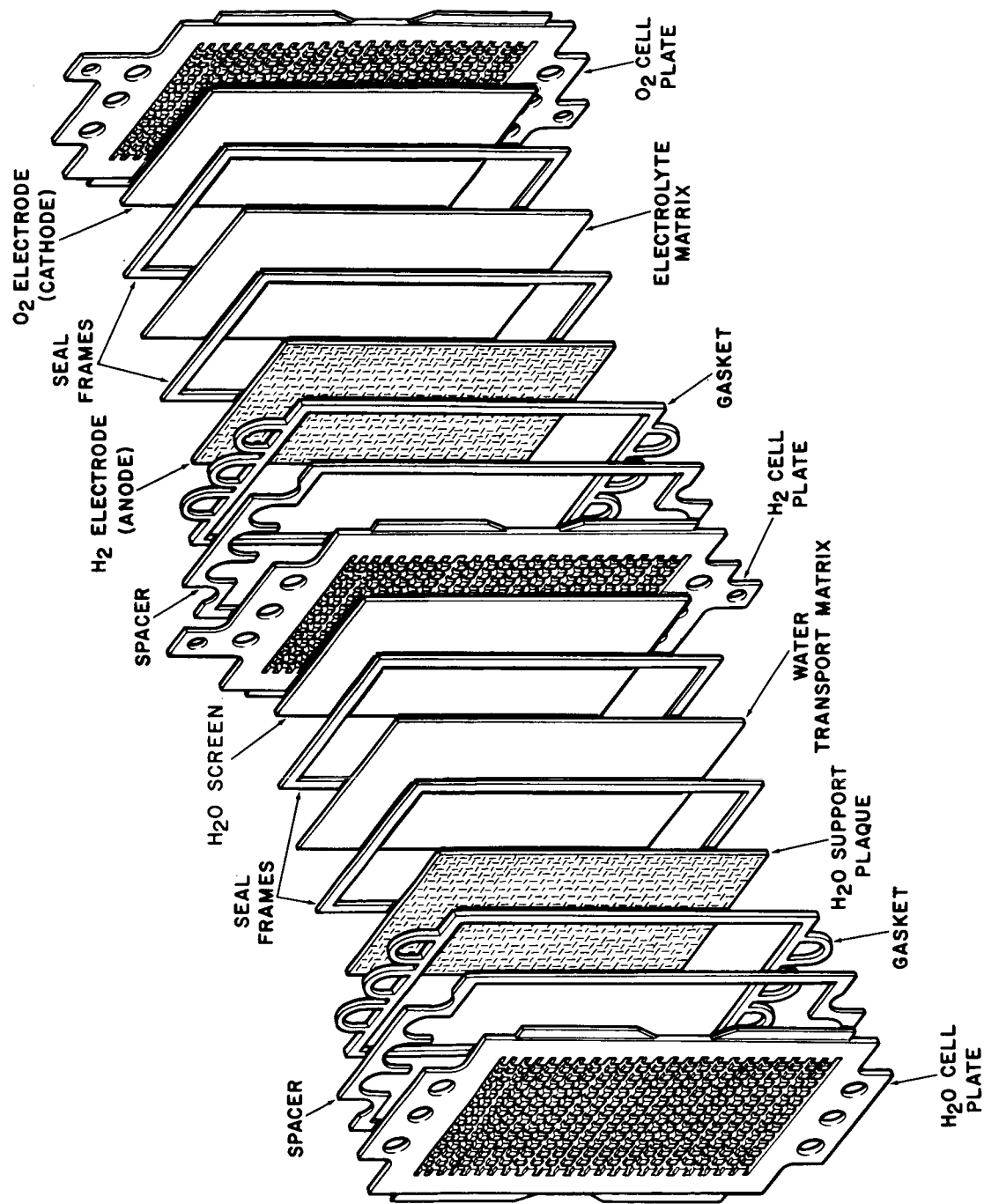


Figure 22. Fuel Cell Construction

Discoloration and Markings. - On Stack 131 every cathode had a portion of the electrode discolored at the oxygen inlet side. The cathode at the top of the stack had half of its area discolored. This discolored area gradually diminished in size progressing down the stack, to about 1 square inch at the bottom cathode. No anodes were discolored. It appears unlikely that the cause of the discoloration is associated with the operation of that particular stack. After completing its test, Stack 131 was held in storage for 3 months before disassembly. Further, the stack was resting on its side during storage. This may or may not be associated with the discoloration. At present, the cause is unknown.

Also, in Stack 131, three cathodes were found to be spotted at the cell matrix interface. The same random pattern of spots were also found on the adjacent cell matrix. Evidently the spots developed on one component and stained the other. The spots ranged in size from barely visible to 3 mm in diameter. The cause is unknown. Test data will be examined to determine if any unusual performance is associated with the three sections having the spotted cathodes.

Corrosion. - When the fuel cell stacks were prepared for flushing after they had accumulated several hundred hours of operating time, removal of the gas and water manifold at the bottom end plate exposed a deposit at the bottom of the oxygen purge port. Analysis of these deposits showed them to be various hydrates of KOH along with small quantities of nickel, copper and magnesium, and trace quantities of other elements used in the stack. Stack disassemblies have shown these same corrosion deposits throughout the entire oxygen purge manifold. This manifold is highly susceptible to corrosion. It is coated with a thin film of KOH which provides an electrical path between sections; it has an abundant supply of oxygen; and the surfaces of the manifold are not well plated because the manifold holes are punched and are not always smooth. The bottom water plate usually shows the most severe corrosion because of the high potential drop ( $\approx 30$  volts) between the bottom section and the bottom end plate. The oxygen inlet manifold is relatively corrosion free due to the dry incoming reactant gas which inhibits the formation of the KOH film.

Several methods that can be employed in future stacks to inhibit corrosion are reaming of fuel cell plate manifold holes to provide a better plating surface, reversing the electrical output leads to eliminate the 30 volt drop to the bottom end plate, and coating manifolds with a substance which will break up the KOH film into discontinuous droplets.

## ANALYTICAL STUDIES

Effect of KOH Concentration on Stack Degradation. - An analysis was performed on Stacks 133 and 135 to show how KOH concentration influences performance.

The degradation rate of stacks is significantly larger than that of single section modules. This is attributed to the fact that single-section modules are operated at their optimum KOH concentration throughout their life whereas a stack, which is composed of 33 sections, is operated at the average optimum concentration of the combined sections. Thus, at least some of the sections in the stack do not operate at optimum conditions. Other factors affecting stack degradation are stack relaxation, purge port blockage, and KOH loading (wet stacking vs vacuum loading) techniques.

Figure 23 shows how the characteristics of optimum concentration shift with time.  $\Delta V_1$  is the measured voltage decrease if the section is operated at optimum conditions at time  $t_0$  and  $t_1$ , as is the case with single section tests.  $\Delta V_2$  represents the measured voltage decrease if the section is operated wet (at a lower concentration than optimum) and at a constant KOH concentration.  $\Delta V_3$  is the measured voltage decrease if the section is operated dry (at a higher concentration than optimum) at a constant KOH concentration. It can be seen from the figure that operating the section wet produces less of a voltage decrease than the optimum, and dry operation produces a greater voltage decrease.

For purposes of this discussion, the true degradation (or the amount the section has degraded) is defined as the voltage decrease at optimum concentration, which is  $\Delta V_1$ .

$\Delta V_2$  and  $\Delta V_3$  are measured voltage decreases that include the voltage decrease due to degradation (as measured by  $\Delta V_1$ ) plus the effects of operation of non-optimum conditions. The latter is defined as pseudo degradation because it is not a true degradation, rather it is the effect of operating at non-optimum conditions. Measured degradation can then be expressed as

$$\text{Measured Degradation} = \text{True Degradation} + \text{Pseudo Degradation}$$

Pseudo degradation is a function of the optimum KOH concentration at  $t_0$ , the percent KOH at which the section was operated at  $t_0$  (this parameter determines the initial voltage output of the section), the percent KOH at which the final voltage measurement was taken, and the change in optimum percent KOH during the elapsed time interval. It is important to note that the true degradation in no way affects the pseudo degradation.

A determination of pseudo degradation can be made by translating the KOH optimization curve at  $t$ , ( $t > t_0$ ), such that the optimum voltages lie on an equipotential line as shown in Figure 24. The measured degradation is then equal to the pseudo degradation because the true degradation is forced to be zero.

The effect of initial optimum concentration, and the initial and final operating concentration on pseudo-degradation is readily understood by considering the following example.

One section of a fuel cell stack optimizes at 37.5% KOH at  $t = 0$  and the stack is initially operated at a concentration of 36.5% KOH. After 500 hours the operating KOH concentration of the stack is changed to 35.0%. The pseudo degradation is calculated for the 500 hour

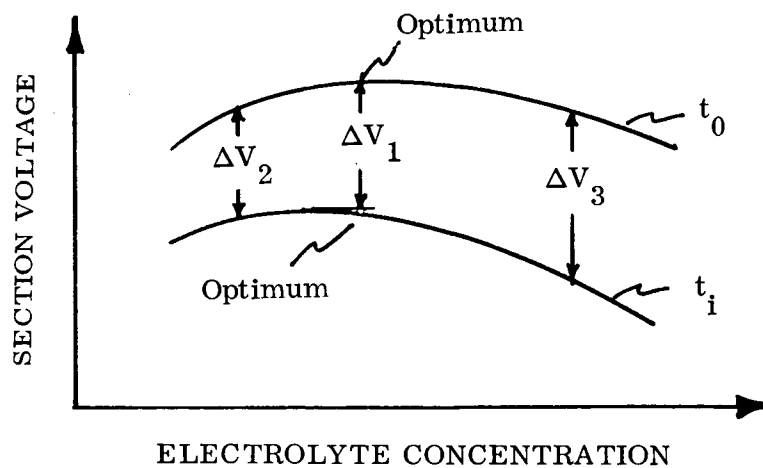


Figure 23. Optimum KOH Concentration Characteristics With Time

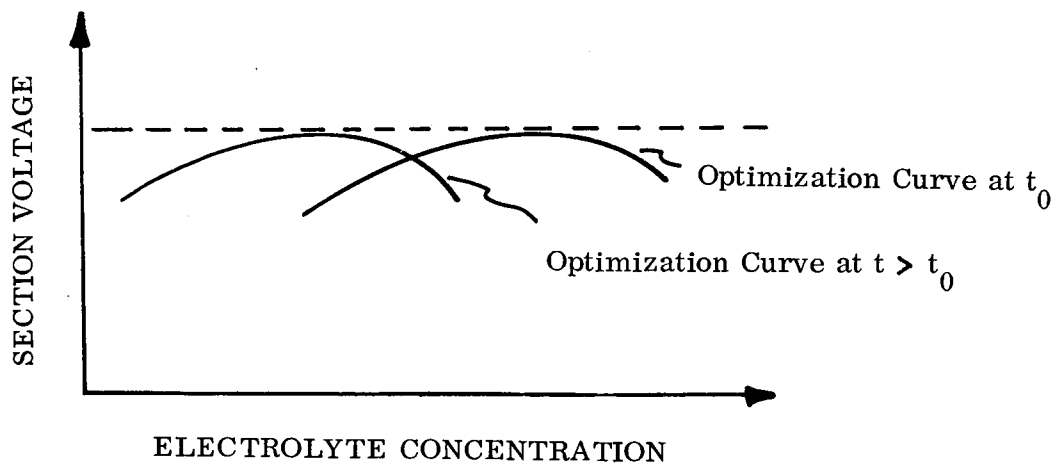


Figure 24. Translation of the Optimization Curves to Determine Pseudo Degradation

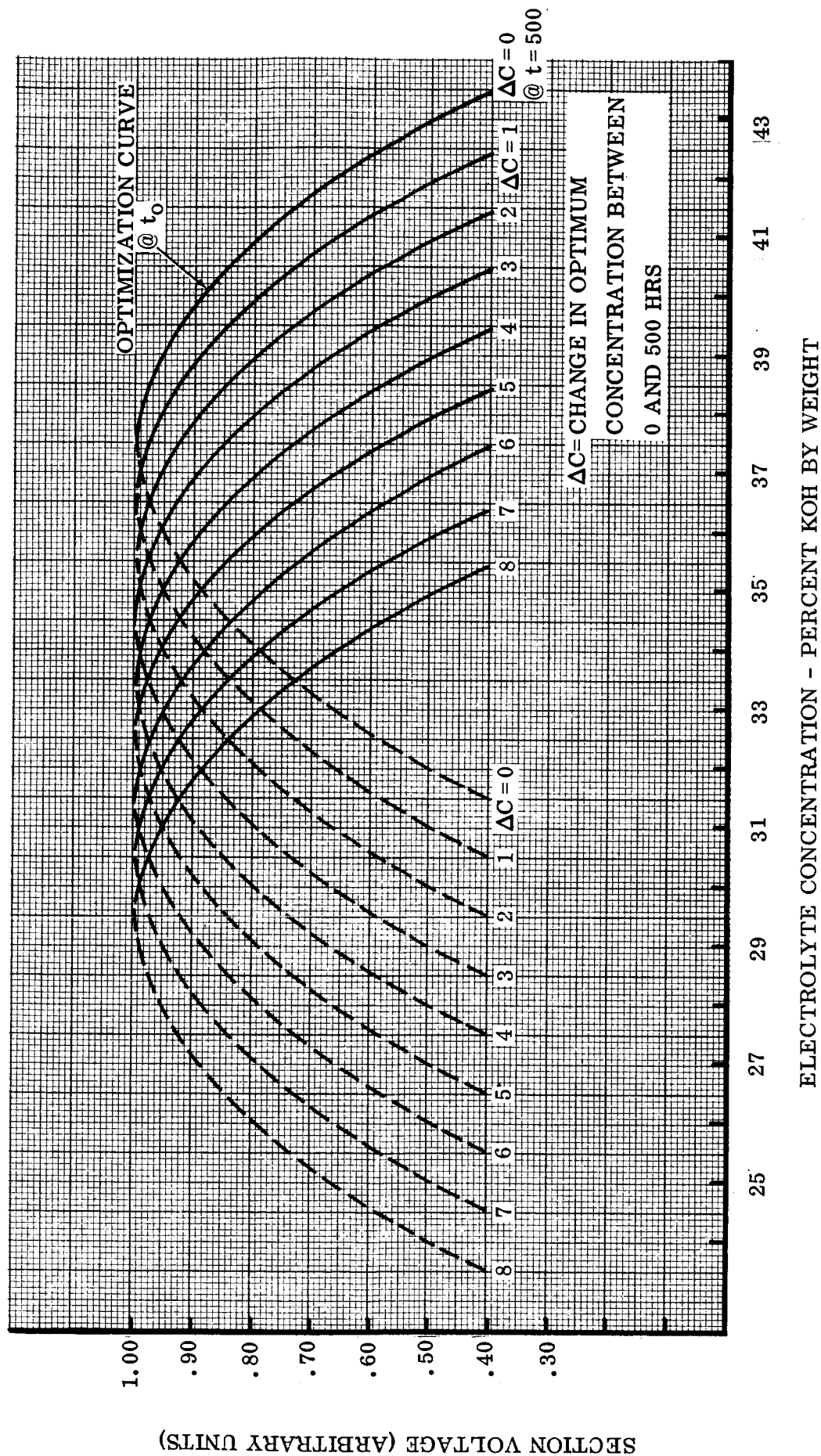


Figure 25. KOH Optimization Curves

period, assuming that the optimum KOH concentration of the section has changed 0, 1, 2, 3, 4, 5, 6, 7, or 8 percent during the time interval. The pseudo-degradation can be determined by translating the KOH optimization curves such that the optimums are on an equipotential line as shown in Figure 25. As can be seen in the figure, the initial voltage is 0.98 (arbitrary units) at the intersection of the optimum curve at  $t_0$  and at a concentration of 36.5 percent. After an elapsed time of 500 hours, the voltage at a concentration of 35.0 percent would be 0.90 volts, if no change in optimum concentration occurred. This value can be read by observing the intersection of 35.0 percent KOH and the optimization curve  $\Delta C = 0$ . An identical approach is used to determine the voltages at  $t = 500$  hours and 35.0% KOH considering that changes in optimum concentration of 1, 2, 3, 4, 5, 6, 7, and 8 percent have taken place; the voltage readings are then 0.96, 0.99, 0.99, 0.96, 0.90, 0.80, 0.66, and 0.50 volts respectively. Subtracting these voltages from the initial voltage of 0.98 volts yields the plot shown in Figure 26.

If the initial operating KOH concentration had been 37.5 percent instead of 36.5 percent, with the rest of the variables the same, the curve would be as shown in Figure 27.

If the final operating KOH concentration had been 34.0 percent instead of 35.0 percent, the rest of the variables being the same as in Figure 26, the curve appears as that shown in Figure 28.

It can be seen from these curves that the pseudo-degradation is a minimum when the section is operating at its most optimum conditions (final operating KOH concentration = final optimum KOH concentration). A negative pseudo degradation (indicating that the measured degradation is less than the true degradation) results when a section initially is operated very wet and the final performance is close to optimum conditions. Thus the initial concentration raises or lowers the curve in the vertical direction depending on the degree of initial wetness or dryness. It can also be observed, by comparing Figures 26 and 28, that a decrease in the final operating KOH concentration shifts the curve to the right.

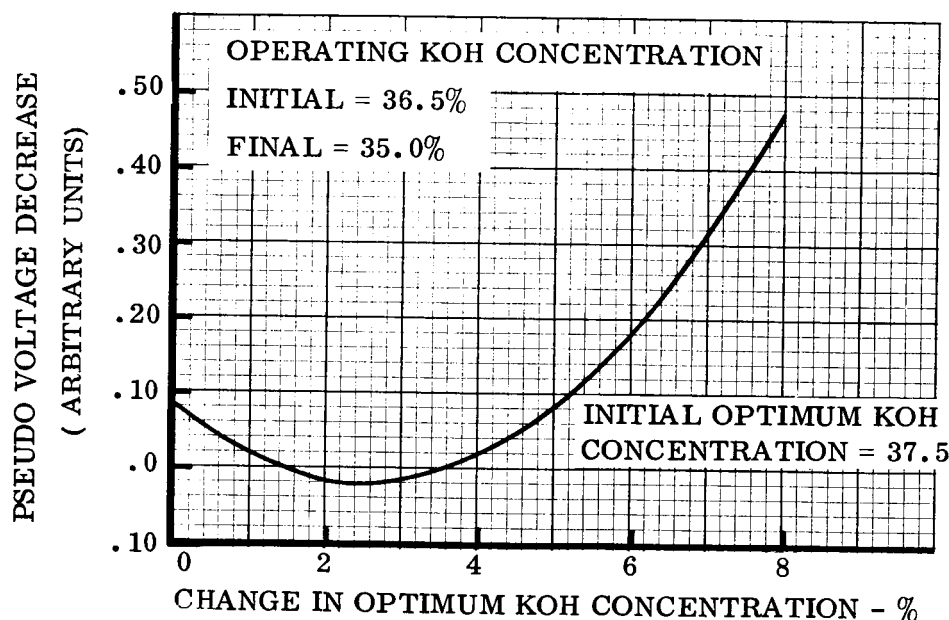


Figure 26. Arbitrary Initial and Final Operating KOH Concentration

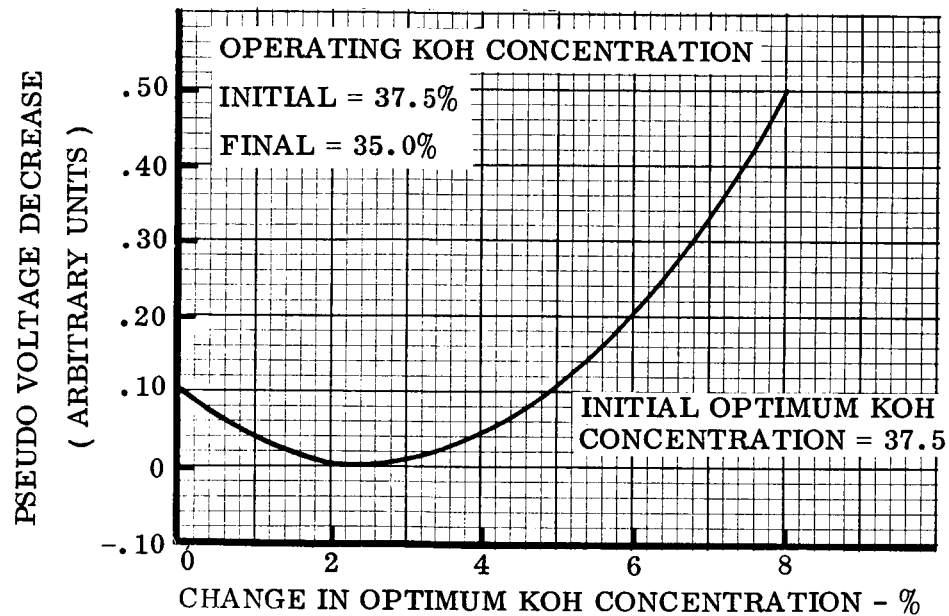


Figure 27. Effect of Increasing Initial Operating Concentration 1 Percent

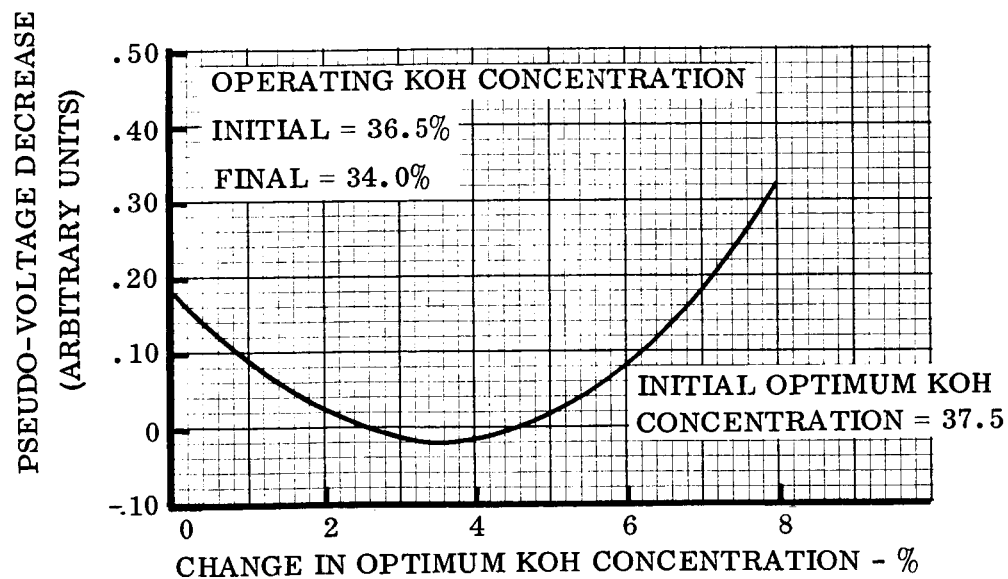


Figure 28. Effect of Decreasing Final Operating Concentration 1 Percent

As can be seen from this model example, the pseudo-degradation resulting from non-optimized performance is a function of several factors: the shape of the optimization curve; the optimum KOH concentration at  $t_0$ ; the optimum KOH concentration at  $t_1$ ; the initial KOH concentration that the section was operated at; and the KOH concentration that the section was operating at when the degradation was determined.

An analysis was performed on stacks 133 and 135 to correlate the effects of non-optimum performance with degradation. The theoretical shapes of these curves were determined by assuming a voltage versus KOH concentration curve, the shape of which is assumed equal for all sections, and determining the pseudo-degradation for the conditions under which the system was operated.

Stack 133 was optimized during the acceptance test and after an elapsed time of 540 hours. The optimum concentration for the individual sections ranged from 33 to 37% KOH and exhibited optimum concentration changes ranging from 2-1/2 to 10% KOH. The system was operated at a constant 34.5% KOH concentration during the 540 hour period. The pseudo-degradation versus change in percent KOH characteristics were calculated in a manner similar to the sample problem, resulting in the family of curves shown in Figure 29. This model predicted the general shape of the pseudo-degradation versus change in percent KOH characteristics for Stack 133 just before the second optimization. The actual pseudo-degradation for Stack 133 was then determined. The measured degradation was calculated by merely subtracting the voltage readings of the sections at  $t = 495$  hours from the readings at 5 hours and dividing by the time interval of 490 hours. The optimization plots of all the sections during both optimizations were then graphed, thereby determining the initial optimization concentrations, the optimum voltages, and the changes in optimum percent KOH between optimizations. The true degradation for each section was then determined by subtracting the optimum voltages at 540 hours from the optimum voltages at minus 20 hours (during the acceptance test) and dividing by the time interval (560 hours). The pseudo-degradation for each of the 33 sections was then determined by subtracting the true degradation from the measured degradation. Thus the pseudo-degradation as a function of change in percent KOH characteristics for Stack 133 was determined and plotted as shown in Figure 30.

Stack 135 was optimized three times in the first 500 hours; during the acceptance test, at 210 and 510 hours. The system was operated at a KOH concentration of 36.5 percent from 0 to 200 hours and at 35.0 percent from 220 to 500 hours. The initial optimum KOH concentration of the sections ranged from 35.5 to 40.5 percent during acceptance test and the exhibited optimum KOH concentration changes ranged from 2 to 7.5 percent KOH during the 520 hour time interval. The theoretical shape of the pseudo-degradation curve, shown in Figure 31, was calculated for these operating conditions. The actual pseudo-degradation was then determined from the data and plotted as shown in Figure 32.

It should be noted that the theoretical shape of the pseudo degradation curves are only intended to predict the relative shape of the pseudo-degradation curve. Considerable deviations can be expected because the concentration versus voltage curves of the sections have different relative shapes, and because of variability in the fuel cell data. Because the pseudo-degradation curves are in good agreement with the theoretical curves, it appears that this model sufficiently explains the effect of operation at non-optimum concentrations.

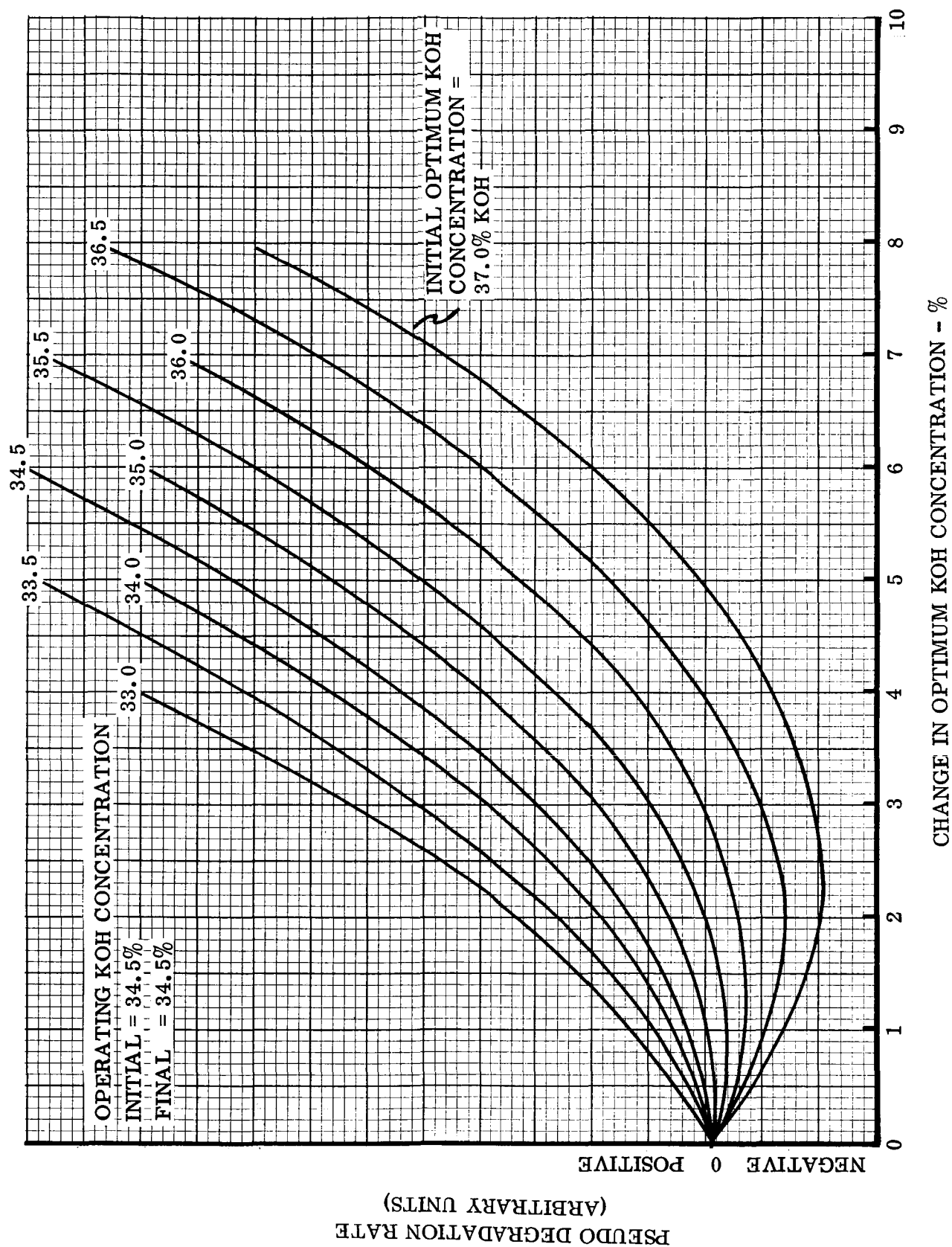


Figure 29. Theoretical Shape of Pseudo-Degradation Rate - Stack 133

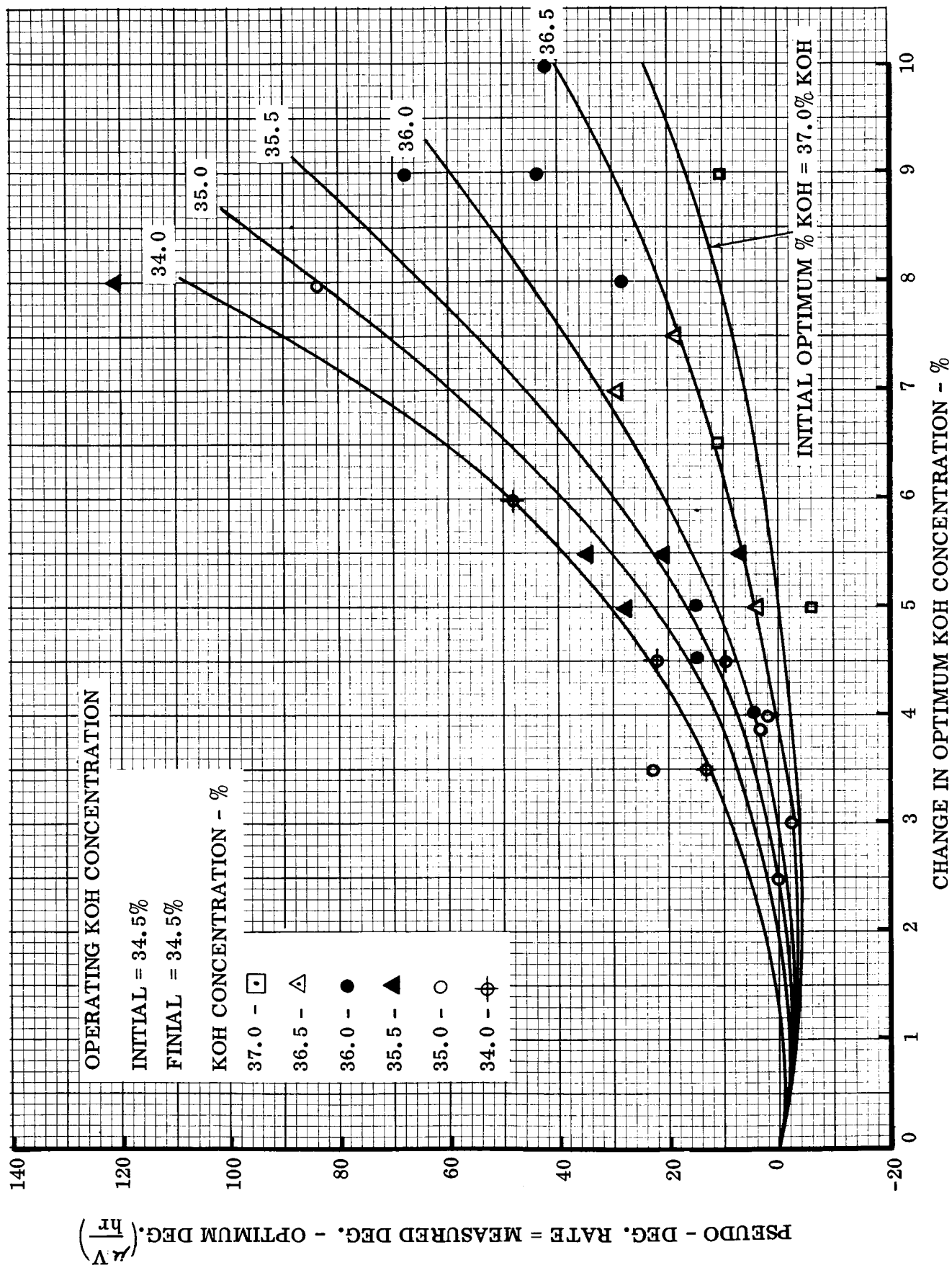


Figure 30. Measured Pseudo-Degradation Rate - Stack 133

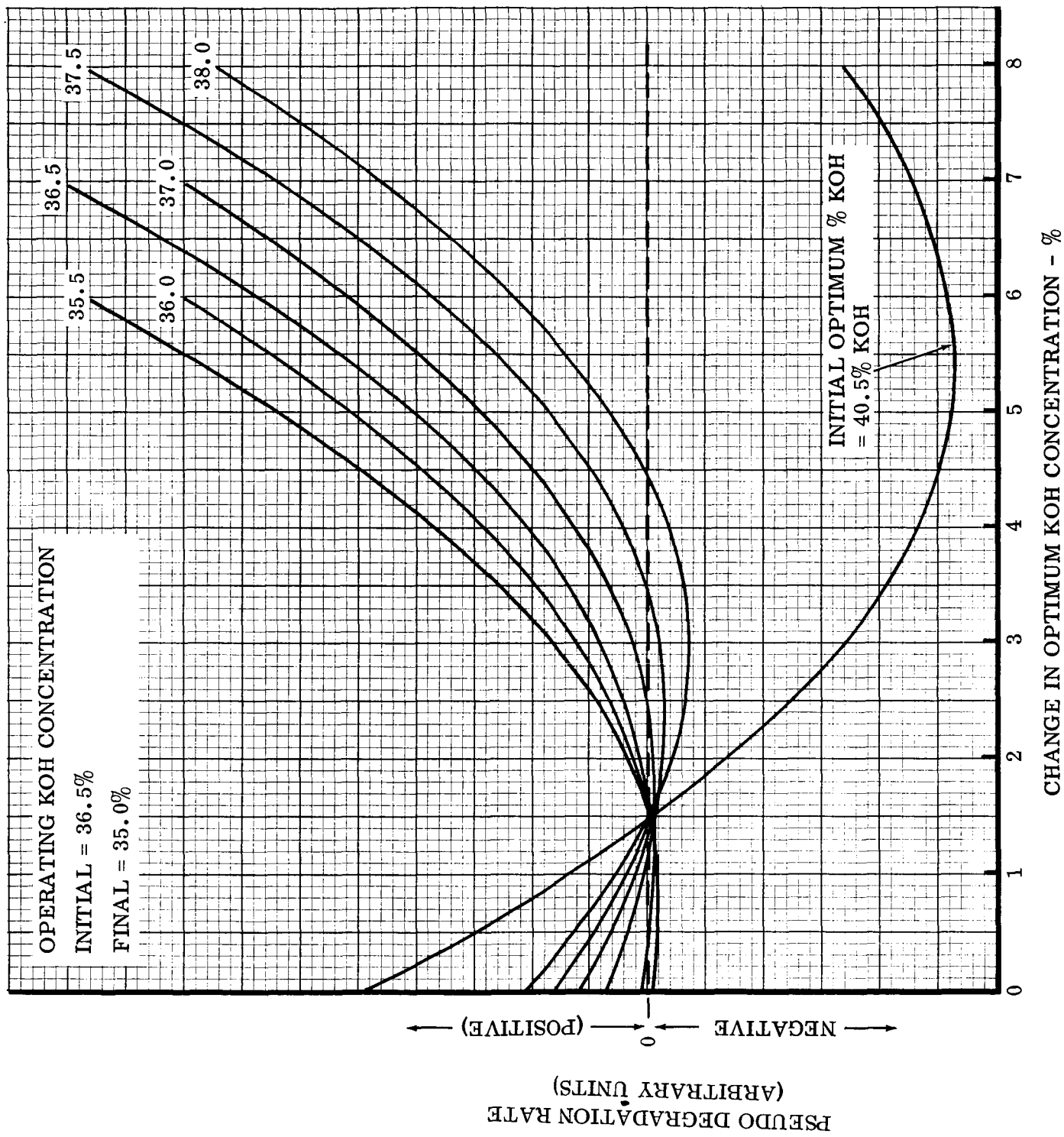


Figure 31. Theoretical Shape of Pseudo-Degradation Rate - Stack 135

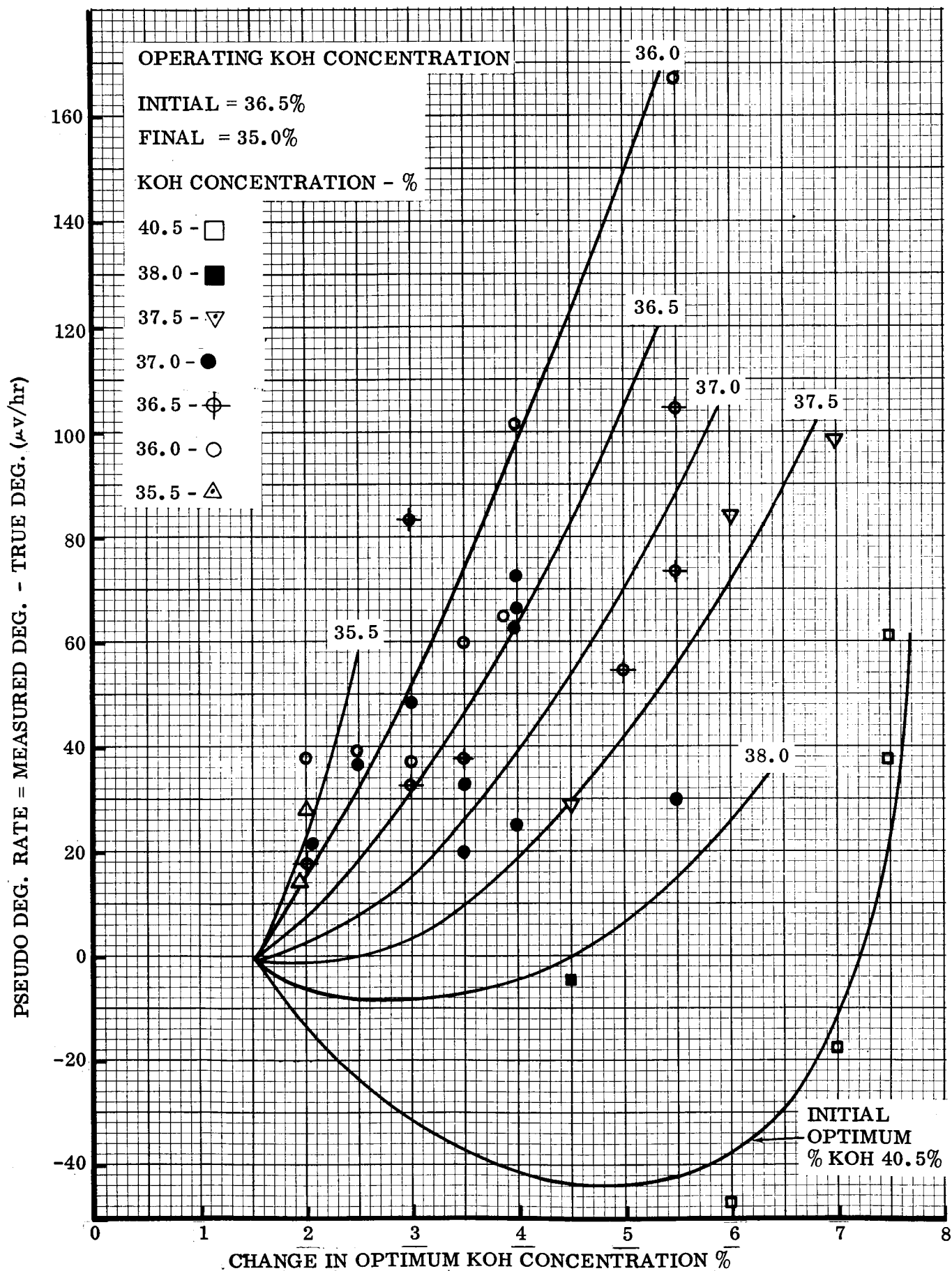


Figure 32. Measured Pseudo-Degradation Rate - Stack 135

The true degradation rate and the measured degradation rate versus change in optimum KOH concentration correlations for stacks 133 and 135 are shown in Figures 33 and 34, respectively. It can be observed from these graphs that there is no apparent relationship between the true degradation rate and the change in optimum KOH concentration. It can also be observed from Figure 35 that there is no relationship between the optimum KOH concentration and the optimum voltage. It follows that if a section could be operated at or near optimum conditions at all times there would be no noticeable change in degradation rate, regardless of the change in optimum KOH concentration the section exhibited. This is supported by the fact that the optimum voltage versus time curves of the individual sections are more linear than the measured voltage versus time curves, which bend downwards due to the steadily increasing measured degradation rate.

On stack 133 the average true degradation rate per section was 44 microvolts per hour with a standard deviation of 17 microvolts per hour. The average measured degradation rate per section was 74 microvolts per hour. Therefore, 40 percent of the measured degradation is a result of operation under non-optimum conditions.

The average true degradation rate per section of stack 135 was 66 microvolts per hour with a standard deviation of 22 microvolts per hour. The average measured degradation rate, however, was 114 microvolts per hour. Thus 24 percent of the measured degradation is a result of operation under non-optimum conditions.

It appears that a significant portion of apparent stack degradation is not really degradation at all but a decrease in performance due to the inability of running every section at its own optimum concentration.

It has been observed from stack performance data that the degradation rate increases with time, sometimes very rapidly. This trend was investigated for the sections of Stack 135 by plotting the approximate volt-time curves for all 33 sections. These curves are shown in Figure 36. The circles at 0, 210, and 510 hours represent the optimum section voltages during the respective optimizations. It can be observed from these curves that almost all the sections have a larger degradation rate from 200 to 500 hours than they had during the first 200 hours, thus exhibiting a degradation rate that increases with time. It can also be observed that if a V-T curve was drawn by connecting the optimum voltages, the characteristics are approximately linear.

This indicates that an increasing degradation rate with time is not necessarily a characteristic of the fuel cell, but an effect produced by operation at non-optimum conditions. Such an effect would be expected because of the increased change in optimum KOH concentration with time. Since some sections exhibit small changes in optimum KOH concentration and some exhibit large changes, the range between the highest and lowest optimum increases with time. Since the stack optimum is approximately equal to the average optimum, the average KOH concentration at which each section operates away from its optimum must increase with time, thus causing an increasing pseudo-degradation rate with time. The increasing degradation rate with time of Stack 135 can be seen in Figure 37. Compare this V-T curve with the relatively optimum V-T curve.

It appears that operating a section wet does not have adverse effects other than slightly lower performance. Several sections in Stacks 133 and 135 were operated as much as 4 percent wet. The resultant performance was approximately 30 millivolts below optimum, but improved with time as the optimum KOH concentration shifted. Sections that were initially 4 percent dry, however, suffered a drastic reduction in performance and developed crossleaks.

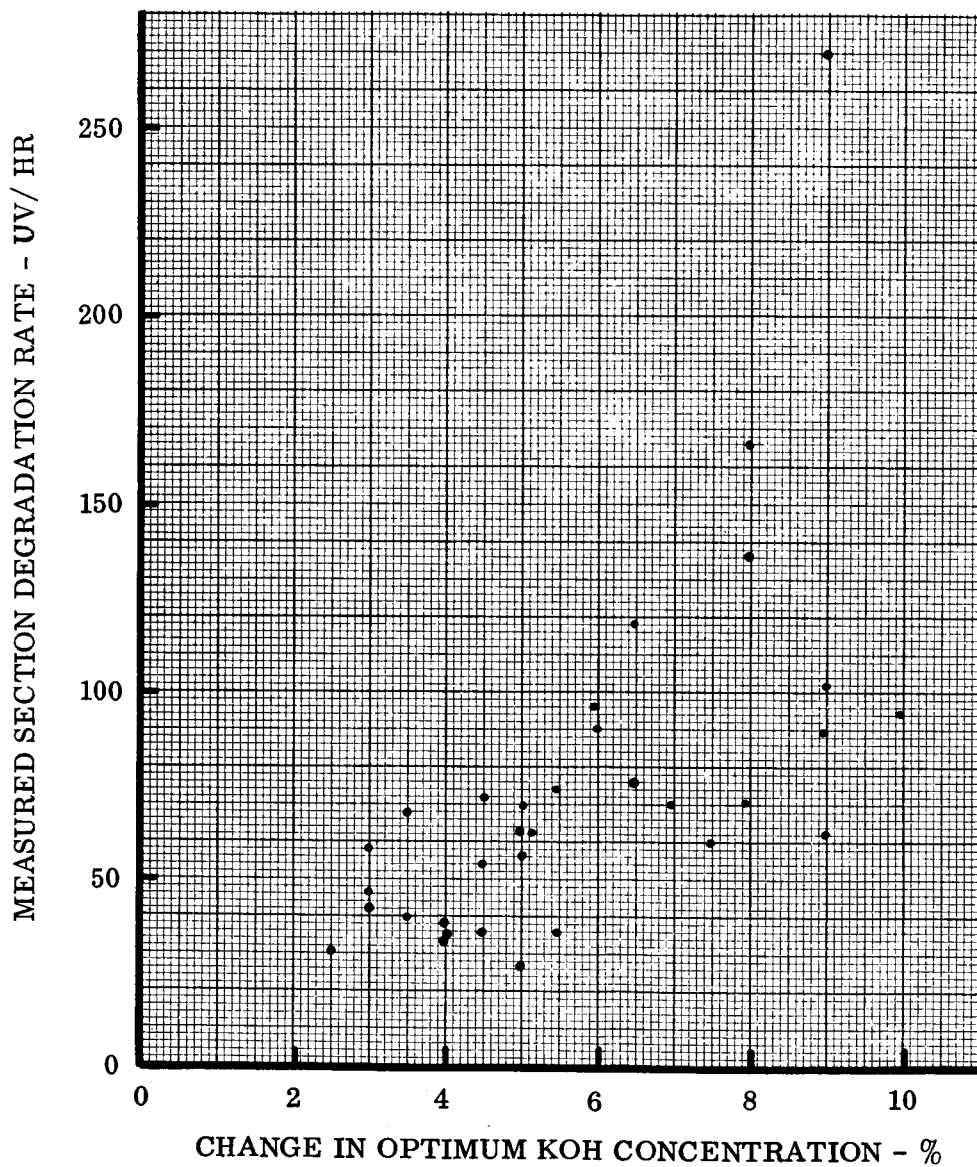
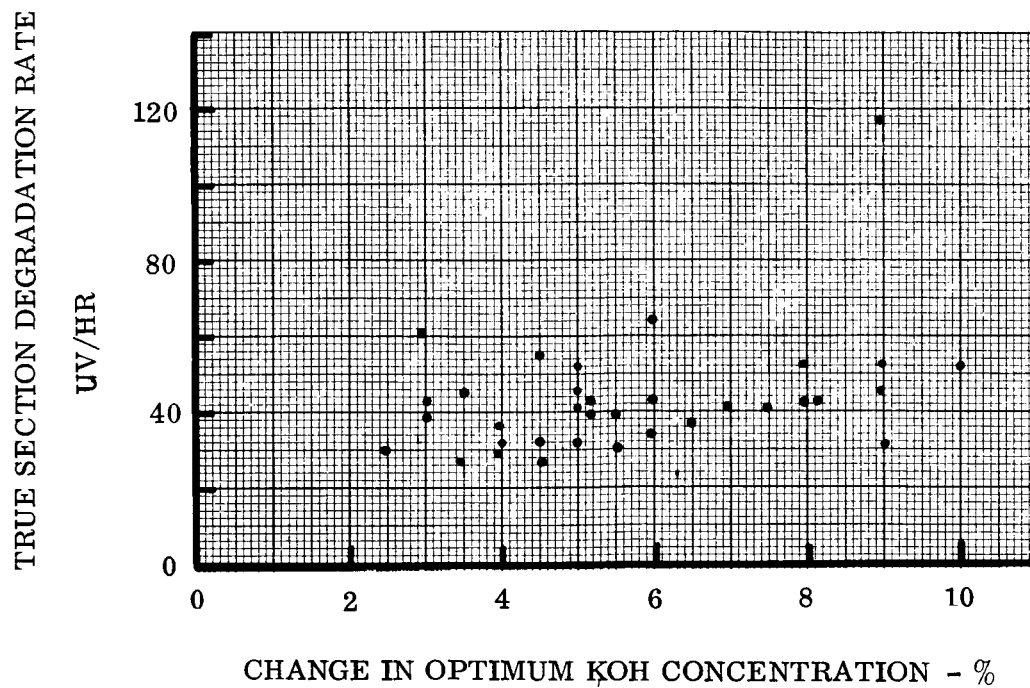


Figure 33. Concentration Deviation - Stack 133

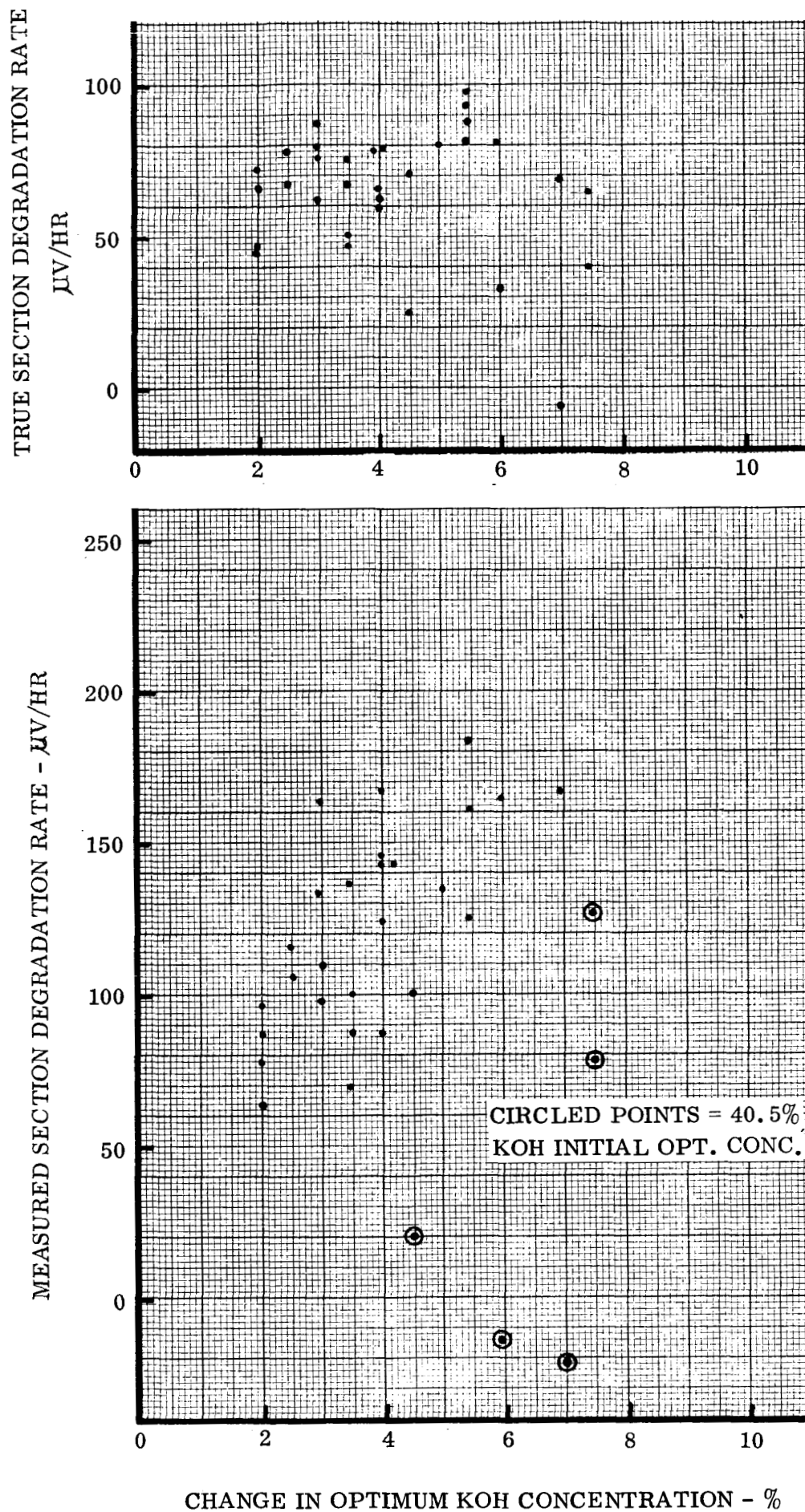
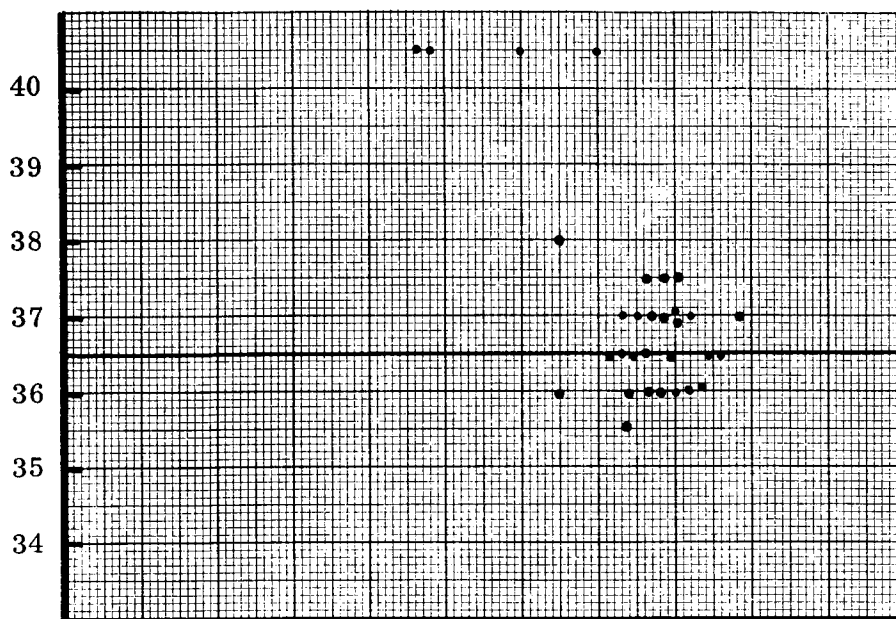


Figure 34. KOH Concentration Deviation - Stack 135

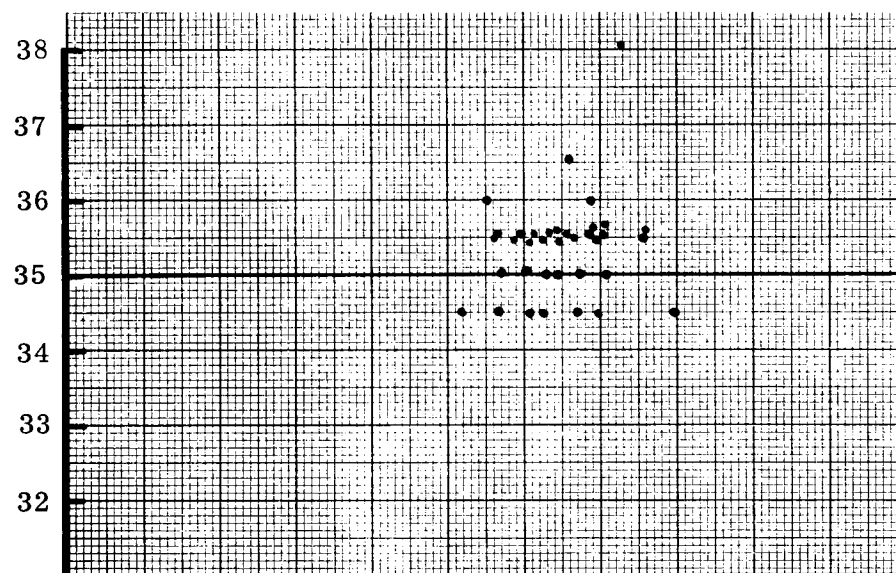
ELECTROLYTE CONCENTRATION

- %KOH BY WEIGHT  
(AT 0 HOURS)



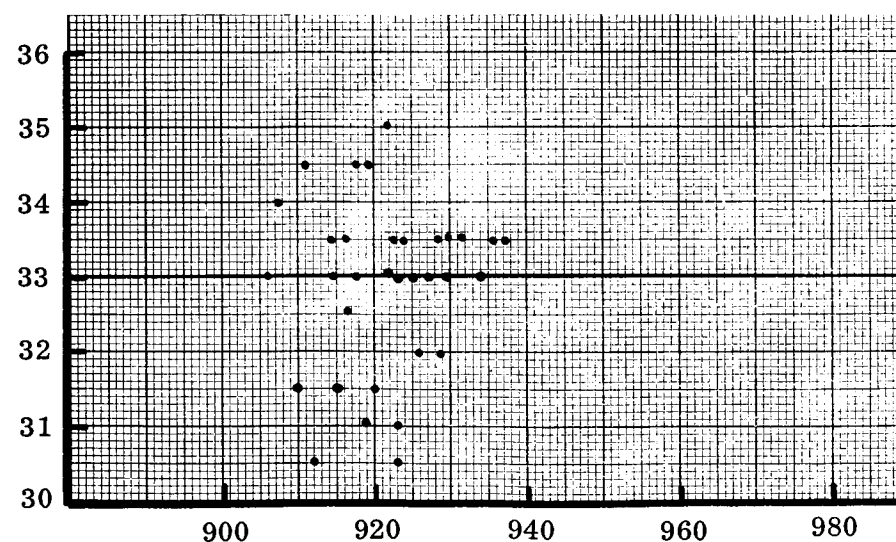
ELECTROLYTE CONCENTRATION

- %KOH BY WEIGHT  
(AT 210 HOURS)



ELECTROLYTE CONCENTRATION

- %KOH BY WEIGHT  
(AT 510 HOURS)

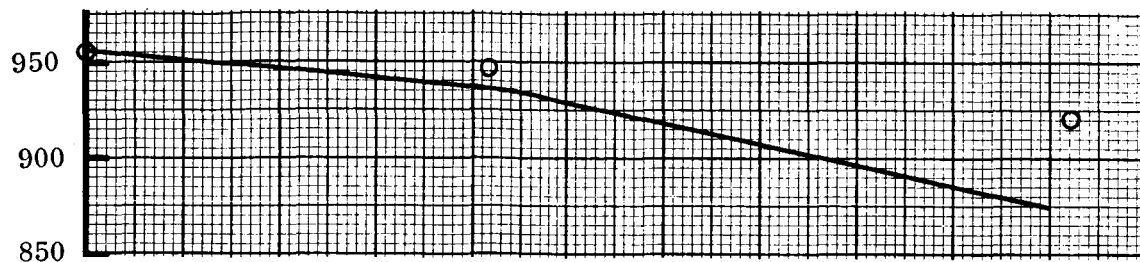


SECTION POTENTIAL - MILLIVOLTS

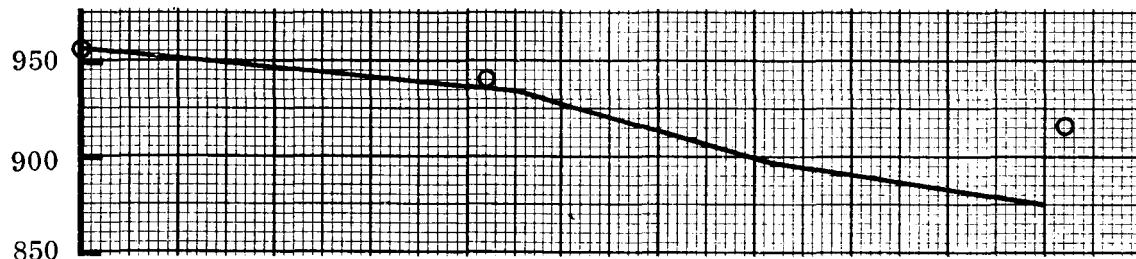
Figure 35. KOH Concentration Optimization - Stack 135

MEASURED SECTION VOLTAGE - MILLIVOLTS

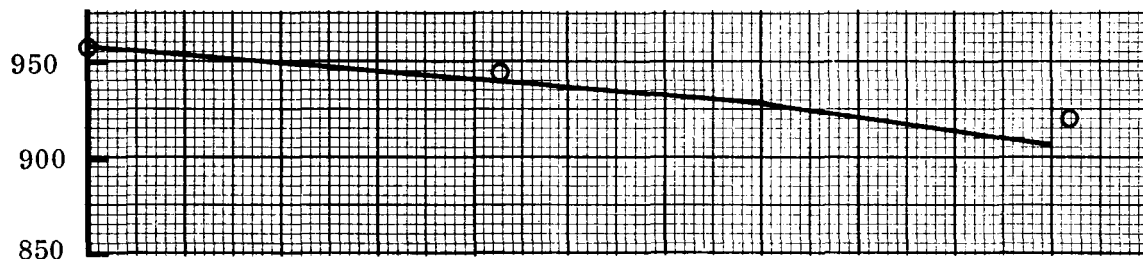
Section No. 1



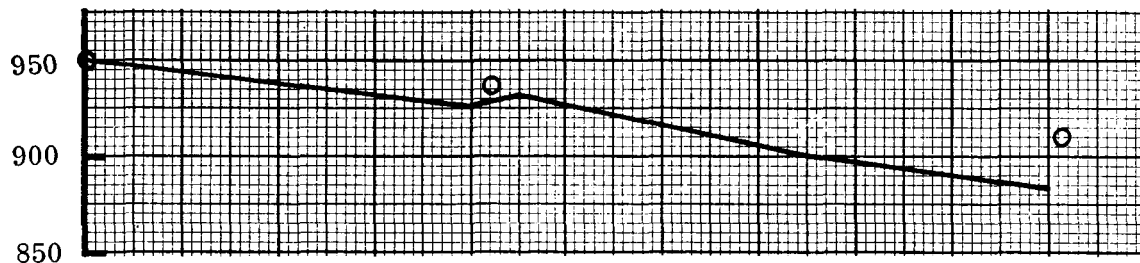
Section No. 2



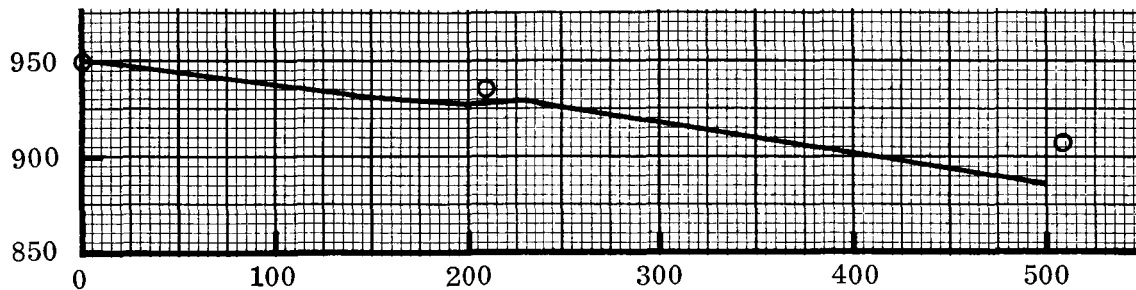
Section No. 3



Section No. 4



Section No. 5



ELAPSED TIME - HOURS

Figure 36. Voltage - Time Curves - Stack 135 (Sheet 1 of 7)

MEASURED SECTION VOLTAGE - MILLIVOLTS

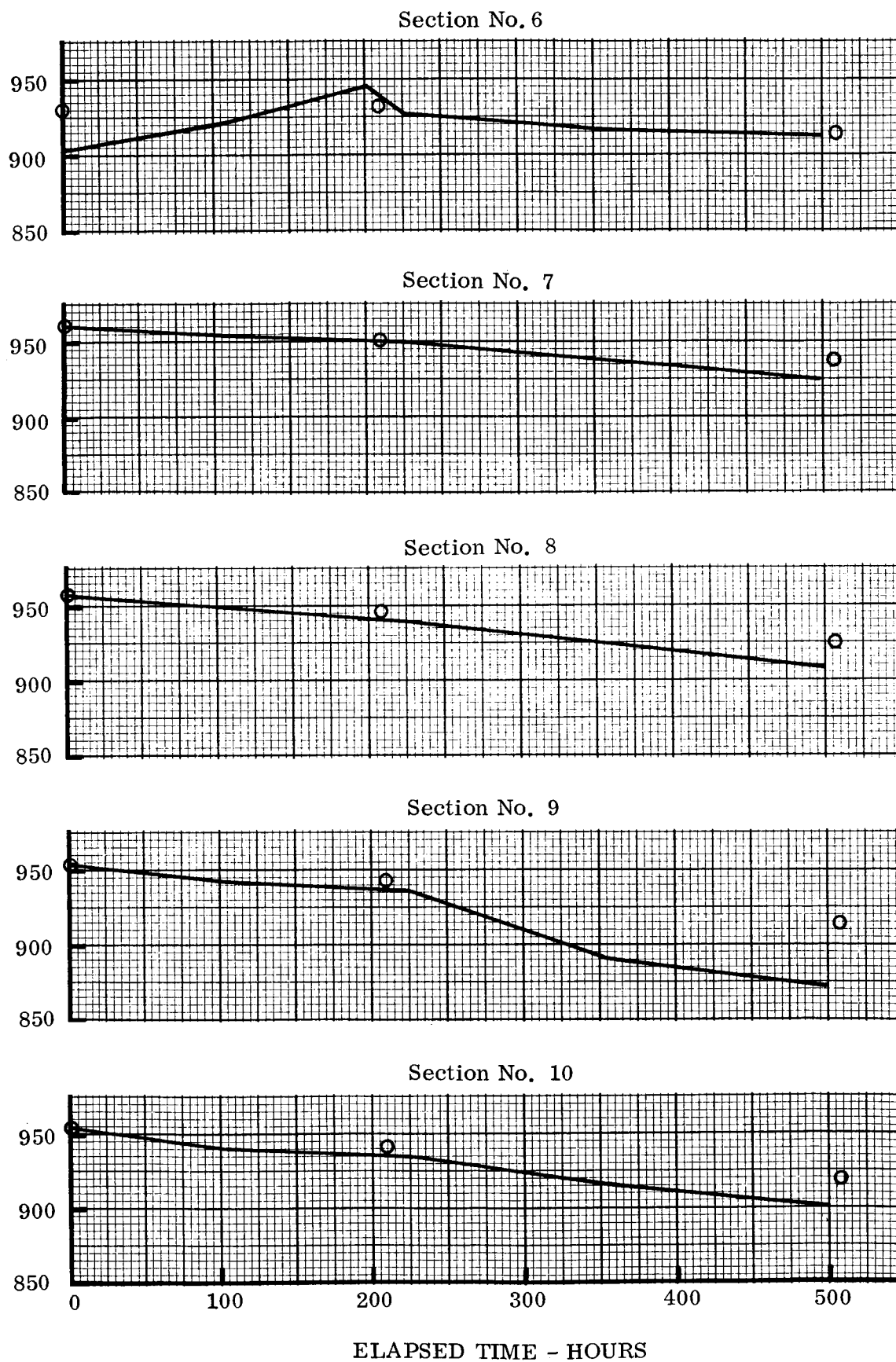


Figure 36. Voltage - Time Curves - Stack 135 (Sheet 2 of 7)

MEASURED SECTION VOLTAGE - MILLIVOLTS

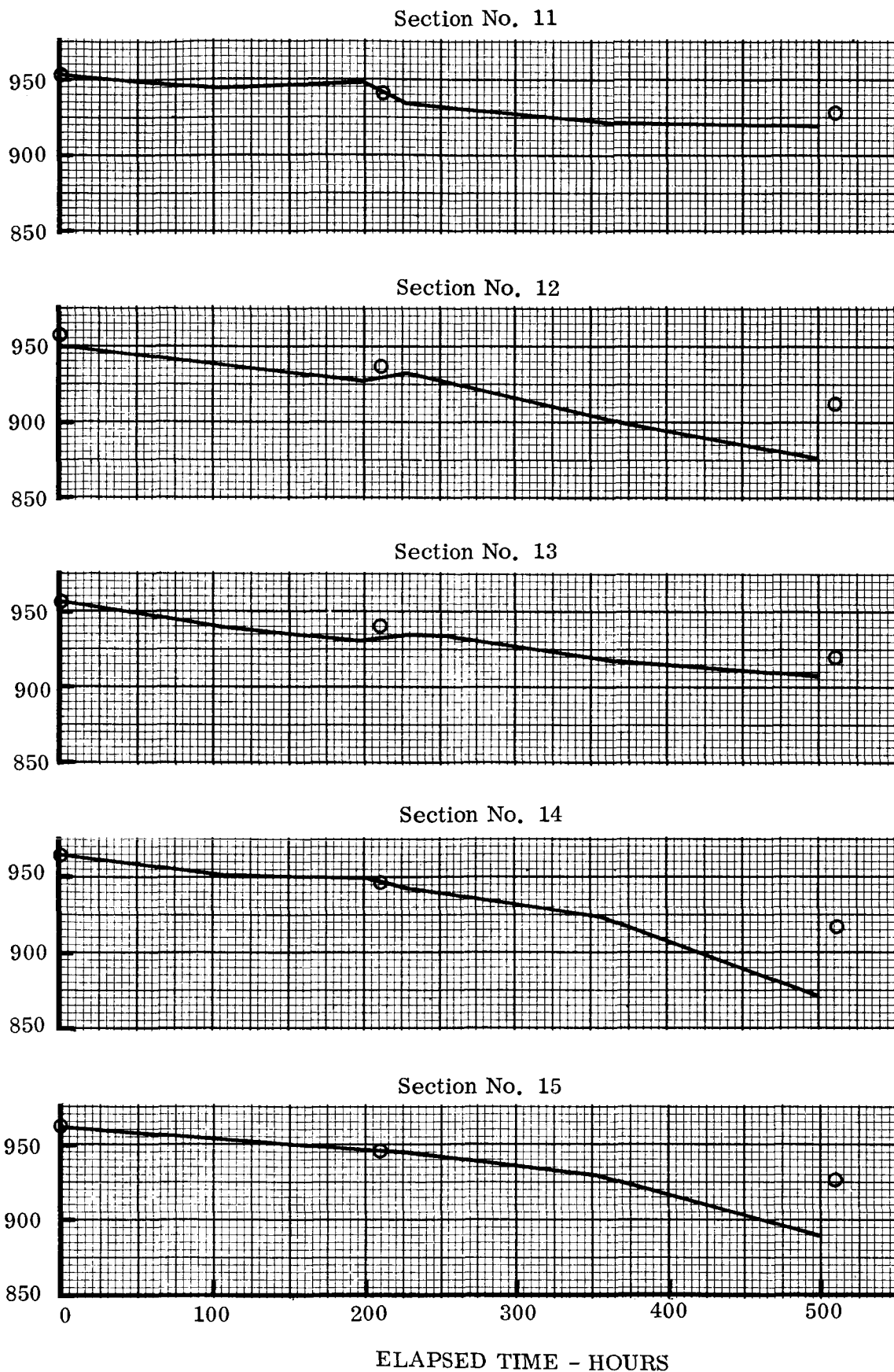
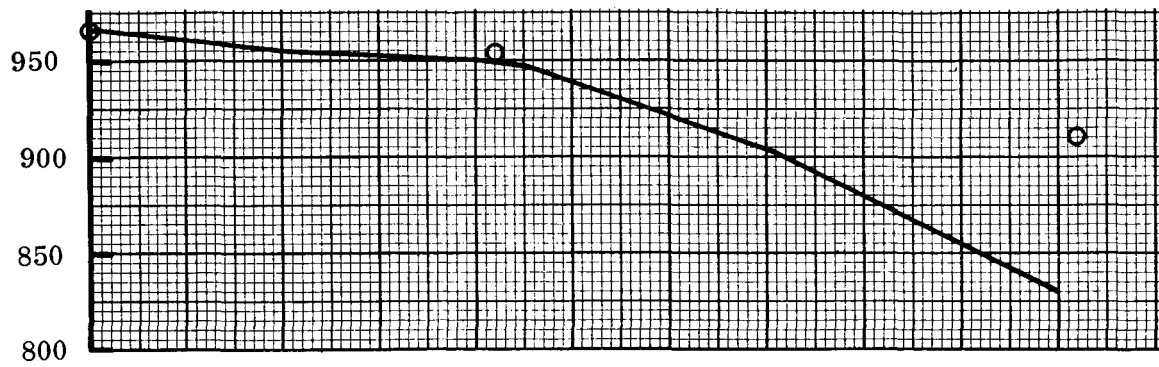


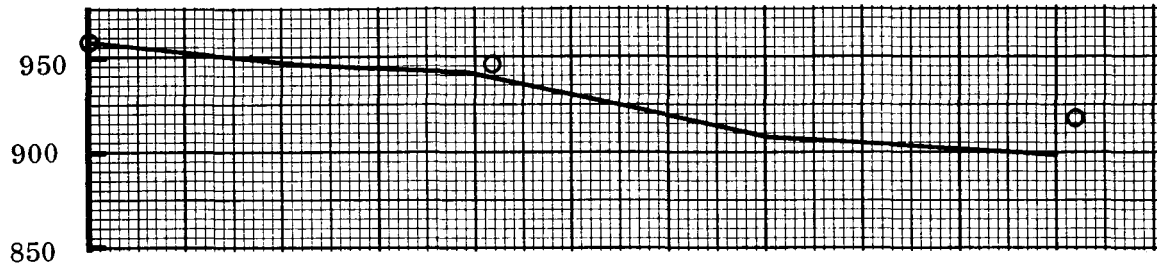
Figure 36. Voltage - Time Curves - Stack 135 (Sheet 3 of 7)

MEASURED SECTION VOLTAGE - MILLIVOLTS

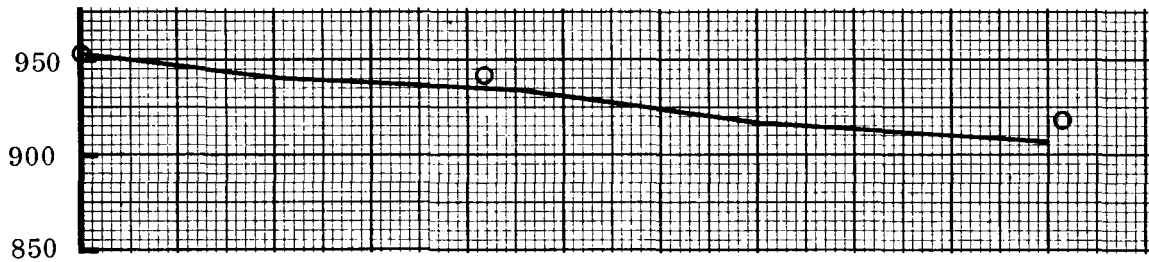
Section No. 16



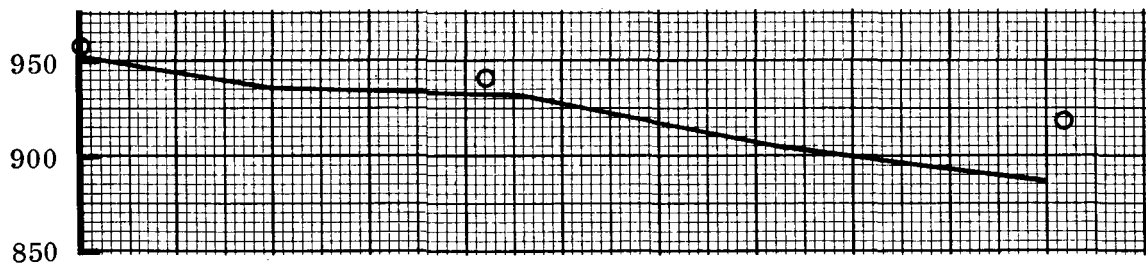
Section No. 17



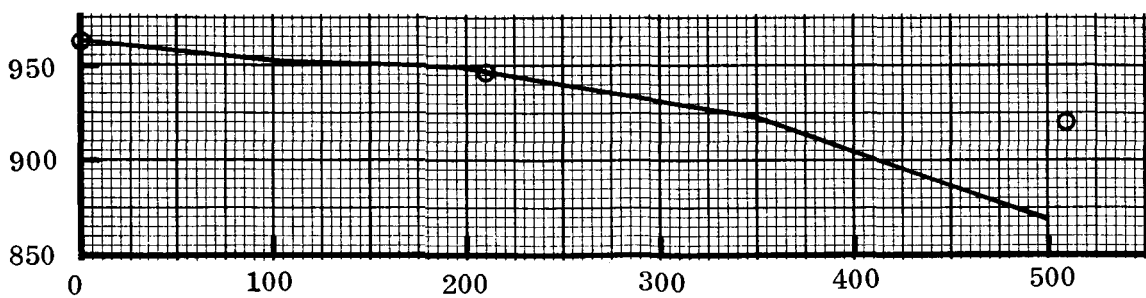
Section No. 18



Section No. 19



Section No. 20



ELAPSED TIME - HOURS

Figure 36. Voltage - Time Curves - Stack 135 (Sheet 4 of 7)

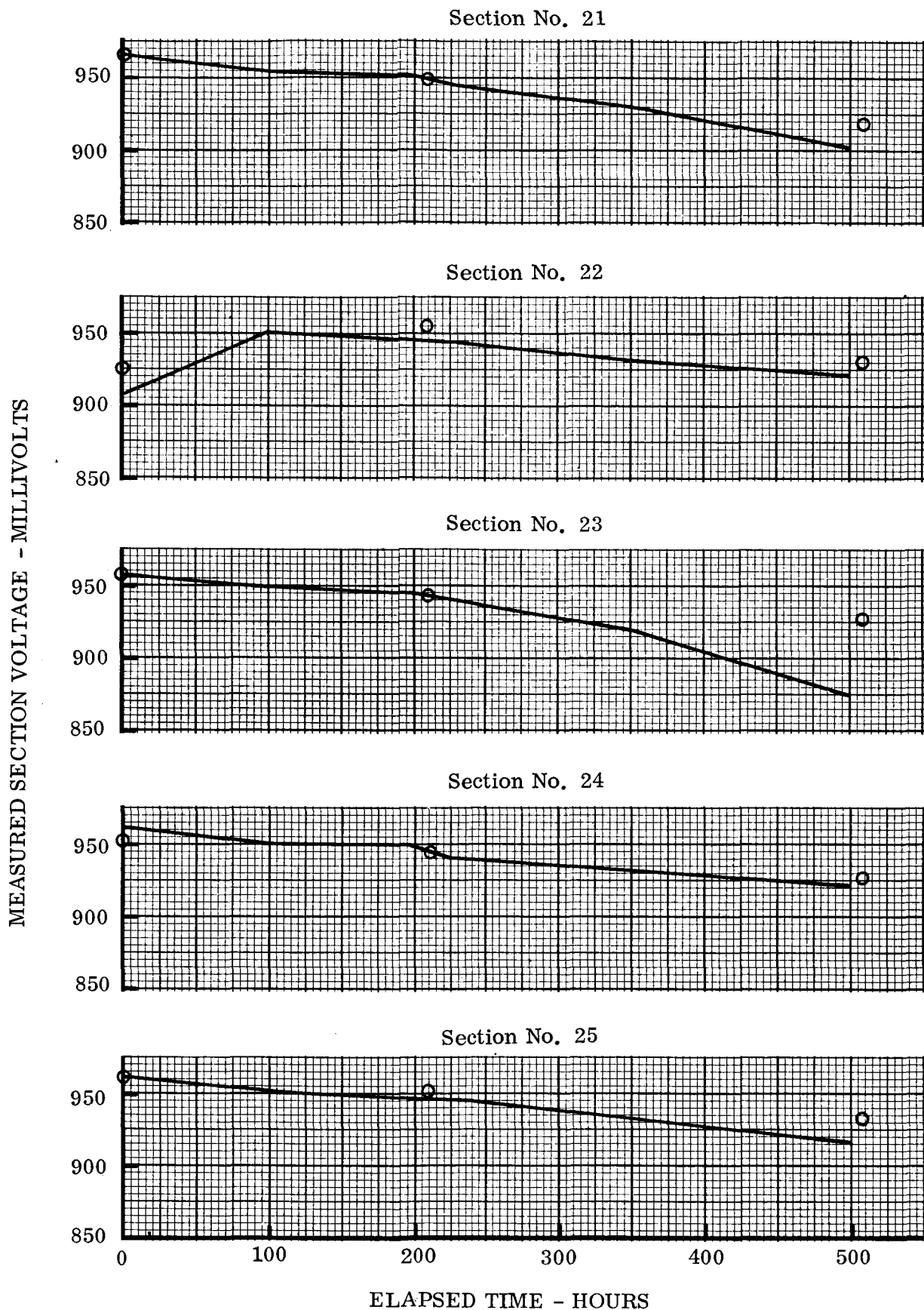
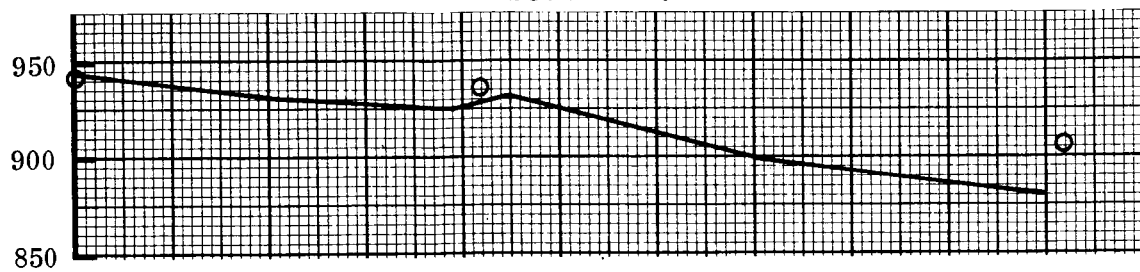


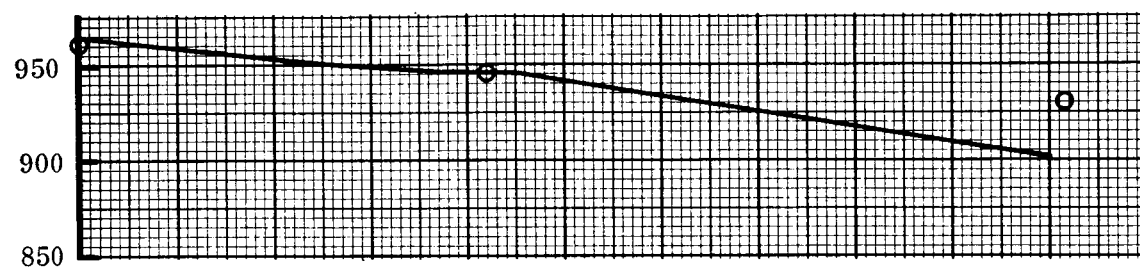
Figure 36. Voltage - Time Curves - Stack 135 (Sheet 5 of 7)

MEASURED SECTION VOLTAGE - MILLIVOLTS

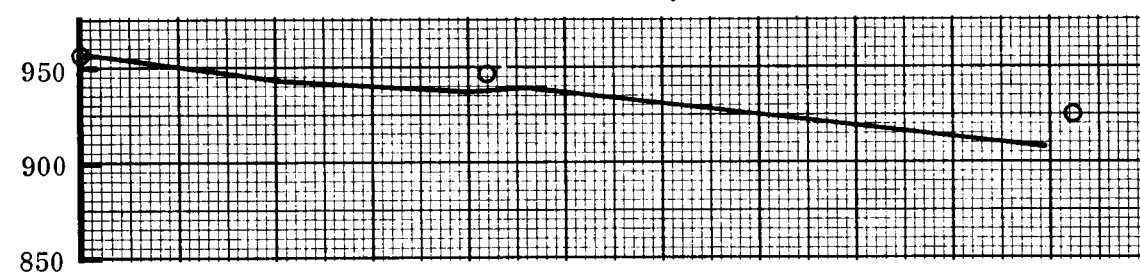
Section No. 26



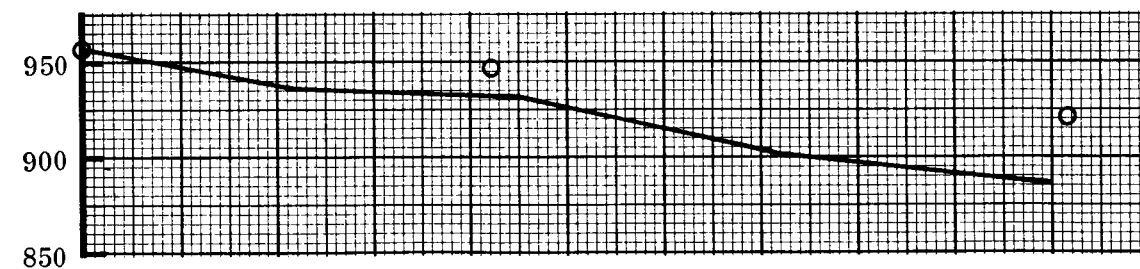
Section No. 27



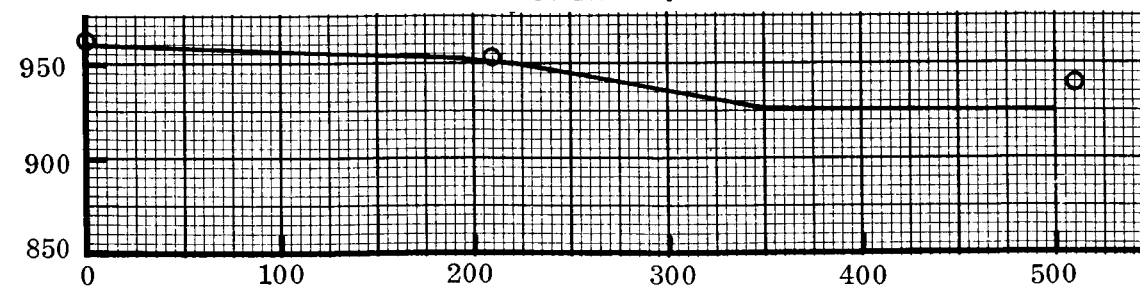
Section No. 28



Section No. 29



Section No. 30



ELAPSED TIME - HOURS

Figure 36. Voltage - Time Curves - Stack 135 (Sheet 6 of 7)

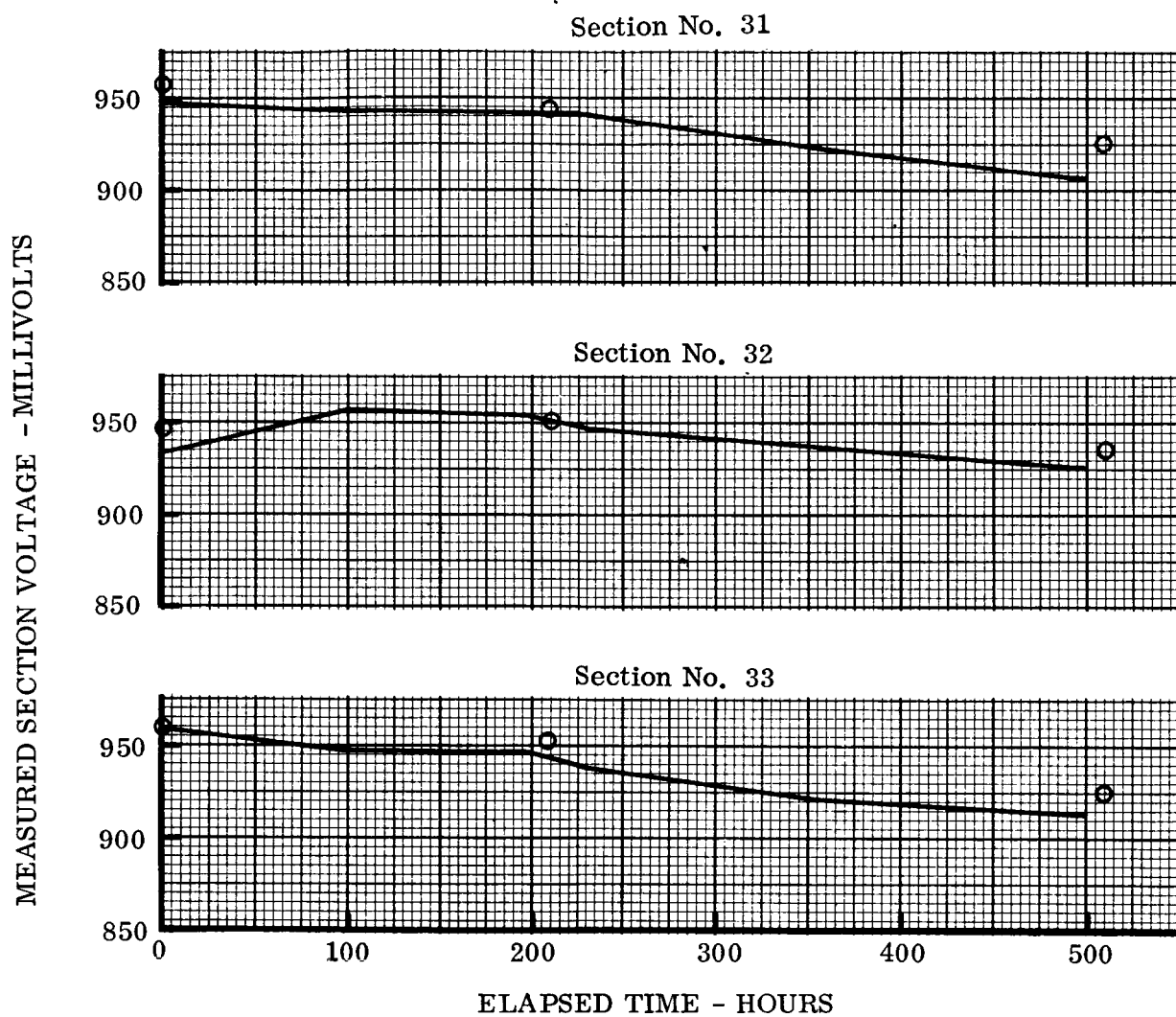


Figure 36. Voltage - Time Curves - Stack 135 (Sheet 7 of 7)

It is evident that the effect of non-optimum performance of the sections in a stack poses some serious problems. It is also evident that this is one of the major reasons why stack performance deviates from single section performance, particularly with increased operating time.

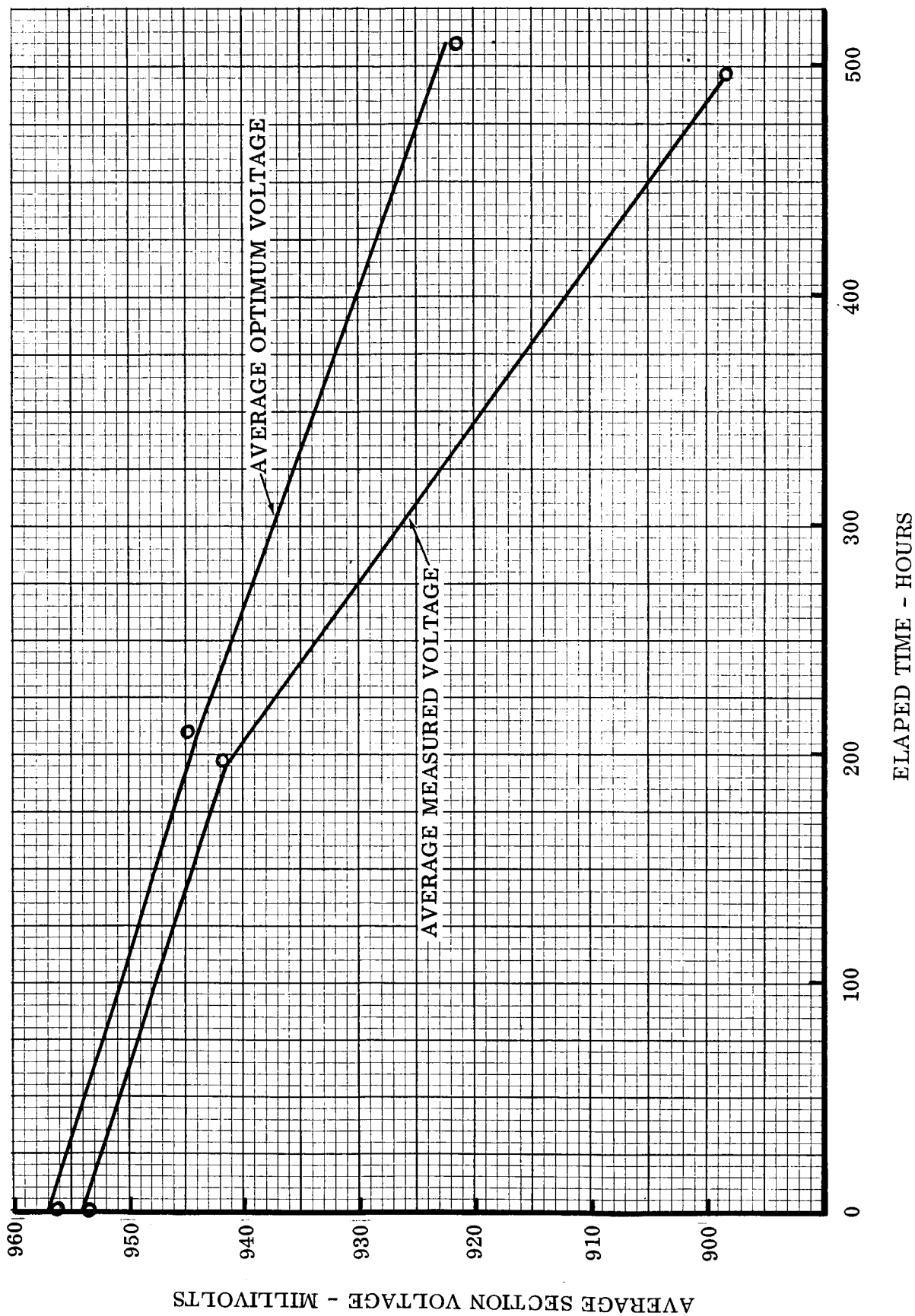


Figure 37. Voltage - Time Characteristics - Stack 135

Reactant Purging. - A study was made of the effect of purging on fuel cell performance. The average, standard deviation and range of the section voltages were used as performance indicators. The voltage data was obtained from Stack 131 operating at a load of 100 amperes. The time segment between 284.5 and 301 hours was chosen because data was recorded at 15 minute intervals for this stack by the Data Acquisition System. A plot of the average section voltage and the standard deviation of the voltages at 15 minute intervals is shown in Figure 38. Eleven automatic purges of 5 second durations were studied.

The degradation rate for the above time period was approximately 110 microvolts per hour per section. Section 26, the high voltage section, had a degradation rate of 31 microvolts per hour. Section 16 had the low voltage throughout the time period studied and degraded at 720 microvolts per hour. Most of the stack degradation and increase in the standard deviation can be attributed to the performance of Section 16. Eliminating the low voltage data points, the standard deviation is 9.7 and 11 millivolts at 285 and 300 hours, respectively.

The average section voltage increased after each of the 11 purges. The average increase was slightly less than 1 millivolt. The standard deviation decreased after 9 of the 11 purges. The range between the high and the low voltage was not uniformly affected by the purges, while increasing from 62 to 73 millivolts at 285 and 300 hours respectively. This is because neither the low nor the high voltage section was uniformly affected by purging.

No significant correlation was found between section number and section voltage although a least-squares-line indicated that the low section numbers had slightly higher voltages. No significant correlation was found between either section number or section voltage rank and voltage change after purging.

For several purges, more sections decreased in voltage than increased. No apparent reason could be found for this. Some sections showed a significant increase in voltage for all of the purges studied. This was especially true for section number 33. Comparison of the KOH optimization curves for several sections showed no cause for some sections to increase voltage after purge and not the others. The sections studied appeared to be operating near their optimum at 35.5 percent KOH.

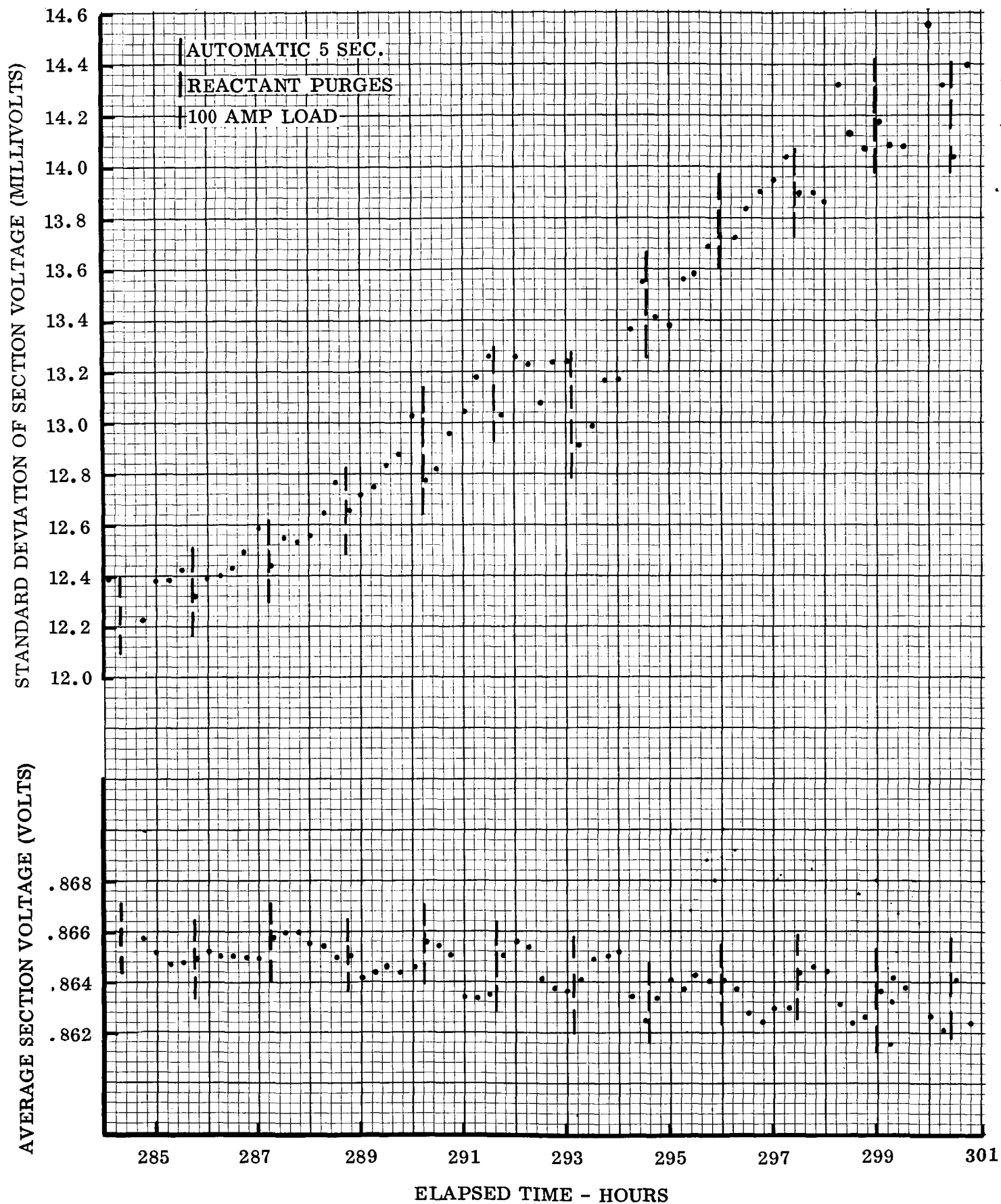


Figure 38. Effects of Purging on Performance - Stack 131

Cell Matrix Compression. - A study was performed to determine if the degree of asbestos matrix compression between the electrodes influences fuel cell performance.

Perhaps the best method of measuring compression is to consider the bulk density of the asbestos, which is determined from the combined weight of the asbestos matrix and the two seal frames (Figure 22) and the available volume in the reactant cavity. The investigation was based upon the premise that the density of the asbestos influences hydroxyl ion and water flow between the electrodes, and, hence, could affect performance. Each section then has two bulk densities (one for each cell). Four combinations of bulk densities were considered, each as the independent variable:

- a. The average of the two bulk densities in a section (gm/cc),
- b. The larger of the two bulk densities in a section (gm/cc),
- c. The smaller of the two bulk densities in a section (gm/cc),
- d. The difference between the two bulk densities in a section as a percentage of the average bulk density of that section.

Three dependent variables were used as indicators of section performance:

- a. The initial section potential at 40 amps (millivolts),
- b. The section degradation rate at 40 amps during the performance evaluation tests (microvolts per hour),
- c. The true degradation rate from the performance evaluation tests (microvolts per hour).

True degradation rate is defined as the measured degradation rate minus the degradation rate due to operation at non-optimum KOH concentration. True degradation rates were available for Stacks 133 (0 to 540 hours) and Stack 135 (0 to 520 hours).

All combinations of the four independent variables with each of the first two dependent variables were studied for Stacks 131 thru 135, and with the third dependent variable for Stacks 133 and 135. In general, all relationships were poor. The highest level of linear correlation was found to exist between the fourth independent variable (d) and the second dependent variable (b). The results of this correlation are presented in Figure 39.

The values of the dependent variable lie between 15 and 85 microvolts per hour, except for point "A" at 172 microvolts per hour. Calculations of the average and standard deviation of the dependent variable show that point "A" lies more than three standard deviations from the average. For a normal distribution, the probability of occurrence for a value more than three standard deviations above or below the average is only 0.0026. Rejecting point "A" and repeating the correlation calculation shows that an insignificant linear correlation exists between these two variables.

Because of the stringent construction tolerances of these stacks, the variation in bulk asbestos density was correspondingly small (1.20 to 1.38 gm/cc for a 30 mil matrix). For variation of asbestos bulk densities within these tolerances, no relationship has been found between matrix compression and fuel cell performance.

⊗ AVERAGE FOR ALL DATA POINTS

× AVERAGE EXCLUDING POINT "A"

— LEAST SQUARES LINE FOR ALL POINTS

---- LEAST SQUARES LINE EXCLUDING POINT "A"

SOLID LINE CORRELATION = 0.293

BROKEN LINE CORRELATION = 0.112

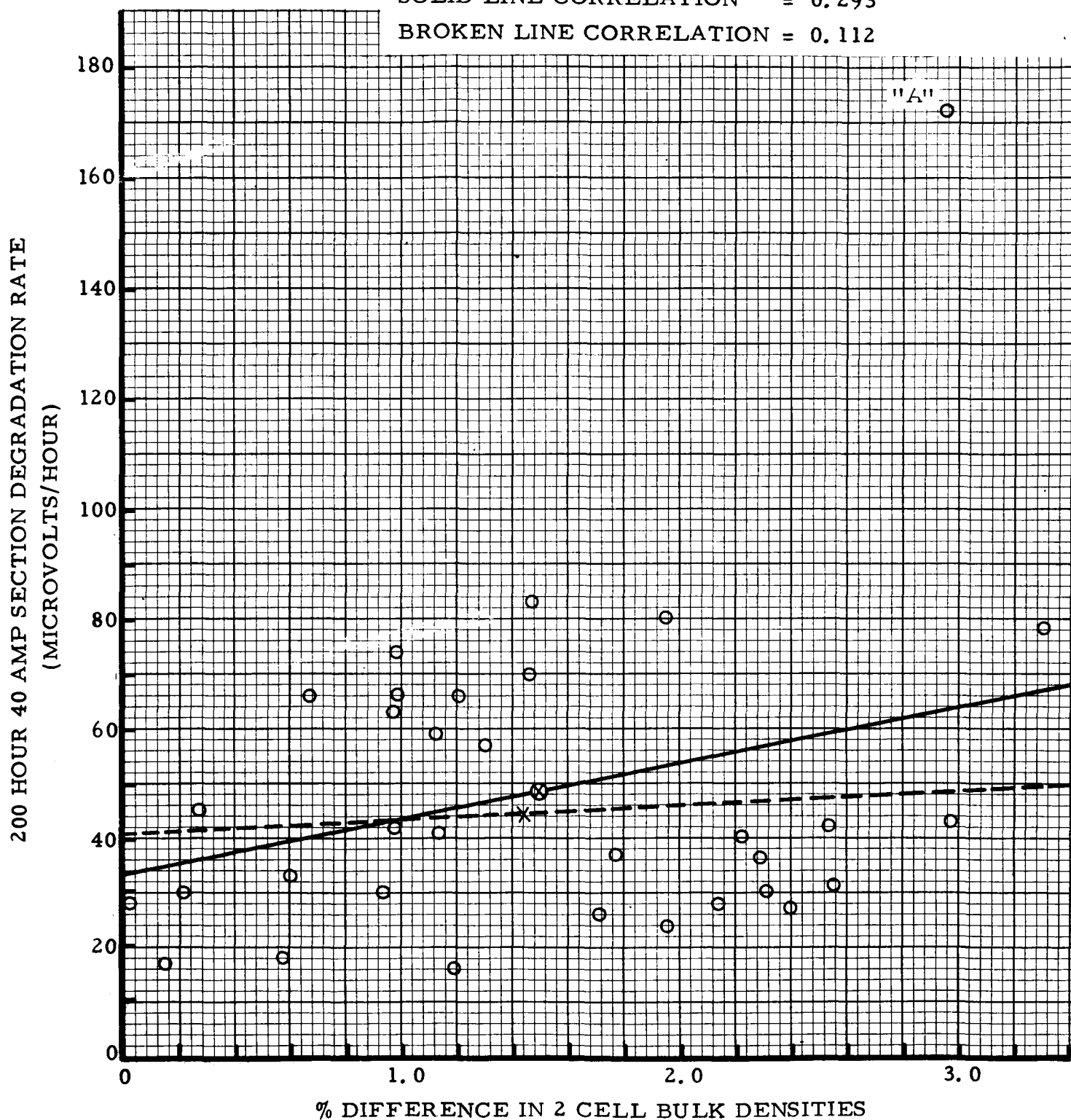


Figure 39. Correlation Between Bulk Matrix Densities and Voltage Degradation